CLASSIFICATION NOTES
No. 30.7

FATIGUE ASSESSMENT OF SHIP STRUCTURES

FEBRUARY 2003

DET NORSKE VERITAS
Veritasveien 1, N-1322 Høvik, Norway Tel.: +47 67 57 99 00 Fax: +47 67 57 99 11

FOREWORD

DET NORSKE VERITAS is an autonomous and independent Foundation with the objective of safeguarding life, property and the environment at sea and ashore.

DET NORSKE VERITAS AS is a fully owned subsidiary Society of the Foundation. It undertakes classification and certification of ships, mobile offshore units, fixed offshore structures, facilities and systems for shipping and other industries. The Society also carries out research and development associated with these functions.

DET NORSKE VERITAS operates a worldwide network of survey stations and is authorised by more than 120 national administrations to carry out surveys and, in most cases, issue certificates on their behalf.

Classification Notes

Classification Notes are publications which give practical information on classification of ships and other objects. Examples of design solutions, calculation methods, specifications of test procedures, as well as acceptable repair methods for some components are given as interpretations of the more general rule requirements.

An updated list of Classification Notes is available on request. The list is also given in the latest edition of the Introduction-booklets to the "Rules for Classification of Ships and the "Rules for Classification of High Speed, Light Craft and Naval Surface Craft".

In "Rules for Classification of Fixed Offshore Installations", only those Classification Notes which are relevant for this type of structure have been listed.

This edition of Classification Note No. 30.7 replaces the issue from January 2001.

Main changes

Figure 2.5 amended
Chapter 8.2.1 Table 8.3 - nomenclature amended
Chapter 8.3.1 Table 8.5 - nomenclature amended
Chapter 8.3.3 nomenclature of the load condition updated

Data processed and typeset by Det Norske Veritas

Printed in Norway

25/02/2003 3:16 PM - CN30.7.doc

CONTENTS

1. General

1.1 Introduction

1.1.1

Fatigue cracks and fatigue damages have been known to ship designers for several decades. Initially the obvious remedy was to improve detail design. With the introduction of higher tensile steels (HTS-steels) in hull structures, at first in deck and bottom to increase hull girder strength, and later on in local structures, the fatigue problem became more imminent.

1.1.2

In the DNV Rules for Classification of Ships, the material factor f_1, which give the ratio of increase in allowable stresses as a function of the material yield point was initially introduced in 1966. The factor is varying with the yield point at a lower than linear rate, this to give some (but insufficient) contribution to the general safety against fatigue fracture of higher tensile steels. However, during recent years a growing number of fatigue crack incidents in local tank structures in HTS steels have demonstrated that a more direct control of fatigue is needed.

1.1.3

This Classification Note is intended to give a general background for the rule requirements for fatigue control of ship structures, and to provide detailed recommendations for such a control. The aim of the fatigue control is to ensure that all parts of the hull structure subjected to fatigue (dynamic) loading have an adequate fatigue life. Calculated fatigue lives, calibrated with the relevant fatigue damage data, may give the basis for the structural design (steel selection, scantlings and local details). Furthermore, they can form the basis for efficient inspection programs during fabrication and throughout the life of the structure.

1.1.4

To ensure that the structure will fulfil its intended function, fatigue assessment, supported where appropriate by a detailed fatigue analysis, should be carried out for each individual type of structural detail which is subjected to extensive dynamic loading. It should be noted that every welded joint and attachment or other form of stress concentration is potentially a source of fatigue cracking and should be individually considered.

1.2 Scope, limitations, and validity

This Classification Note includes procedures for evaluation of fatigue strength, but not limited to, for the following:

- Steel ship structures excluding high speed light crafts.
- Foundations welded to hull structures.
- Any other areas designated primary structures on the drawings of ship structures
- Attachment by welding to primary ship structures, such as double plates, etc.

This Classification Note may be adapted for modification to existing ship structures, subject to the limitations imposed by the original material and fabrication techniques.

This Classification Note is valid for steel material with yield stress less than 500 MPa.

1.3 Methods for fatigue analysis

1.3.1

Fatigue design may be carried out by methods based on fatigue tests (S-N data) and estimation of cumulative damage (Palmgrens - Miner rule).

1.3.2

The long term stress range distribution is a fundamental requirement for fatigue analysis. This may be determined in various ways. This Classification Note outlines two methods for stress range calculation:

1) A postulated form of the long-term stress range distribution with a stress range based on dynamic loading as specified in the rules.
2) Spectral method for the estimation of long-term stress range

In the first method a Weibull distribution is assumed for the long term stress ranges, leading to a simple formula for calculation of fatigue damage. The load effects can be derived directly from the ship rules. The nominal stresses have to be multiplied by relevant stress concentration factors for calculation of local notch stresses before entering the S-N curve.

The second method implies that the long-term stress range distribution is calculated from a given (or assumed) wave climate. This can be combined with different levels of refinement of structural analysis.

Thus a fatigue analysis can be performed based on simplified analytical expressions for fatigue lives or on a more refined analysis where the loading and the load effects are calculated by numerical analysis. The fatigue analysis may also be performed based on a combination of simplified and refined techniques as indicated by the diagonal arrows in Figure 1.1.

1.3.3

The requirement to analysis refinement should be agreed upon based on

- experience with similar methods on existing ships and structural details with respect to fatigue

– consequences of a fatigue damage in terms of service problems and possible repairs

In general, the simplified method for fatigue life calculation is assumed to give a good indication as to whether fatigue is a significant criterion for design or not. The reliability of the calculated fatigue lives is, however, assumed to be improved by refinement in the design analysis.

1.3.4

It should further be kept in mind that real fatigue lives are a function of workmanship related to fabrication and corrosion protection. Therefore, to achieve the necessary link between the calculated and the actual fatigue lives for ships, the fabrication has to be performed according to good shipbuilding practice with acceptance criteria as assumed in the calculation.

1.4 Fatigue accumulation

1.4.1

The fatigue life under varying loading is calculated based on the S-N fatigue approach under the assumption of linear cumulative damage (Palmgrens-Miner rule). The total damage that the structure is experiencing may be expressed as the accumulated damage from each load cycle at different stress levels, independent of the sequence in which the stress cycles occur.

The design life assumed in the fatigue assessment of ships is normally not to be taken less than 20 years. The accumulated fatigue damage is not to exceed a usage factor of 1.0. The acceptance criteria is related to design S-N curves based on mean- minus-two-standard-deviations curves for relevant experimental data.

1.5 Definitions

1.5.1

The following general symbols are used in this Classification Note:

A	Cross sectional area
B	Greatest moulded breadth of ship in m measured at the summer waterline
C_B	Block coefficient = $\Delta/1.025LBT_{RULE}$
C_W	Wave coefficient as given in DNV Rules for Ships Pt.3, Ch.1.
D	Moulded depth of ship, cfr, Rules Pt.3 Ch.1 Sec.1
D	Fatigue damage
$F_{\Delta\sigma}(\Delta\sigma)$	Weibull distribution
$H(\omega)$	Transfer function
H_S	Significant wave height
I	Moment of inertia
I_a	Moment of inertia for the transverse frame
I_b	Moment of inertia for the longitudinal stringer/ girder
K	Stress concentration factor
K_g	Geometric stress concentration factor
K_n	Un-symmetrical stiffeners with lateral loading stress concentration factor
K_{te}	Eccentric tolerance stress concentration factor (normally plate connections)
K_t	Angular mismatch stress concentration factor (normally plate connections)
K_w	Weld geometry stress concentration factor
L	Rule length of ship in m, cfr. Rules Pt.3 Ch.1 Sec.1.
L_{pp}	Length between perpendiculars
M	Moment
M_{wo}	Wave induced vertical moment
M_H	Wave induced horizontal moment
N_S	Number of cross ties
$Q(\Delta\sigma)$	Probability level for exceedance of stress range $\Delta\sigma$
$S_\eta(\omega)$	Wave spectrum
$S_\sigma(\omega)$	Stress response spectrum
T_d	Design life
T_{act}	Draught actual
T	vessel mean moulded summer draught in m
T_z	Zero crossing period
Z	Section modulus
$\bar{a}$	S-N fatigue parameter
a	Local / global load combination factor
b	Local / global load combination factor
b_f	Flange width
a_i	Acceleration in direction i
f_1	Material factor as specified in the Rules
f_e	Environmental reduction factor
f_m	Mean stress reduction factor
f_r	Factor for calculation of load effects at 10^{-4} probability level
g	Acceleration of gravity (= 9.81 m/s^2)
h	Weibull shape parameter
h_o	Basic Weibull shape parameter
h_w	Web height
i_a	I_a / S
i_b	I_b / l_s
l	Stiffener length
log( )	10th logarithm
ln( )	Natural logarithm
m	S-N fatigue parameter
m_n	Spectral moment of order n
p	Lateral pressure
p_{ij}	Occurrence probability of sea condition i and heading j
p_S	Sailing rate = fraction of design life at sea

q	Weibull scale parameter
s	Stiffener spacing
t	Plate thickness
t_p	Plate thickness
t_f	Flange thickness
t_w	Web thickness
t_n	Net plate thickness
δ	Deformation
v_{ij}	Zero crossing frequency in short-term condition *i*, *j*
ω	Wave frequency
v_o	Long-term average zero frequency
ρ	Correlation coefficient
σ	Stress amplitude
σ_2	Secondary stress amplitude resulting from bending of girder system
σ_3	Tertiary stress amplitude produced by bending of plate elements between longitudinal and transverse frames/stiffeners
$\sigma_{nominal}$	Nominal stress amplitude, e.g. stress derived from beam element or finite element analysis
η	Fatigue usage factor
Δ	moulded displacement in t in salt water (density 1.025 t/m^3) on draught T
$\Delta\sigma$	Stress range
$\Delta\sigma_g$	Global stress range
$\Delta\sigma_l$	Local stress range
$\Delta\sigma_h$	Nominal stress range due to horizontal bending
$\Delta\sigma_v$	Nominal stress range due to vertical bending
$\Gamma(\ )$	Gamma function

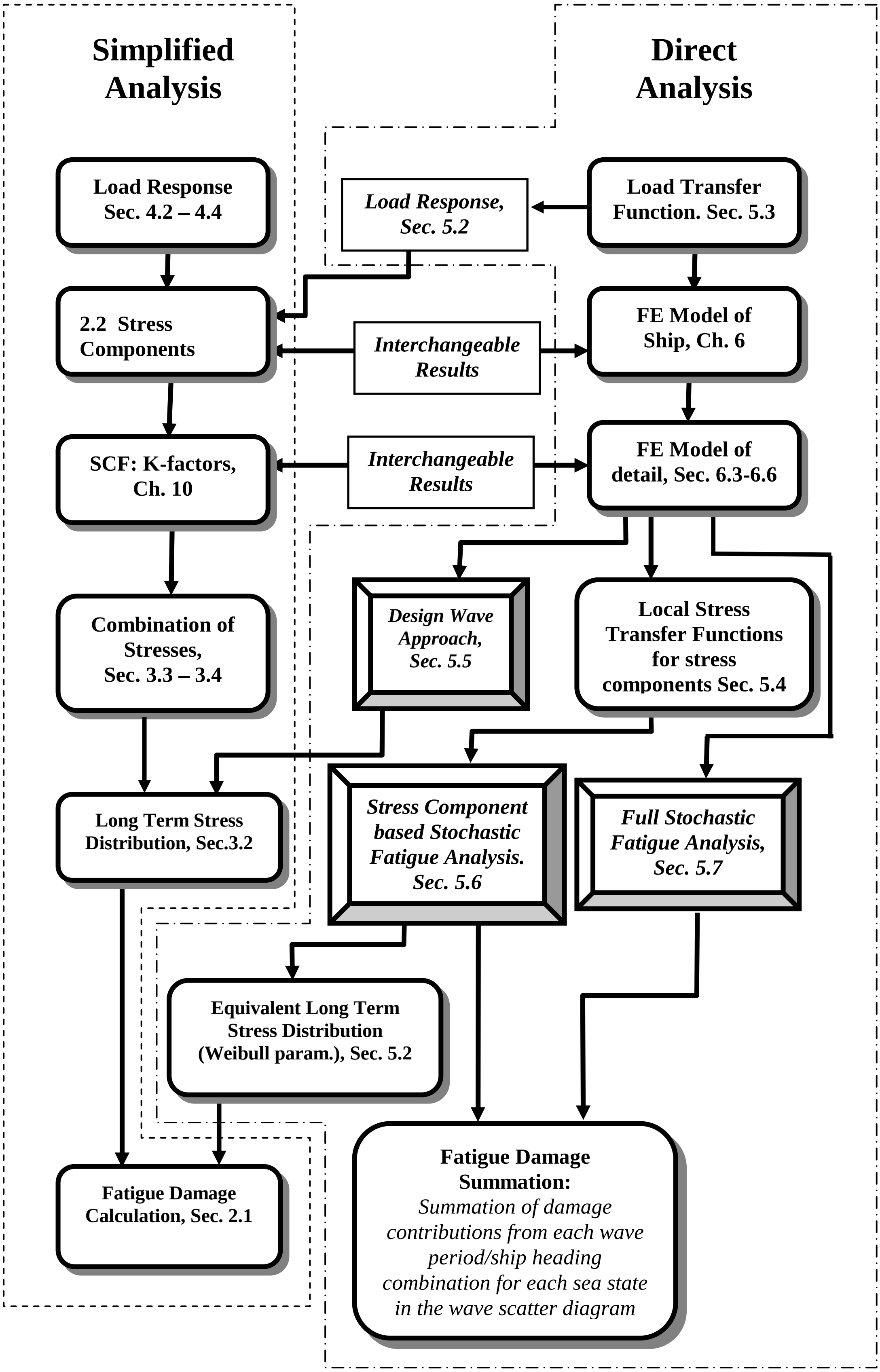

Figure 1.1 Flow diagram over possible fatigue analysis procedures

2. Fatigue Analysis

2.1 Cumulative damage

2.1.1

The fatigue life may be calculated based on the S-N fatigue approach under the assumption of linear cumulative damage (Palmgrens-Miner rule).

When the long-term stress range distribution is expressed by a stress histogram, consisting of a convenient number of constant amplitude stress range blocks $\Delta\sigma_i$ each with a number of stress repetitions n_i the fatigue criterion reads

$$D = \sum_{i=1}^{k} \frac{n_i}{N_i} = \frac{1}{\bar{a}} \sum_{i=1}^{k} n_i \cdot (\Delta\sigma_i)^m \leq \eta$$

where

D	=	accumulated fatigue damage
$\bar{a}$, m	=	S-N fatigue parameters
k	=	number of stress blocks
n_i	=	number of stress cycles in stress block i
N_i	=	number of cycles to failure at constant stress range $\Delta\sigma_i$
η	=	usage factor. Accepted usage factor is defined as $\eta = 1.0$

Applying a histogram to express the stress distribution, the number of stress blocks, k, is to be large enough to ensure reasonable numerical accuracy, and should not be less than 20. Due consideration should be given to selection of integration method as the position of the integration points may have a significant influence on the calculated fatigue life dependent on integration method.

2.1.2

When the long-term stress range distribution is defined applying Weibull distributions for the different load conditions, and a one-slope S-N curves is used, the fatigue damage is given by,

$$D = \frac{\nu_0 T_d}{\bar{a}} \sum_{n=1}^{N_{load}} p_n q_n^m \Gamma(1 + \frac{m}{h_n}) \leq \eta$$

where

N_{load}	=	total number load conditions considered
p_n	=	fraction of design life in load condition n, $\Sigma p_n \leq 1$, but normally not less than 0.85
T_d	=	design life of ship in seconds (20 years = 6.3 10^8 secs.)
h_n	=	Weibull stress range shape distribution parameter for load condition n, see Section 3.2
q_n	=	Weibull stress range scale distribution parameter for load condition n
ν_0	=	long-term average response zero-crossing frequency
$\Gamma(1+\frac{m}{h_n})$	=	gamma function. Values of the gamma function are listed in Table 2.1

h	*m = 3.0*	*h*	*m=3.0*
0.60	120.000	0.86	11.446
0.61	104.403	0.87	10.829
0.62	91.350	0.88	10.263
0.63	80.358	0.89	9.741
0.64	71.048	0.90	9.261
0.65	63.119	0.91	8.816
0.66	56.331	0.92	8.405
0.67	50.491	0.93	8.024
0.68	45.442	0.94	7.671
0.69	41.058	0.95	7.342
0.70	37.234	0.96	7.035
0.71	33.886	0.97	6.750
0.72	30.942	0.98	6.483
0.73	28.344	0.99	6.234
0.74	26.044	1.00	6.000
0.75	24.000	1.01	5.781
0.76	22.178	1.02	5.575
0.77	20.548	1.03	5.382
0.78	19.087	1.04	5.200
0.79	17.772	1.05	5.029
0.80	16.586	1.06	4.868
0.81	15.514	1.07	4.715
0.82	14.542	1.08	4.571
0.83	13.658	1.09	4.435
0.84	12.853	1.10	4.306
0.85	12.118		

Table 2.1 Numerical values for Γ(1+m/h)

The Weibull scale parameter is defined from the stress range level, $\Delta\sigma_0$, as

$$q_n = \frac{\Delta\sigma_0}{(\ln n_0)^{1/h_n}}$$

where n_0 is the number of cycles over the time period for which the stress range level $\Delta\sigma_0$ is defined. ($\Delta\sigma_0$ includes mean stress effect)

In combination with calculation of stress range $\Delta\sigma_0$ by the simplified method given in Chapters 3, 4 and 10, the zero-crossing-frequency may be taken as,

$$\nu_0 = \frac{1}{4 \cdot \log_{10}(L)}$$

where L is the ship Rule length in meters.

Alternatively, in combination with calculation of stress range $\Delta\sigma_o$ by direct analyses, the average zero-crossing-frequency can be derived as given in Chapter 5.

2.1.3

When the long term stress range distribution is defined through a short term Rayleigh distribution within each short term period for the different loading conditions, and a one-slope S-N curve is used, the fatigue criterion reads,

$$D = \frac{\nu_0 T_d}{\bar{a}} \Gamma(1+\frac{m}{2}) \sum_{n=1}^{N_{load}} p_n \cdot \sum_{i=1, j=1}^{\substack{\text{all seastates}\\ \text{all headings}}} r_{ijn} (2\sqrt{2m_{0ijn}})^m \le \eta$$

where

r_{ij} = the relative number of stress cycles in short-term condition *i, j*, see also 5.2.6

ν_o = long-term average response zero-crossing-frequency, see 5.2.6

m_{oij} = zero spectral moment of stress response process

The Gamma function, $\Gamma(1+\frac{m}{2})$ is equal to 1.33 for m = 3.0.

Expressions for fatigue damage applying bi-linear S-N curves are given in Appendix D

2.2 Stresses to be considered

2.2.1

The procedure for the fatigue analysis is based on the assumption that it is only necessary to consider the ranges of cyclic principal stresses in determining the fatigue endurance. However, some reduction in the fatigue damage accumulation can be credited when parts of the stress cycle range are in compression.

It should be noted that in welded joints, there may be several locations at which fatigue cracks can develop, e.g. weld toe and weld root of fillet joints. It is recommended to check potential hot spot locations for fatigue cracks by comparing the principal stress level with the maximum allowable notch stress ranges in Tables 2.8 and 2.9.

2.2.2

When the potential fatigue crack is located in the parent material at the weld toe, the relevant local notch stress is the range of maximum principal stress adjacent to the potential crack location with stress concentrations being taken into account.

This stress concentration is due to the gross shape of the structure and the local geometry of the weld. As an example, for the weld shown in Figure 2.1 a), the relevant local notch stress for fatigue design would be the tensile stress, σ, multiplied by the stress concentration factor due to the weld K_w. For the weld shown in Figure 2.1 b), the stress concentration factor for the local geometry must in addition be accounted for, giving the relevant local notch stress equal to $K_g K_w \sigma$, where K_g is the stress concentration factor due to the hole. For butt-welds with the weld surface dressed flush and small local bending stress across the plate thickness, K_w of 1.0 is to be used. Otherwise K_w of 1.5 is to be used.

The maximum principal stress range within 45° of the normal to the weld toe should be used for the analysis.

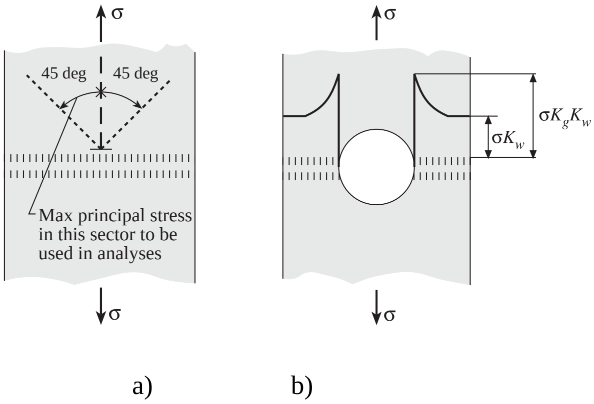

Figure 2.1 Explanation of local notch stresses

2.2.3

For fatigue analysis of regions in the base material not significantly effected by residual stresses due to welding, the stress range may be reduced dependent on whether mean cycling stress is tension or compression. This reduction may e.g. be carried out for cut-outs in the base material. Mean stress means that the static notch stress including relevant stress concentration factors. The calculated stress range obtained may be multiplied by the reduction factor f_m as obtained from Figure 2.2 before entering the S-N curve. For variable amplitude stresses, Δσ can be taken as the stress range at the 10^{-4} probability level of exceedance.

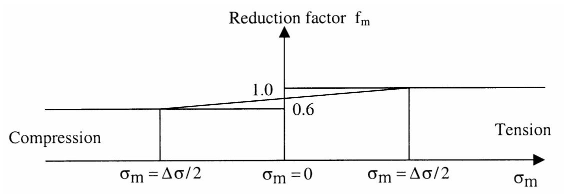

Figure 2.2 Stress range reduction factor to be used with the S-N curve for base material

2.2.4

Residual stresses due to welding and construction are reduced over time as the ship is subjected to loading. If a hot spot region is subjected to a tension force implying local yielding at the considered region, the effective stress range for fatigue analysis can be reduced due to the mean stress effect also for regions effected by residual stresses from welding. Mean stress means that the static notch stress including relevant stress concentration factors. The following reduction factor on the derived stress range may be applied, see Figure 2.3.

f_m = reduction factor due to mean stress effects

= 1.0 for tension over the whole stress cycle

= 0.85 for mean stress equal to zero

= 0.7 for compression over the whole stress cycle

For parts of the structure being exposed to both compressive and tensile mean stress depending on the loading situation, the reduction factor f_m = 0.85 may be applied on the long-term stress range distribution. For variable amplitude stresses, $\Delta\sigma$ can be taken as the stress range at the 10^{-4} probability level of exceedance.

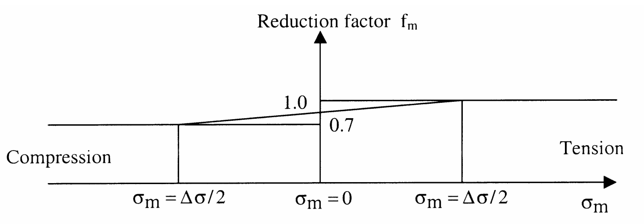

Figure 2.3 Stress range reduction factor that may be used with S-N curve for welded structures

2.3 S-N curves

2.3.1

The fatigue design is based on use of S-N curves which are obtained from fatigue tests. The design S-N curves which follow are based on the mean-minus-two-standard-deviation curves for relevant experimental data. The S-N curves are thus associated with a 97.6% probability of survival.

2.3.2

The S-N curves are applicable for normal and high strength steels used in construction of hull structures.

2.3.3

The S-N curves are presented as straight lines in a log-log scale. S-N curves in air are often presented as bi-linear with a change in slope beyond 10^7 cycles. S-N curves for welded joints and base material in air/cathodic protected environment and for corrosive environment are given in Table 2.2. The background for the S-N curves are described in Appendix E.

2.3.4

The use of bi-linear S-N curves complicates the expression for fatigue damage, ref. Appendix D. In order to reduce the computational effort, simplified one-slope S-N curves have been derived for typical long term stress range distributions in ship structures. Use of the one-slope S-N curves, defined by parameters as given in Table 2.3, leads to results on the safe side for calculated fatigue lives exceeding 20 years.

2.3.5

The basic design S-N curve is given as,

$$\log N = \log\bar{a} - m\log\Delta\sigma$$

with S-N curve parameters given in Tables 2.2 and 2.3.

N = predicted number of cycles to failure for stress range $\Delta\sigma$

$\Delta\sigma$ = stress range

m = negative inverse slope of S-N curve

$\log\bar{a}$ = intercept of log$N$-axis by S-N curve

$$\log\bar{a} = \log a - 2s$$

where

a = is constant relating to mean S-N curve

s = standard deviation of log N;

s = 0.20

In combination with the fatigue damage criteria given in Section 2.1.2 and 2.1.3, curves Ib, II, IIIb and IV should be used.

S-N Curve	Material	$N \le 10^7$		$N > 10^7$	
		$\log\bar{a}$	m	$\log\bar{a}$	m
I	Welded joint	12.65	3.0	16.42	5.0
III	Base Material	12.89	3.0	16.81	5.0

a) Air or with cathodic protection:

S-N Curve	Material	$\log\bar{a}$	m
II	Welded joint	12.38	3.0
IV	Base material	12.62	3.0

b) Corrosive Environment:

Table 2.2 S-N parameters

S-N Curve	Material	$\log \overline{a}$	m
Ib	Welded joint	12.76	3.0
IIIb	Base material	13.00	3.0

Table 2.3 Alternative one-slope S-N parameters

Figure 2.4 Design S-N Curves

2.3.6

The design S-N curves given here correspond to test results from smooth specimens having a stress concentration factor K = 1.0. The curves for base material assume that flame cut- or otherwise rough surfaces are ground. For base material where the surface and edge corners are machined or ground smooth and protected against corrosion, the fatigue life may be increased by a factor of 2.0. The curves for welded joints assume welds proven free from significant defects.

For fatigue analysis of details with $K \neq 1.0$, the stress range must incorporate the stress concentration factors, see Chapter 10.

2.3.7

The fatigue strength of welded joints is to some extent dependent on plate thickness and on the stress gradient over the thickness. Thus for thickness larger than 25 mm, the S-N curve in air reads

$$logN = log\overline{\alpha} - \frac{m}{4}\ log\left(\frac{t}{25}\right) - m\ log\ \Delta\sigma$$

where *t* is thickness (mm) through which the potential fatigue crack will grow. This S-N curve in general applies to all types of welds. For fatigue analysis of details where the stress concentration factor is less than 1.3, the thickness effect can be neglected and the basic S-N curve can be used. Such stress concentration factors are normally only achieved through grinding or machining of the weld/base material transition. See 10.4 for a description of normal workmanship associated with use of these S-N curves.

2.4 Corrosion

2.4.1

It is recognised that the fatigue life of steel structures is considerably shorter in freely corroding condition submerged in sea water than in air, i.e. in dry indoor atmosphere such as common laboratory air. For steel submerged in sea water and fully cathodically protected, approximately the same fatigue life as in dry air is obtained.

An intact coating system will also protect the steel surface from the corrosive environment, so that the steel can be considered to be as in dry air condition.

The basic S-N curve for welded regions in air is only to be applied for joints situated in dry spaces or joints effectively protected against corrosion. For joints efficiently protected only a part of the design life and exposed to corrosive environment the remaining part, the fatigue damage may be calculated as a sum of partial damages according to 2.4.3.

Estimating the efficient life time of coating- and cathodic protection systems, due consideration is to be given to specification, application and maintenance of the systems. A guideline for effective life times for common corrosion protection systems is listed in Table 2.4.

Full cathodic protection is defined as: Steel surfaces submerged in normal, aerated sea water having a potential of - 0.80 volts measured with a silver/silver chloride reference cell (or - 0,79 volts versus a calomel cell, etc.). The potential limit for cathodic overprotection will vary with the degree of steel strength. For normal strength carbon manganese steel (yield strength min. 235 MPa) it will be - 1,1 volts versus silver/silver chloride. Cathodic overprotection, especially in hydrogen sulphide H_2S containing environment, can lead to hydrogen embrittlement of high strength steels.

Coating system	*5 years Prep. I* [2] *Coats x mic.*	*10 years Prep II* [2] *Coats x mic.*	*15 years Prep III* [2] *Coats x mic.*
Epoxy based (light coloured) Epoxy coal tar (Coal Tar Epoxy) Other recognised coating systems [1]	1 x 200 1 x 200		
As above		2 x 175	
As above			2 x 175 (to 2 x 225)

1. Other-than-epoxy based with well documented performance
2. **Prep. I:** Steel plates shop primed on blast cleaned surface to Sa 2 - Sa 2,5. Welds and burns mechanically cleaned to min. St 3. To obtain a coating durability ≥ 5 years the steel surface preparation for shop priming should be Sa 2,5
   Prep. II: Zinc rich shop primer on surface blast cleaned to Sa 2,5 or better. Sharp edges broken. Welds and burns cleaned to min. St 3. Dry conditions: Air humidity ≤ 85 % and steel temperature ≥ 3 C above the dew point during blast cleaning and coating application.
   Prep. III: Zinc rich shop primer on surface blast cleaned to Sa 2,5 or better. Sharp edges broken. Welds, burns and broken edges blast cleaned to Sa 2,5 or better. Clean conditions: Any oil, grease, dust, weld smoke or salt contamination on shop primed or other surface to be coated, removed by cleaning before final blasting operations. Dry conditions: Air humidity ≤ 85 % and steel temperature ≥ 3 ˚C above the dew point during blast cleaning and coating application.

Table 2.4 Duration of corrosion protection

2.4.2

Global stress components may be calculated based on gross scantlings.

Local stress components should be calculated based on reduced scantlings, i.e. gross scantlings minus corrosion addition t_k as given in Table 2.5. (The corrosion addition specified below is similar to that specified in the Rules [1])

Tank/hold region	*Location*	
Internal members and plate boundary between spaces of the given category	Within 1.5 m below weather deck tank or hold top	Elsewhere
Ballast tank[1)]	3.0	1.5
Cargo oil tank only	2.0	1.0 (0)[2)]
Hold of dry bulk cargo carriers 4)	1.0	1.0 (3)[5)]
Plate boundary between given space categories	Within 1.5 m below weather deck tank or hold top	Elsewhere
Ballast tank [1)] / Cargo oil tank only	2.5	1.5 (1.0) [2)]
Ballast tank [1)] / Hold of dry bulk cargo carrier [4)]	2.0	1.5
Ballast tank [1)] / Other category space [3)]	2.0	1.0
Cargo oil tank only / Other category space 3)	1.0	0.5 (0) [2)]
Hold of dry bulk carrier [4)] / Other category space [3)]	0.5	0.5

1) The term ballast tank includes also combined ballast and cargo oil tanks, but not cargo oil tanks which may carry water ballast according to Regulation 13 (3), of MARPOL 73/78, see Rules
2) The figure in bracket refers to non-horizontal surfaces.
3) Other category space denotes the hull exterior and all spaces other than water ballast and cargo oil tanks and holds of dry bulk cargo carriers.
4) Hold of dry bulk cargo carriers refers to the cargo holds of vessels with class notations **Bulk Carrier** and **Ore Carrier**
5) The figure in bracket refers to lower part of main frames in bulk carrier holds.

Table 2.5 Corrosion addition tk in mm

2.4.3

Fatigue strength may normally be assessed with the S-N curve in air for the effective corrosion protection period, i.e. the corrosion protection period of coating plus 5 years. The S-N curve in corrosive environment is to be used for the remaining time.

Carriage of sour crude oil cargoes may reduce the fatigue strength of structures in cargo tanks, while the sweet oil cargoes may not reduce the fatigue life. As type of oil cargoes and actual corrosion protection period of the coating system are uncertain at the design stage, for new building of oil tankers it is assumed that cargo tanks are exposed to sweet cargoes for the loaded condition. Thus, for cargo tanks, the S-N curve in air may normally be used for new building of oil tankers. If sour cargoes and the other cargoes causing corrosion are to be carried out frequently in cargo tanks, the S-N curve in corrosive environment may normally be used.

For the ballast condition, as there is no cargo in the cargo tanks, the S-N curve in air may normally be used for new building of vessels. For ballast tanks, the effective corrosion protection period of 15 years may normally be used for new building of vessels.

For dry cargo holds, fuel oil tanks, void spaces, cofferdam, and hull external surfaces, the S-N curve in air may normally be used.

2.5 Maximum allowable notch stress ranges

2.5.1

Depending on the required accuracy of the fatigue evaluation it may be recommended to divide the design life into a number of time intervals due to different loading conditions and limitations of durability of the corrosion protection. For example, the design life may be divided into one interval with good corrosion protection and one interval where the corrosion protection is more questionable for which different S-N data should be used, see Section 2.3. Each of these intervals should be divided into that of loaded and ballast conditions.

The effect of varying degree of corrosion protection of ballast tanks during design life may, as a simplification, be accounted for by multiplying the calculated fatigue damage by a factor χ from Table 2.6. It is then assumed that the fatigue damage has been calculated for the total life time using only one of the S-N curves I or III. Guidance on expected effective corrosion protection period of coating is given in 2.4 and in Guidelines No 8. For ballast tanks protected by anodes only, it is recommended to apply S-N curves II or IV.

As a simplification therefore, the fatigue damage may be calculated applying S-N curves for air and then multiply the fatigue damage by the factor χ given in Table 2.6.

The procedure can be described as:

1. Calculate the fatigue life according to I or III (In Air)
2. If the calculated fatigue life is greater than the effective corrosion protection period, i.e. T_c +5 years, the corrected life is calculated as

$$T = T_c + 5 + \left(\frac{T_{design}}{D_{InAir}} - T_c - 5 \right) \frac{D_{InAir}}{D_{Corrosive}}$$

where $\frac{1}{D_{InAir}}$ correspond to the calculated fatigue life (In Air), T_c = coating life time, T_{design} = design life time in years.

The factor χ as given in the table below is determined assuming $\frac{D_{corrosive}}{D_{InAir}} \approx 2.3$

		Ballast tanks *Effective corrosion protection period (Yrs)*					*Tanks for cargo oil*
S-N curve used for calculation of fatigue damage	Design life (years)	5	10	15	20	25	
	20	2	1.7	1.3	1	-	1.7
I or III	25	2.1	1.8	1.5	1.3	1.	1.7
	30	2.1	1.9	1.7	1.5	1.2	1.7

Table 2.6 Factor χ on fatigue damage to account for corrosion protection of structure exposed to a corrosive environment.

Example: Assume that a fatigue damage of ballast tank structure D_{air} has been calculated for a design life equal to 25 years based on S-N curve I. Assume further that the considered detail is exposed to a corrosive environment but with an effective corrosion protection period lasting 15 years. Then the resulting fatigue damage is obtained as $D = 1.5 \cdot D_{air}$

2.5.2

It can be assumed as a simplification that the long-term stress range distribution over the design life is a Weibull distribution. Any stress range in this distribution is a particular quantile, i.e. it is associated with a particular probability of exceedance. The maximum allowable stress range at a particular probability of exceedance is a design stress range, defined as the stress range that results from using the Weibull distribution in conjunction with a characteristic S-N curve and requiring the accumulated damage in the design life to be equal to 1.0. The characteristic S-N curve is obtained as the mean S-N curve shifted two standard deviations of logN to the left. Under the current safety format, the characteristic S-N curve is used as the design S-N curve.

Different maximum allowable notch stress ranges result for different Weibull shape parameters *h* and for different characteristic S-N curves. (For background see Chapter 10 of Ref. [8].) In Tables 2.8 and 2.9, the maximum allowable notch stress range ($\Delta\sigma_o$) at probabilities of exceedance 10^{-4} and 10^{-8}, respectively, has been calculated for total design lives of $0.5{\cdot}10^8$, $0.7{\cdot}10^8$ and $1.0{\cdot}10^8$ cycles. An example of use of the tables is shown in Figure 2.5. The S-N parameters for S-N curves I, II, III, and IV are given in Table 2.2.

The maximum allowable notch stress range includes the stress concentration factors (K-factors), such that the maximum allowable nominal stress range to be used for design is obtained as

$$\Delta\sigma_{\text{nominal}} = \frac{\Delta\sigma_0}{K}$$

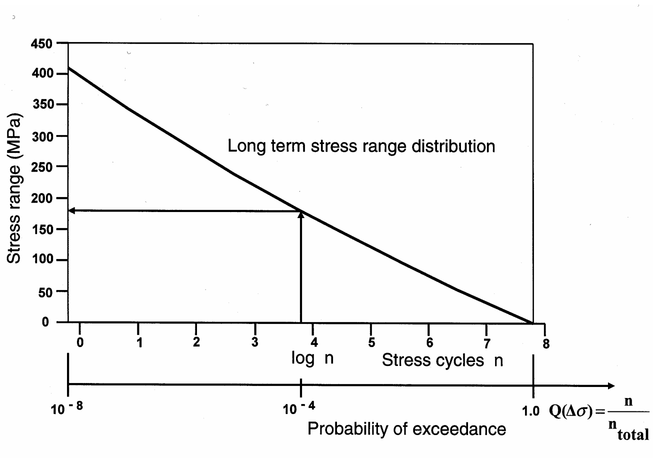

Figure 2.5 Stress range versus probability of exceedance

Example:

Weibull shape parameter h = 0.87

Total number of stress cycles $n_{total} = 0.7{\cdot}10^8$

Welded joint, corrosive environment, S-N curve II

It follows from Tables 2.9 that the maximum allowable notch stress range at 10^{-8} probability level of exceedance is 417.9 MPa and from Table 2.8 that maximum notch stress range at 10^{-4} probability level of exceedance is 188.4 MPa

The maximum allowable nominal stress range taking into account that the considered detail is exposed to a corrosive environment, but protected against corrosion for a fraction of the design life, can be approximated as

$$\Delta\sigma_{\text{nominal}} = \frac{\Delta\sigma_0}{K \cdot \chi^{1/3}}$$

where $\Delta\sigma_0$ is taken from Tables 2.8 and 2.9 assuming S-N curve I or III and χ is given in 2.5.1.

Example: Assume a welded detail with resulting stress concentration factor K = 3.1, h = 0.9, design life 20 years and number of cycles $0.7 \cdot 10^8$. From Table 2.9 we get $\Delta\sigma_0$ = 516.2 MPa. Assume effective corrosion protection 10 years, then it follows from 2.5.1 that χ = 1.7. Maximum allowable nominal stress range (extreme value) is then $\Delta\sigma_{\text{nominal}} = 516.2 / 3{,}1{\cdot}1.7^{1/3} = 140$ MPa

Weibull Shape-parameter h	S-N Curve I Welded joint Air/Cathodic, $\Delta\sigma_0$			S-N Curve II Welded joint Corrosive, $\Delta\sigma_0$			S-N Curve III Base material Air/Cathodic, $\Delta\sigma_0$			S-N Curve IV Base material Corrosive, $\Delta\sigma_0$		
	Design life cycles			Design life cycles			Design life cycles			Design life cycles		
	$0.5 \cdot 10^8$ cycles	$0.7 \cdot 10^8$ cycles	$1.0 \cdot 10^8$ cycles	$0.5 \cdot 10^8$ cycles	$0.7 \cdot 10^8$ cycles	$1.0 \cdot 10^8$ cycles	$0.5 \cdot 10^8$ cycles	$0.7 \cdot 10^8$ cycles	$1.0 \cdot 10^8$ cycles	$0.5 \cdot 10^8$ cycles	$0.7 \cdot 10^8$ cycles	$1.0 \cdot 10^8$ cycles
0.60	376.8	338.6	303.0	298.3	266.6	236.6	452.7	406.8	364.0	358.6	320.4	284.6
0.61	371.6	334.1	299.1	294.1	262.8	233.3	446.4	401.4	359.4	353.5	315.9	280.5
0.62	366.6	329.8	295.3	289.9	259.0	230.0	440.4	396.1	354.7	348.5	311.4	276.5
0.63	361.6	325.4	291.5	285.8	255.4	226.8	434.5	391.0	350.2	343.5	307.2	272.6
0.64	356.8	321.2	287.9	281.8	251.8	223.6	428.7	386.0	345.7	338.7	302.8	268.8
0.65	352.2	317.1	284.3	277.9	248.4	220.5	423.1	381.0	341.4	334.1	298.6	265.1
0.66	347.6	313.1	280.7	274.0	245.0	217.5	417.6	376.1	337.1	329.5	294.5	261.5
0.67	343.1	309.1	277.3	270.3	241.5	214.5	412.3	371.3	333.0	325.1	290.5	257.9
0.68	338.7	305.3	273.9	266.6	238.3	211.6	407.0	366.6	328.9	320.6	286.5	254.4
0.69	334.4	301.5	270.6	263.1	235.1	208.9	401.8	362.1	324.9	316.3	282.7	251.0
0.70	330.3	297.8	267.3	259.6	232.0	206.0	396.8	357.7	321.0	312.1	278.9	247.6
0.71	326.2	294.2	264.2	256.1	229.0	203.3	391.7	353.3	317.2	308.0	275.3	244.4
0.72	322.3	290.7	261.1	252.8	226.0	200.7	387.0	349.0	313.5	303.8	271.7	241.2
0.73	318.3	287.2	258.1	249.5	223.1	198.1	382.3	344.9	309.9	300.0	268.2	238.1
0.74	314.5	283.8	255.1	246.3	220.2	195.5	377.8	340.9	306.3	296.1	264.7	235.1
0.75	310.8	280.5	252.2	243.2	217.4	193.0	373.3	336.9	302.8	292.4	261.3	232.1
0.76	307.1	277.3	249.3	240.2	214.7	190.6	368.8	333.0	299.4	288.7	258.1	229.2
0.77	303.6	274.2	246.6	237.2	212.0	188.2	364.6	329.3	296.1	285.1	254.9	226.4
0.78	300.0	271.1	243.6	234.3	209.4	185.9	360.4	325.5	292.8	281.6	251.7	223.6
0.79	296.6	268.1	241.3	231.4	206.9	183.7	356.3	321.9	289.6	278.1	248.7	220.8
0.80	293.3	265.1	238.7	228.6	204.3	181.5	352.3	318.3	286.5	274.8	245.7	218.2
0.81	290.1	262.2	236.2	225.9	201.9	179.3	348.5	314.9	283.5	271.6	242.8	215.6
0.82	286.9	259.4	233.7	223.2	199.5	177.2	344.6	311.4	280.5	268.4	240.0	213.0
0.83	283.8	256.6	231.3	220.6	197.2	175.1	340.8	308.1	277.6	265.2	237.1	210.5
0.84	280.7	254.0	228.9	218.1	194.9	173.1	337.2	304.9	274.8	262.2	234.4	208.1
0.85	277.7	251.3	226.6	215.5	192.7	171.1	333.6	301.7	271.9	259.2	231.7	205.7
0.86	274.8	248.7	224.3	213.1	190.5	169.2	330.1	298.6	269.2	256.3	229.1	203.4
0.87	272.0	246.3	222.1	210.8	188.4	167.3	326.6	295.6	266.6	253.5	226.5	201.1
0.88	269.2	243.8	219.9	208.5	186.3	165.5	323.3	292.6	264.0	250.7	224.0	198.9
0.89	266.5	241.4	217.8	206.2	184.3	163.7	320.0	289.7	261.4	247.9	221.5	196.7
0.90	263.8	239.0	215.7	204.0	182.4	161.9	316.8	286.8	258.9	245.2	219.2	194.6
0.91	261.2	236.7	213.7	201.8	180.4	160.2	313.7	284.1	256.5	242.6	216.8	192.5
0.92	258.7	234.4	211.7	199.6	178.5	158.5	310.6	281.4	254.2	240.0	214.6	190.5
0.93	256.2	232.2	209.8	197.6	176.6	156.8	307.6	278.7	251.8	237.5	212.3	188.5
0.94	253.8	230.0	207.9	195.5	174.8	155.2	304.6	276.1	249.5	235.1	210.1	186.6
0.95	251.3	227.8	206.0	193.5	173.0	153.6	301.7	273.6	247.2	232.6	208.0	184.7
0.96	249.0	225.8	204.1	191.6	171.3	152.1	298.9	271.1	245.0	230.3	205.9	182.9
0.97	246.7	223.8	202.4	189.7	169.6	150.5	296.2	268.6	242.9	228.0	203.8	181.0
0.98	244.4	221.8	200.6	187.8	167.9	149.1	293.5	266.3	240.8	225.8	201.8	179.2
0.99	242.2	219.8	198.9	186.0	166.3	147.6	290.8	263.9	238.7	223.6	199.9	177.5
1.00	240.1	217.9	197.3	184.2	164.7	146.2	288.2	261.6	236.7	221.4	198.0	175.8
1.01	237.9	216.1	195.6	182.4	163.1	144.8	285.7	259.3	234.6	219.3	196.1	174.1
1.02	235.9	214.2	194.0	180.7	161.5	143.4	283.2	257.1	232.7	217.2	194.2	172.4
1.03	233.9	212.4	192.4	179.0	160.0	142.1	280.8	254.9	230.8	215.2	192.4	170.8
1.04	231.9	210.7	190.8	177.4	158.5	140.8	278.4	252.8	229.0	213.2	190.6	168.3
1.05	229.9	209.0	189.3	175.8	157.1	139.4	276.1	250.7	227.1	211.3	188.9	167.8
1.06	228.0	207.2	187.8	174.2	155.7	138.2	273.7	248.7	225.3	209.4	187.2	166.2
1.07	226.1	205.6	186.4	172.6	154.3	137.0	271.5	246.6	223.6	207.5	185.5	164.7
1.08	224.3	204.0	185.0	171.1	152.9	135.8	269.3	244.7	221.8	205.7	183.9	163.2
1.09	222.5	202.4	183.6	169.6	151.6	134.6	267.1	242.8	220.2	203.9	182.3	161.8
1.10		200.8	182.2		150.3	133.4		240.9	218.5		180.7	160.4

Table 2.7 Maximum allowable notch stress range (MPa) at a probability of exceedance 10^{-4} to keep the fatigue damage less than 1.0 for different design life cycles. (A Weibull distribution for the long-term stress range is assumed.)

Weibull Shape-parameter h	*S-N Curve I Welded joint Air/Cathodic, $\Delta\sigma_0$*			*S-N Curve II Welded joint Corrosive, $\Delta\sigma_0$*			*S-N Curve III Base material Air/Cathodic, $\Delta\sigma_0$*			*S-N Curve IV Base material Corrosive, $\Delta\sigma_0$*		
	Design life cycles			*Design life cycles*			*Design life cycles*			*Design life cycles*		
	$0.5\cdot10^8$ cycles	*$0.7\cdot10^8$ cycles*	*$1.0\cdot10^8$ cycles*	*$0.5\cdot10^8$ cycles*	*$0.7\cdot10^8$ cycles*	*$1.0\cdot10^8$ cycles*	*$0.5\cdot10^8$ cycles*	*$0.7\cdot10^8$ cycles*	*$1.0\cdot10^8$ cycles*	*$0.5\cdot10^8$ cycles*	*$0.7\cdot10^8$ cycles*	*$1.0\cdot10^8$ cycles*
0.60	1196.1	1075.0	962.1	946.9	846.3	751.3	1437.2	1291.6	1155.8	1138.4	1017.3	903.4
0.61	1157.6	1040.9	931.7	916.1	818.6	726.7	1390.6	1250.6	1119.6	1101.1	984.1	873.8
0.62	1121.2	1008.6	903.1	886.6	792.1	703.5	1346.9	1211.7	1084.9	1065.8	952.6	845.8
0.63	1086.5	977.9	876.0	858.7	767.4	681.4	1305.6	1174.8	1052.2	1032.2	923.0	819.3
0.64	1053.9	948.6	850.2	832.2	743.9	660.4	1266.3	1140.0	1021.2	1000.5	894.5	793.8
0.65	1023.0	921.1	825.9	807.1	721.5	640.8	1229.0	1106.6	991.6	970.4	867.4	770.0
0.66	993.5	894.8	802.5	783.1	700.1	621.6	1193.6	1074.9	963.6	941.7	841.8	747.4
0.67	965.4	869.8	780.2	760.5	679.6	603.6	1160.1	1044.8	937.0	914.6	817.4	725.7
0.68	938.6	846.0	759.1	738.9	660.4	586.5	1127.8	1016.0	911.6	888.5	793.9	705.1
0.69	913.3	823.4	738.9	718.3	642.1	570.3	1097.2	988.8	887.2	863.7	771.9	685.5
0.70	889.0	801.7	719.5	698.7	624.5	554.6	1068.0	962.8	864.2	840.0	750.8	666.6
0.71	865.9	781.0	701.2	679.7	607.8	539.7	1039.8	937.9	842.1	817.5	730.7	648.7
0.72	844.0	761.2	683.7	661.9	591.8	525.5	1013.5	914.0	821.0	795.7	711.5	631.7
0.73	822.7	742.3	667.0	644.8	576.5	511.9	988.1	891.4	801.0	775.2	693.1	615.4
0.74	802.5	724.1	650.9	628.5	562.0	498.9	963.8	869.7	781.6	755.6	675.3	599.7
0.75	783.1	706.8	635.6	612.8	547.9	486.3	940.6	848.9	763.1	736.8	658.5	584.8
0.76	764.5	690.3	620.7	597.8	534.4	474.4	918.1	829.0	745.4	718.7	642.4	570.7
0.77	746.8	674.4	606.7	583.5	521.6	463.1	896.9	810.1	728.4	701.5	627.0	556.9
0.78	729.6	659.2	593.1	569.8	509.2	452.1	876.4	791.7	712.0	684.9	612.2	543.6
0.79	713.3	644.6	580.2	556.5	497.4	441.6	856.8	774.1	696.4	668.8	598.0	531.0
0.80	697.6	630.4	567.7	543.8	485.9	431.6	837.9	757.2	681.5	653.6	584.4	518.9
0.81	682.6	617.0	555.7	531.6	475.1	421.8	819.9	740.9	667.1	639.0	571.4	507.2
0.82	668.1	604.0	544.3	519.8	464.6	412.6	802.4	725.1	653.2	625.0	558.8	496.0
0.83	654.1	591.6	533.2	508.6	454.6	403.7	785.6	710.2	639.9	611.4	546.6	485.1
0.84	640.6	579.6	522.4	497.7	444.9	395.1	769.5	695.9	627.1	598.4	535.0	474.9
0.85	627.7	568.0	512.1	487.1	435.6	386.8	753.9	682.0	614.6	585.9	523.7	465.0
0.86	615.3	556.9	502.2	477.2	426.5	378.9	739.0	668.6	602.8	573.8	512.9	455.4
0.87	603.4	546.3	492.7	467.5	417.9	371.1	724.4	655.7	591.3	562.3	502.5	446.2
0.88	591.8	535.9	483.5	458.2	409.6	363.7	710.6	643.3	580.3	551.0	492.5	437.3
0.89	580.7	525.9	474.6	449.2	401.6	356.6	697.2	631.1	569.6	540.2	482.7	428.6
0.90	569.9	516.2	465.9	440.6	393.9	349.7	684.3	619.6	559.3	529.7	473.4	420.4
0.91	559.5	506.9	457.7	432.2	386.4	343.1	671.8	608.5	549.4	519.6	464.5	412.4
0.92	549.6	497.9	449.7	424.0	379.2	336.7	659.8	597.7	539.9	509.9	455.8	404.8
0.93	539.9	489.3	442.0	416.3	372.1	330.5	648.1	587.3	530.5	500.5	447.4	397.3
0.94	530.5	480.9	434.5	408.8	365.4	324.5	636.7	577.2	521.5	491.4	439.3	390.1
0.95	521.4	472.6	427.3	401.5	358.9	318.6	625.8	567.4	512.8	482.5	431.5	383.1
0.96	512.6	464.8	420.3	394.5	352.6	313.0	615.3	558.0	504.4	474.1	423.8	376.4
0.97	504.1	457.2	413.5	387.6	346.5	307.6	605.1	548.9	496.3	465.9	416.5	369.8
0.98	495.9	449.9	407.0	381.0	340.6	302.4	595.3	540.1	488.4	458.0	409.4	363.5
0.99	487.9	442.8	400.6	374.7	334.9	297.3	585.7	531.5	480.7	450.3	402.6	357.4
1.00	480.2	435.9	394.6	368.4	329.3	283.4	576.4	523.2	473.3	442.9	395.9	351.5
1.01	472.6	429.2	388.5	362.3	323.9	287.6	567.5	515.1	466.1	435.6	389.4	345.8
1.02	465.4	422.6	382.8	356.5	318.7	283.0	558.7	507.3	459.1	428.5	383.2	340.2
1.03	458.4	416.3	377.2	350.9	313.6	278.5	550.3	499.7	452.4	421.8	377.2	334.9
1.04	451.5	410.2	371.7	345.4	308.7	274.2	542.2	492.3	445.9	415.2	371.2	329.7
1.05	444.9	404.3	366.4	340.1	304.0	270.0	534.2	485.2	439.5	408.8	365.5	324.6
1.06	438.5	398.5	361.2	335.0	299.4	265.8	526.4	478.2	433.3	402.7	359.9	319.6
1.07	432.2	392.9	356.2	330.0	294.9	261.8	518.9	471.4	427.3	396.6	354.5	314.8
1.08	426.2	387.5	351.4	325.1	290.6	258.0	511.6	464.9	421.4	390.8	349.3	310.2
1.09	420.2	382.2	346.7	320.3	286.3	254.2	504.5	458.6	415.8	385.1	344.2	305.6
1.10	414.5	377.1	342.1	315.7	282.2	250.6	497.6	452.4	410.3	379.6	339.3	301.3

Table 2.8 Maximum allowable notch stress range (MPa) at a probability of exceedance 10^{-8} to keep the fatigue damage less than 1.0 for different design life cycles. (A Weibull distribution for the long-term stress range is assumed.)

2.6 Uncertainties in fatigue life prediction

2.6.1

There are a number of different uncertainties associated with fatigue life predictions. The calculated loading on the ship is uncertain due to uncertainties in wave heights, periods and distribution of waves. The resulting stresses in the ship are uncertain due to uncertainties in the loading, calculation of response and calculation of stress concentrations.

2.6.2

Because of the sensitivity of calculated fatigue life to the accuracy of estimates of stresses, particular care must be taken to ensure that stresses are realistic. Fatigue damage is proportional to stress raised to the power of the inverse slope of the S-N curve. I.e. small changes in stress result in much greater changes in fatigue life. Special attention should be given to stress raisers like eccentricities and secondary deformations and stresses due to local restraints. Due considerations should, therefore, be given to the fabrication tolerances during fatigue design.

2.6.3

There is a rather large uncertainty associated with the determination of S-N curves. The scatter in the test results which form the basis for the S-N curves is generally accepted to relate to the normal variation of weld imperfections within normal workmanship, indicated in Table 10.14 . The ratio between calculated fatigue lives based on the mean S-N curve and the mean minus two standard deviations S-N curve is significant as shown in Figure 2.6.

2.6.4

There is also uncertainty associated with the determination of stress concentration factor. The error introduced in the calculated fatigue life by wrong selection of stress concentration factor is indicated in Figure 2.7.

2.6.5

It should be kept in mind that a high fatigue life is an efficient means to reduce probability of fatigue failure, see Figure 2.8. It also reduces the need for in-service inspection. In order to arrive at a cost optimal design, effort should be made to design details such that stress concentrations, including that of fabrication tolerances, are reduced to a minimum. Stresses may also be reduced by increasing the thickness of parent metal or weld metal, which will improve fatigue life.

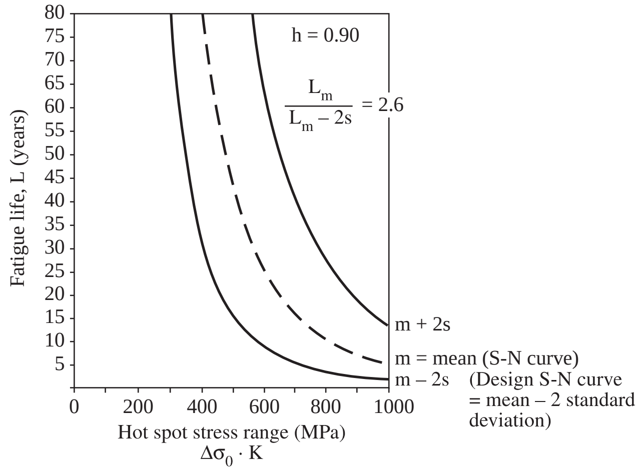

Figure 2.6 Fatigue life influence of stress level and S-N data for welded connections

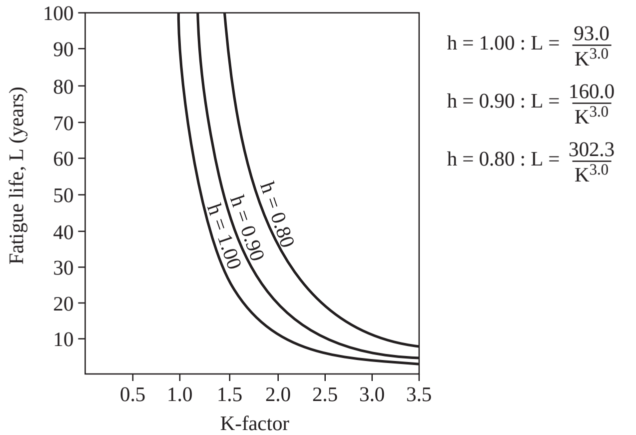

Figure 2.7 Fatigue life sensitivity to stress concentration factor K and Weibull shape factor h

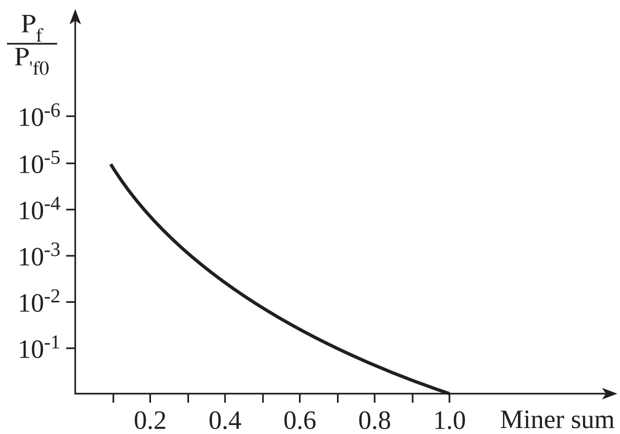

Figure 2.8 Relative probability of failure versus Miner sum. P_{fo} is probability of failure in lifetime for a Miner sum equal 1.0

3. Simplified Stress Analysis

3.1 General

3.1.1

This section outlines a simplified approach to determine the distributions of long-term stress ranges for closed or semi-closed hull cross sections, expressed as Weibull distributions. Simple formats for combination of global and local stress components are given, and alternative models for simplified calculations of stress response in ship structures are given.

3.1.2

Stress response may be calculated by different levels of accuracy:

Calculation of hull girder stresses is the simplest way of getting reasonable approximations to the stress level in longitudinal hull girder elements and connections and can be used for quick evaluation of stress levels in important details.

Dynamic pressure load analysis combined with manual calculation of stiffener bending response is the simplest way for determining the stress response of longitudinal and transverse frames due to external and internal pressure loads. The member end restraints/moments must, however be evaluated with great care in order to arrive at reliable results. A frame analysis is generally more reliable and should be performed if it is uncertainty about used restraints/moments.

Frame Analysis should be applied in order to assess stresses in hull elements like transverse frames, floors and girders. Both 2-D and 3-D models can be used (Section 6.4).

In order to obtain a more precise stress estimation of the response in the hull, Finite Element Analysis should be applied (Section 6).

3.2 Long term distribution of stresses

3.2.1

The long term distribution of stress ranges at local details may be described by Weibull distribution

$$Q(\Delta\sigma) = \exp\left[-\left(\frac{\Delta\sigma}{q}\right)^{h}\right]$$

where:

Q = probability of exceedance of the stress range $\Delta\sigma$

h = Weibull shape parameter

q = Weibull scale parameter, defined as

$$q = \frac{\Delta\sigma_0}{(\ln n_0)^{1/h}}$$

The stress range distribution may also be expressed as

$$\Delta\sigma = \Delta\sigma_0\left[\frac{\ln n}{\ln n_0}\right]^{1/h}$$

where

$\Delta\sigma_o$ = reference stress range value at the local detail exceeded once out of n_o cycles

n_o = total number of cycles associated with the stress range level $\Delta\sigma_o$

When the long term stress range follows a Weibull distribution with shape parameters in the range 0.8 -1.0, the main contribution to the cumulative fatigue damage comes from the smaller waves, see Figure 3.1. The long term stress range should generally be based on a reference stress range $\Delta\sigma_o$ being the highest stress range out of 10^4 stress cycles.

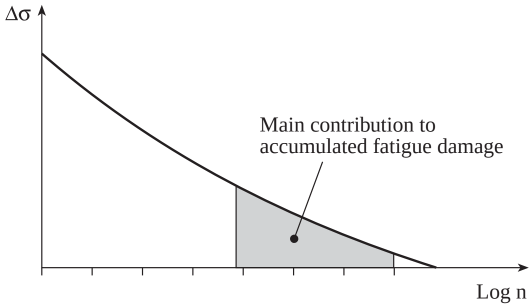

Figure 3.1 Contribution to fatigue damage from different stress blocks

If the highest stress range out of 10^8 stress cycles are used to describe the long-term stress range distributions, the calculated fatigue damage is very sensitive to the estimate of the Weibull shape parameter h.

3.2.2

The Weibull shape parameter may be established from long-term wave load analysis. In lieu of more accurate calculations, the shape parameter may be taken as

$h = h_o$	For deck longitudinals	
$h = h_o + h_a (D - z) / (D - T_{act})$	For ship side above the waterline	$T_{act} < z < D$
$h = h_o + h_a$	For ship side at the waterline	$z = T_{act}$
$h = h_o + h_a z/T_{act} - 0.005(T_{act} - z)$	For ship side below the waterline	$z < T_{act}$
$h = h_o - 0.005\ T_{act}$	For bottom longitudinals	

$h = h_o + h_a$ For longitudinal and transverse bulkheads

where:

h_o = basic shape parameter

= $2.21 - 0.54 \log_{10}(L)$

(In lieu of more accurate calculations h_0 may, for open type vessels, be taken as 1.05 in connection with fatigue assessment of deck structure subjected to dynamic, torsional stresses.)

h_a = additional factor depending on motion response period

= 0.05 in general

= 0.00 for plating subjected to forces related to roll motions for vessels with roll period $T_R > 14$ sec.

z = vertical distance from baseline to considered longitudinal (m)

The above Weibull shape parameters are based on results from the study in [2].

For hopper knuckle connections, the Weibull shape parameter for ship side at the waterline may be used.

3.3 Definition of stress components

3.3.1

Dynamic stress variations are referred to as either *stress range* ($\Delta\sigma$) or *stress amplitude* (σ). For linear responses, the following relation applies

$$\Delta\sigma = 2\sigma$$

3.3.2

The global dynamic stress components (primary stresses) which should be considered in fatigue analysis are

σ_v= wave induced vertical hull girder bending stress

σ_{hg}= wave induced horizontal hull girder bending stress

3.3.3

The local dynamic stress amplitudes which should be considered are defined as follows

σ_e = total local stress amplitude due to dynamic external pressure loads

σ_i = total local stress amplitude due to dynamic internal pressure loads or forces

while the local stress components are defined as

σ_2 = secondary stress amplitude resulting from bending of girder systems

σ_{2A} = stress amplitude produced by bending of stiffeners between girder supports

σ_3 = tertiary stress amplitude produced by bending of un-stiffened plate elements between longitudinals and transverse frames.

See also Figure 3.3

3.4 Combination of stresses

3.4.1

For each loading condition, combined local stress components due to simultaneous internal and external pressure loads are to be combined with global stress components induced by hull girder wave bending. The procedures described in the following is applicable for ships with closed or semi-closed cross sections only. For open type vessels (e.g. container vessels), torsional stresses may have to be included. ref. 9.3.

3.4.2

The stress components to be combined are the notch stresses, i.e. stresses including stress concentration factors, K. The resulting stress concentration factor of a structural detail depends on weld geometry, structural geometry and type of loading.

3.4.3

The combined global and local stress range may be taken as

$$\Delta\sigma_o = f_m \, \Delta\sigma$$

$$\Delta\sigma = f_e \max \begin{cases} \Delta\sigma_g + b \cdot \Delta\sigma_l \\ a \cdot \Delta\sigma_g + \Delta\sigma_l \end{cases}$$

f_e = Reduction factor on derived combined stress range accounting for the long- term sailing routes of the ship considering the average wave climate the vessel will be exposed to during the lifetime. Assuming world wide operation the factor may be taken as 0.8. For shuttle tankers and vessels that frequently operates in the North Atlantic or in other harsh environments, f_e = 1.0 should be used.

f_m = Reduction factor on derived combined stress range accounting for the effect of mean stresses, see Sections 2.2.3 and 2.2.4.

a, b = Load combination factors, accounting for the correlation between the wave induced local and global stress ranges. (The below factors are based on [2]).

a = 0.6

b = 0.6

$\Delta\sigma_l$ = combined local stress range due to lateral pressure loads

$\Delta\sigma_g$ = combined global stress range

3.4.4

The combined global stress range may in general be taken as

$$\Delta\sigma_g = \sqrt{\Delta\sigma_V{}^2 + \Delta\sigma_{hg}{}^2 + 2\rho_{vh}\Delta\sigma_V\Delta\sigma_{hg}}$$

except for ships with large hatch openings (i.e. container carriers and open hatch type bulk carriers) for which torsional stresses must be included, see 9.3.

$\Delta\sigma_V$ = stress range due to wave induced vertical hull girder bending

$\Delta\sigma_{hg}$ = stress range due to wave induced horizontal hull girder bending.

= $2\sigma_h$ in general (for tankers and vessels without large hatch openings)

ρ_{vh} = 0.10, average correlation between vertical and horizontal wave induced bending stress (from [2])

3.4.5

The combined local stress range, $\Delta\sigma_l$, due to external and internal pressure loads may be taken as

$$\Delta\sigma_l = 2\sqrt{\sigma_e^2 + \sigma_i^2 + 2\rho_p\sigma_e\sigma_i}$$

where

σ_e = total local stress amplitude due to the dynamic sea pressure loads (tension = positive)

σ_i = total local stress amplitude due to internal pressure loads (tension = positive)

ρ_p = average correlation between sea pressure loads and internal pressure loads (from [2])

$$= \frac{1}{2} - \frac{z}{10 \cdot T_{act}} + \frac{|x|}{4 \cdot L} + \frac{|y|}{4 \cdot B} - \frac{|x| \cdot z}{5 \cdot L \cdot T_{act}}$$

where: $z \le T_{act}$

For $z > T_{act}$, z may be taken equal to T_{act}

Origo of the coordinate system has co-ordinates (midship, centerline, baseline), see Figure 3.2. x, y and z are longitudinal, transverse and vertical distance from origo to load point of considered structural member.

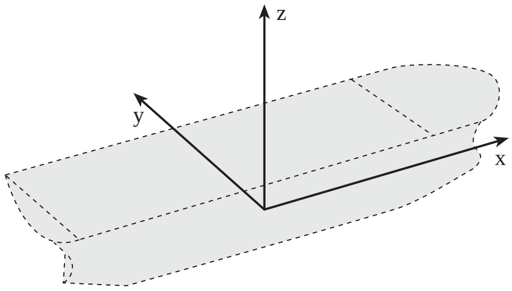

Figure 3.2 Coordinate system

3.4.6

The total local stress amplitudes due to external or internal pressure loads are the sum of individual local stress components as follows (Figure 3.3)

$$\sigma_{e,i} = \sigma_2 + \sigma_{2A} + \sigma_3$$

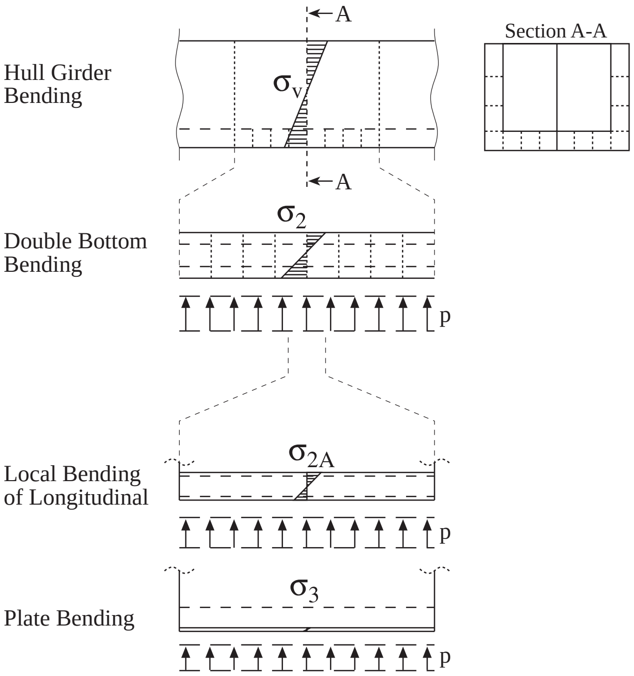

Figure 3.3 Definition of Stress Components

3.5 Calculation of stress components

3.5.1

The wave induced vertical hull girder stress is given by

$$\sigma_v = 0.5\,K\,[M_{wo,h} - M_{wo,s}]\,10^{-3}\,|\,z - n_0\,|/\,I_N$$

where

$M_{wo,s(h)}$	=	vertical wave sagging (hogging) bending moment amplitude
$\vert z - n_0 \vert$	=	vertical distance in m from the horizontal neutral axis of hull cross section to considered member
I_N	=	moment of inertia of hull cross-section in m^4 about transverse axis
K	=	stress concentration factor for considered detail and loading

The corresponding stress range is

$$\Delta\sigma_v = 2\sigma_v$$

3.5.2

The wave induced horizontal hull girder stress is given by

$$\sigma_h = K\, M_H\, 10^{-3}\, |y| / I_C$$

where

M_H	=	horizontal wave bending moment amplitude
y	=	distance in m from vertical neutral axis of hull cross section to member considered
I_C	=	the hull section moment of inertia about the vertical neutral axis
K	=	stress concentration factor for considered detail and loading

The corresponding stress range is

$$\Delta\sigma_{hg} = 2\,\sigma_h$$

3.5.3

Local secondary bending stresses (σ_2) are the results of bending due to lateral pressure of stiffened single skin or double hull cross-stiffened panels between transverse bulkheads, see Figure 3.3. This may be bottom or deck structures, sides or longitudinal bulkheads.

The preferred way of determining secondary stresses is by means of FEM analysis or alternatively by 3(2)-dimensional frame analysis models . When such analysis are not available, secondary stresses may be estimated by the expressions given in Appendix B.

Dynamic secondary bending stresses should be calculated for dynamic sea pressure p_e and for internal dynamic pressure p_i The pressures to be used should generally be determined at the mid-position for each cargo hold or tank.

3.5.4

The local bending stress of stiffeners with effective plate flange between transverse supports (e.g. frames, bulkheads) may be approximated by

$$\sigma_{2A} = K\frac{M}{Z_s} + K\frac{m_\delta EI}{l^2 Z_s}\; r_\delta \cdot \delta$$

where

K	=	stress concentration factor. Note that the stress concentration factor in front of each term may be different. (K_n is to be included in the first term)
M	=	moment at stiffener support adjusted to hot spot position at the stiffener (e.g. at bracket toe) $= \frac{p\,s\,l^2}{12} r_p$
p	=	lateral dynamic pressure
	=	p_e for dynamic sea pressure
	=	p_i for internal dynamic pressure
s	=	stiffener spacing
l	=	effective span of longitudinal/stiffener as shown in Figure 3.4
Z_s	=	section modulus of longitudinal/stiffener with associated effective plate flange. For definition of effective flanges, see 3.5.7
I	=	moment of inertia of longitudinal/stiffener with associated effective plate flange.
m_δ	=	moment factor due to relative deflection between transverse supports. For designs where all the frames obtain the same deflection relative to the transverse bulkhead, e.g. where no stringers or girders supporting the frames adjacent to the bulkhead exist, m_δ may be taken as 4.4 at the bulkhead. At termination of stiff partial stringers or girders, m_δ may be taken as 4.4.

When the different deflections of each frame are known from a frame and girder analysis, m_δ should be calculated due to the actual deflections at the frames by using a beam model or a stress concentration model of the longitudinal. A beam model of a longitudinal covering ½ + ½ cargo hold length is shown in Figure 3.6. Normally, representative m_δ may be calculated for side and bottom, using one load condition, according to

$$m_\delta = \frac{M_\delta l^2}{\delta_i EI}$$

where

M_δ is the calculated bending moment at the bulkhead due to the prescribed deflection at the frames, δ_1, δ_2 … δ_n. δ_i is the relative support deflection of the longitudinal at the nearest frame relative to the transverse bulkhead. The frame where the deflection for each longitudinal in each load condition, δ, is to be taken, should be used.

δ = deformation of the nearest frame relative to the transverse bulkhead (positive inwards - net external pressure).

r_δ r_p = moment interpolation factors for interpolation to hot spot position along the stiffener length, Figure 3.5.

$$r_\delta = 1 - 2\left(\frac{x}{l}\right) \quad ; \quad 0 \le x \le l$$

$$r_p = 6\left(\frac{x}{l}\right)^2 - 6\left(\frac{x}{l}\right) + 1.0 \; ; \quad 0 \le x \le l$$

where

x = distance to hot spot, see Fig.3.5.

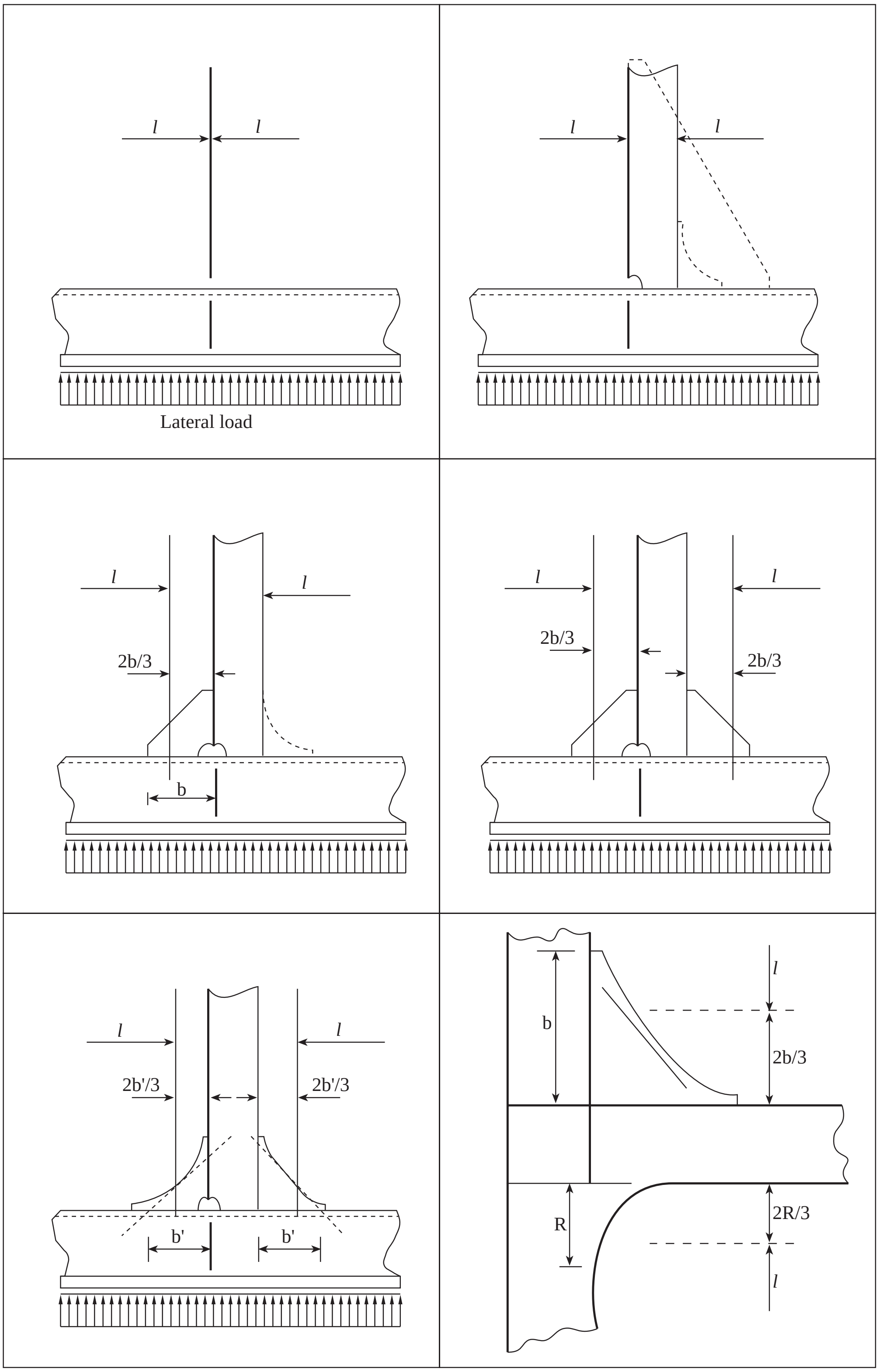

Figure 3.4 Definition of effective span lengths

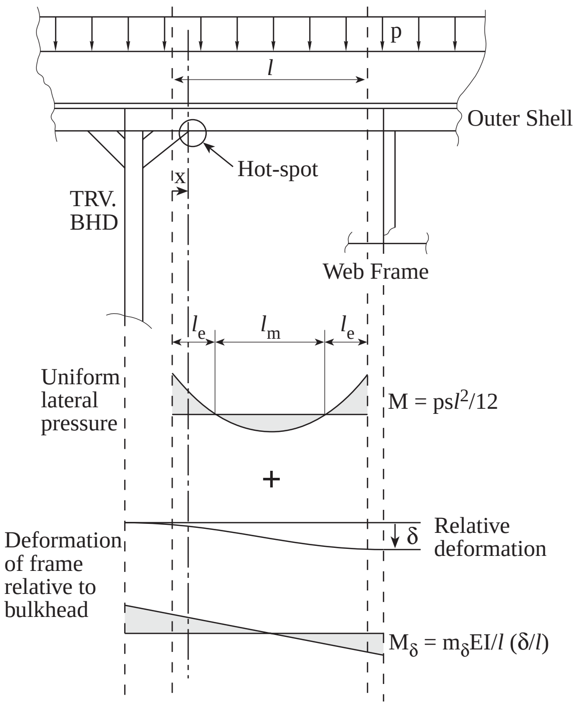

Figure 3.5 Stresses in stiffener

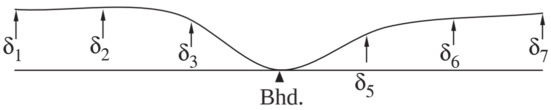

Figure 3.6 Beam element model of longitudinal through 6 frame spacings

3.5.5

It is of great importance for a reliable fatigue assessment that bending stresses in longitudinals caused by relative deformation between supports are not underestimated. The appropriate value of relative deformation δ has to be determined in each particular case, e.g. by beam- or element analyses

(Classification Note Nos. 31.1 and 31.3 show modelling examples).

3.5.6

Longitudinal local tertiary plate bending stress amplitude in the weld at the plate/transverse frame/bulkhead intersection is midway between the longitudinals given by

$$\sigma_3 = 0.343\, p\, (s/t_n)^2\, K$$

where

p = lateral pressure

= p_e for dynamic sea pressure

= p_i for internal dynamic pressure

s = stiffener spacing

t_n = "net" plate thickness

Similarly, the transverse stress amplitude at stiffener mid-length is

$$\sigma_{3T} = 0.50\, p\, (s/t_n)^2\, K$$

3.5.7

Effective breadth of plating can be taken as follows:

Flat and curved plate flanges of web frames and girders is to be taken as given in the Ship Rules[1].

Effective breadth of plate flanges of stiffeners (longitudinals) in bending (due to the shear lag effect) exposed to uniform lateral load can be taken as

For bending at midspan:

$$\frac{s_e}{s} = \begin{cases} \sin\left[\dfrac{\pi}{6}\left(\dfrac{l_m}{s}\right)\right] & ;\ for\ \left(\dfrac{l_m}{s}\right) \le 9 \\ 1.0 & ;\ for\ \left(\dfrac{l_m}{s}\right) \ge 9 \end{cases}$$

For bending at ends:

$$\frac{s_e}{s} = \begin{cases} 0.67\sin\left[\dfrac{\pi}{6}\left(\dfrac{l_e}{s}\right)\right] & ;\ for\ \left(\dfrac{l_e}{s}\right) \le 3 \\ 0.67 & ;\ for\ \left(\dfrac{l_e}{s}\right) \ge 3 \end{cases}$$

where

$l_m = l/\sqrt{3}$	length of stiffener between zero moment inflection points (at midspan - uniformly loaded and clamped stiffener)
$l_e = l\left(1 - 1/\sqrt{3}\right)/2$	length of stiffener at ends, i.e. outside zero moment inflection points

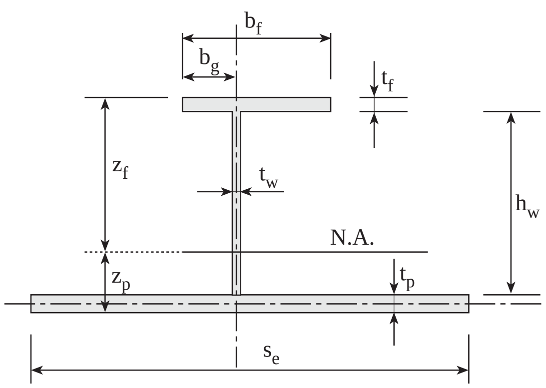

Figure 3.7 Stiffener geometry

4. Simplified Calculation of Loads

4.1 General

4.1.1

This section outlines a simplified approach for calculation of dynamic loads. Formulas are given for calculation of global wave bending moments, external sea pressure acting on the hull and internal pressure acting on the tank boundaries.

The simple formula for calculation of loads in this section are based on the linear dynamic part of the loads as defined in the Rules [1]. The design loads as defined in the Rules do also includes non-linear effects such as bow-flare and roll damping, and are not necessarily identical with the dynamic loads presented herein.

4.1.2

Fatigue damage should in general be calculated for all representative load conditions accounting for the expected operation time in each of the considered conditions. For tankers, bulk carriers and container vessels, it is normally sufficient to consider only ballast- and fully loaded conditions, see also 7.2, 8.2 and 9.2. The loads are calculated using actual draughts, T_{act}, metacentric heights GM_{act} and roll radius of gyration, $k_{r,act}$ for each considered loading condition.

4.2 Wave induced hull girder bending moments

4.2.1

The vertical wave induced bending moments may be calculated using the bending moment amplitudes specified in the Rules Pt. 3, Ch.1[1].

The moments, at 10^{-4} probability level of exceedance, may be taken as

$$M_{wo,s} = -0.11 f_r\, k_{wm}\, C_w\, L^2\, B\, (C_B + 0.7) \quad \text{(kNm)}$$

$$M_{wo,h} = 0.19 f_r\, k_{wm}\, C_w\, L^2\, B\, C_B \quad \text{(kNm)}$$

where

$M_{wo,s}$ = wave sagging moment amplitude

$M_{wo,h}$ = wave hogging moment amplitude

C_w = wave coefficient

=	$0.0792L$	$L < 100$ m
=	$10.75 - [(300-L)/100]^{3/2}$	100 m $<L<$ 300 m
=	10.75	300 m $<L<$ 350 m
=	$10.75 - [(L-350)/150]^{3/2}$	350 m $< L$

k_{wm} = moment distribution factor

= 1.0 between 0.40L and 0.65L from A.P., for ships with low/moderate speed.

= 0.0 at A.P. and F.P. (Linear interpolation between these values.)

f_r = factor to transform the load from 10^{-8} to 10^{-4} probability level.

= $0.5^{1/h_o}$

h_o = long-term Weibull shape parameter

= $2.21 - 0.54 \log(L)$

L = Rule length of ship (m)

B = Greatest moulded breath of ship in meters measured at the summer waterline

C_B = Block coefficient

For the purpose of calculating the vertical hull girder bending moment by direct global finite element analyses, simplified loads may be obtained from Appendix C.

4.2.2

The horizontal wave bending moment amplitude at 10^{-4} probability level may be taken as follows (ref. Rules Pt.3, Ch.1 [1])

$$M_H = 0.22 f_r\, L^{9/4}\, (T_{act} + 0.30\, B)\, C_B\, (1-\cos(2\pi x/L)) \quad \text{(kNm)}$$

x = distance in m from A.P. to section considered.

L, B, C_B, f_r, as defined in 4.2.1

4.2.3

Wave torsional loads and moments which may be required for analyses of open type vessels (e.g. container vessels) are defined in 9.3 and Appendix C.

4.3 External pressure loads

4.3.1

Due to intermittent wet and dry surfaces, the range of the pressure is reduced above $T_{act}-z_{wl}$, see Figure 4.1. The dynamic external pressure amplitude (half pressure range) , p_e, related to the draught of the load condition considered, may be taken as:

$$p_e = r_p\, p_d \quad \text{(kN/m}^2\text{)}$$

where ;

p_d = dynamic pressure amplitude below the waterline.

The dynamic pressure amplitude may be taken as the largest of the combined pressure dominated by pitch motion in head/quartering seas, p_{dp}, or the combined pressure dominated by roll motion in beam/quartering seas, p_{dr}, as:

$$p_d = \max \begin{cases} p_{dp} = p_l + 135\dfrac{|\bar{y}|}{B+75} - 1.2(T_{act} - z_w) \\ p_{dr} = 10\left[|y|\dfrac{\phi}{2} + C_B\dfrac{|y|+k_f}{16}\left(0.7 + 2\dfrac{z_w}{T_{act}}\right)\right] \end{cases} \quad (\mathrm{kN/m^2})$$

where

$$p_l = k_s C_W + k_f$$

$$= (k_s C_W + k_f)\left(0.8 + 0.15\frac{V}{\sqrt{L}}\right) \quad \text{if} \quad \frac{V}{\sqrt{L}} > 1.5$$

k_s = $3C_B + \dfrac{2.5}{\sqrt{C_B}}$ at AP and aft.

= $3C_B$ between 0.2 L and 0.7 L from AP.

= $3C_B + \dfrac{4.0}{C_B}$ at FP and forward.

Between specified areas k_s is to be varied linearly.

z_w = vertical distance from the baseline to the loadpoint

= maximum T_{act} (m).

y = horizontal distance from the centre line to the loadpoint

$\bar{y}$ = y, but minimum B/4 (m).

C_W = as given in 4.2.1

k_f = the smallest of T_{act} and f

f = vertical distance from the waterline to the top of the ship's side at transverse section considered (m)

= maximum $0.8 \cdot C_W$ (m).

L = ship length

ϕ = rolling angle, single amplitude(rad) as defined in 4.5.1

V = vessels design speed in knots

r_p = reduction of pressure amplitude in the surface zone

= 1.0 for $z < T_{act} - z_{wl}$

= $\dfrac{T_{act} + z_{wl} - z}{2z_{wl}}$ for $T_{act} - z_{wl} < z < T_{act} + z_{wl}$

= 0.0 for $T_{act} + z_{wl} < z$

z_{wl} = distance in m measured from actual water line. In the area of side shell above $z = T_{act} + z_{wl}$ it is assumed that the external sea pressure will not contribute to fatigue damage.

= $\dfrac{3}{4}\dfrac{p_{dT}}{\rho g}$

p_{dT} = p_d at $z = T_{act}$

T_{ac} = the draught in m of the considered load condition

ρ = density of sea water = 1.025 (t / m³).

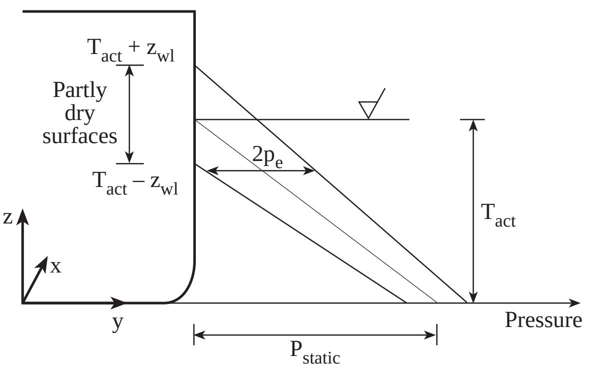

Figure 4.1 Reduced pressure ranges in the surface region

4.4 Internal pressure loads due to ship motions

4.4.1

The dynamic pressure from liquid cargo or ballast water should be calculated based on the combined accelerations related to a fixed co-ordinate system. The gravity components due to the motions of the vessel should be included. The dynamic internal pressure amplitude, p_i in kN/m², may be taken as the maximum pressure due to acceleration of the internal mass:

$$p_i = f_a \max \begin{cases} p_1 = \rho\, a_v\, h_s \\ p_2 = \rho\, a_t\, |y_s| \\ p_3 = \rho\, a_l\, |x_s| \end{cases} \quad (\mathrm{kN/m^2})$$

where;

p_1 = pressure due to vertical acceleration (largest pressure in lower tank region)

p_2 = pressure due to transverse acceleration

p_3 = pressure due to longitudinal acceleration

ρ = density of sea water, 1.025 (t/m³)

x_s = longitudinal distance from centre of free surface of liquid in tank to pressure point considered (m)

y_s = transverse distance from centre of free surface of liquid in tank to the pressure point considered (m), see Figure 4.5.

h_s = vertical distance from point considered to surface inside the tank (m), Figure 4.5

a_v, a_t and a_l = accelerations in vertical-, transverse-, or longitudinal direction (m/s^2)

f_a = factor to transform the load effect to probability level 10^{-4} , when the accelerations are specified at the 10^{-8} probability level.

= $0.5^{1/h}$

h = $h_0 + 0.05$

= $2.26 - 0.54 \log_{10}(L)$,

Note that the factor f_a is estimated for ships with a roll period $T_R < 14$ sec., and may otherwise be less for roll induced pressures and forces, see also Section 3.2.2

The accelerations a_v, a_t and a_l are given in Section 4.5.

The effect of ullage (void space in top of tank) will add to the pressure in one half cycle and subtract in the other, and is therefore omitted in the above description of the half pressure range. Similarly, the effect of the tank top geometry may be omitted. For partly subdivided tanks, where the fluid is prevented to flow through swash bulkheads during one half motion cycle, the pressures may be reduced accordingly.

Note that the above scaling of pressures, by use of the factor f_a, is only valid for fatigue assessment and may be justified as the dominating fatigue damage is caused mainly by moderate wave heights.

For bulk and ore cargoes, only p_1 need to be considered. The appropriate density and pressure height should be specially considered.

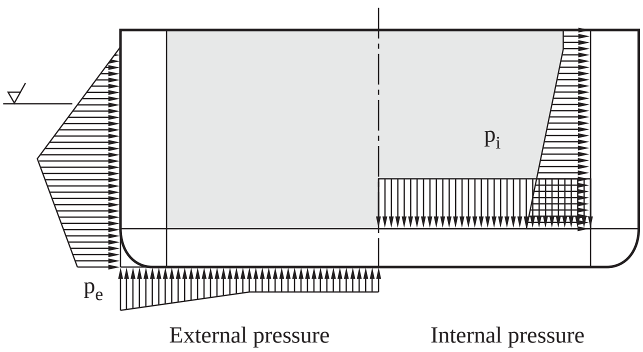

Figure 4.2 Distribution of pressure amplitudes for tankers in the fully loaded condition.

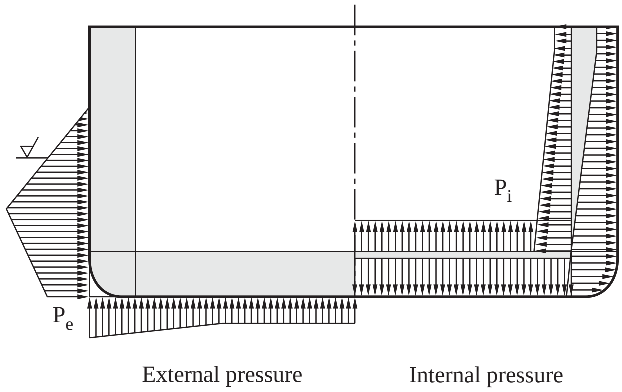

Figure 4.3 Distribution of pressure amplitudes for tankers in ballast condition

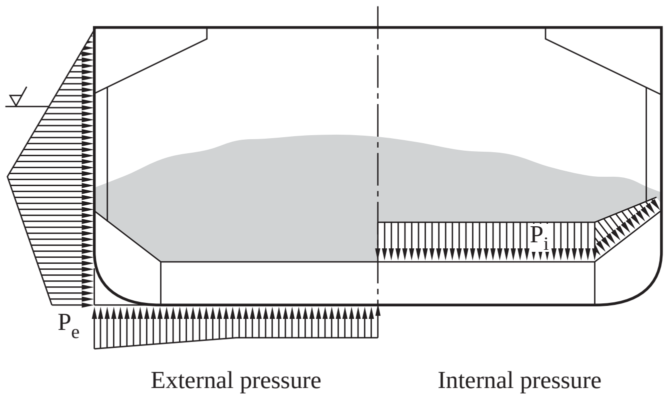

Figure 4.4 Distribution of pressure amplitudes for a bulk carrier in the ore loading condition.

4.5 Ship accelerations and motions

4.5.1

The formula for ship accelerations and motions given below are derived from the Rules, Ch.1. ,Pt.3, Sec.4, [1]. The acceleration and motions are extreme values corresponding to a probability of occurrence of 10^{-8}.

Combined accelerations :

a_t = combined transverse acceleration (m/s^2)

$$a_t = \sqrt{a_y^2 + \left(g_0 \sin\phi + a_{ry}\right)^2}$$

a_l = combined longitudinal acceleration (m/s^2)

$$a_l = \sqrt{a_x^2 + \left(g_0 \sin\theta + a_{px}\right)^2}$$

a_v = combined vertical acceleration (m/s^2)

$$a_v = max\begin{cases}\sqrt{a_{rz}^2 + a_z^2}\\ \sqrt{a_{pz}^2 + a_z^2}\end{cases}$$

Acceleration components :

a_x = surge acceleration (m/s^2)
= $0.2\ g\ a_o \sqrt{C_B}$

a_y = acceleration due to sway and yaw (m/s^2)
= $0.3\ g\ a_o$

a_z = heave acceleration (m/s^2)
= $0.7\ g\ a_o / \sqrt{C_B}$

a_o = acceleration constant
= $3C_w/L + C_V\ V/\sqrt{L}$

C_V = $\sqrt{L}/50$, max. 0.2

V = ship design speed (knots).

Roll motions:

a_{ry} = horizontal component of roll acceleration (m/s^2)
= $\phi\ (2\pi / T_R)^2\ R_{RZ}$

a_{rz} = vertical component of roll acceleration (m/s^2)
= $\phi\ (2\pi / T_R)^2\ R_{RY}$

R_R = distance from the axis of rotation to centre of mass (m).

The distance is related to the roll axis of rotation that may be taken at z_r (m) above the baseline, where z_r is the smaller of [D / 4 + T / 2] and [D / 2].

For double hull ballast tanks the R_R may be approximated by the horizontal distance from the centreline to the tank surface centre.

R_{RZ} = vertical distance from axis of rotation to centre of tank/mass (m)

R_{RY} = transverse distance from axis of rotation to centre of tank/mass (m)

T_R = period of roll
= $2\ k_r / \sqrt{GM}$, maximum 30 (s)

In case the values of roll radius, k_r, and metacentric height, GM, have not been calculated for the relevant loading conditions, the following approximate values may be used:

k_r = roll radius of gyration (m), k_r in the main rules Pt.3 ch.1 sec.17 shall be used unless the calculated value of k_r is available
= 0.39 B for ships with even distribution of mass and double hull tankers in ballast.
= 0.35 B for single skin tankers in ballast.
= 0.25 B for ships loaded with ore between longitudinal bulkheads.

GM = metacentric height (m)
= 0.07 B in general
= 0.12 B for single skin tankers, bulk carriers and fully loaded double hull tankers.
= 0.17 B for bulk and ore carriers in the ore loading condition.
= 0.33 B for double hull tankers in the ballast loading condition.
= 0.25 B for bulk carriers in the ballast condition
= 0.04 B for container carriers

ϕ = maximum roll angle, single amplitude (rad)
= $50\ c / (B + 75)$

c = $(1.25 - 0.025\ T_R)\ k$

k = 1.2 for ships without bilge keel
= 1.0 for ships with bilge keel
= 0.8 for ships with active roll damping facilities

Pitch motions:

a_p = tangential pitch acceleration (m/s^2)
= $\theta\ (2\pi / T_P)^2\ R_P$

a_{px} = longitudinal component of pitch acceleration (m/s^2)
= $\theta\ (2\pi / T_P)^2\ R_{PZ}$

a_{pz} = vertical component of pitch acceleration (m/s^2)
= $\theta\ (2\pi / T_P)^2\ R_{PX}$

R_P = distance from the axis of rotation to the tank centre (m)

R_{PZ} = vertical distance from axis of rotation to centre of tank/mass (m)

R_{PX} = longitudinal distance from axis of rotation to centre of tank/mass (m)

T_P = period of pitch (s)
= $1.80 \sqrt{L / g}$

θ = maximum pitch angle (rad)
= $0.25\ a_o / C_B$

Axis of rotation may be taken as 0.45L from A.P., at centreline, z_r above baseline.

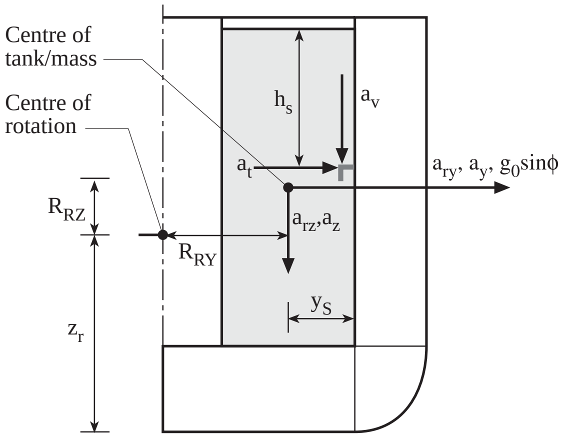

Figure 4.5 Illustration of acceleration components

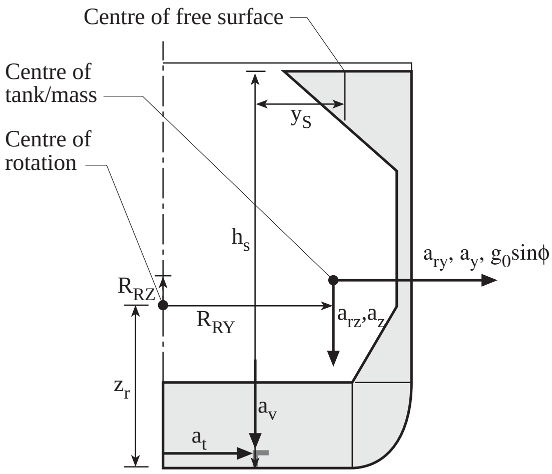

Figure 4.6 Illustration of acceleration components and centre of mass for double hull tankers or bulk carriers with connected top wing- and hopper/bottom ballast tanks

5. Wave Loading by Direct Computation

5.1 General

5.1.1

This section gives a brief description of the necessary steps in a direct load analysis for fatigue assessment. The loads computed by direct computations may substitute the simplified load components defined in Section 4 and is mainly intended for use in combination with finite element analysis.

5.1.2

A linear modelling of the ship response is in general sufficient for fatigue assessment purposes. The response is then described by a superposition of the response of all regular wave components that make up the irregular sea, leading to a frequency domain analysis. The resulting stress may be established as a summation over all contributing dynamic loads/load effects.

The linear frequency domain results should normally be applied without any corrections for large wave effects as most of the fatigue damage is related to moderate wave heights.

5.1.3

Transfer function values must be determined for a sufficient number of frequencies (>15) and headings (≥ 8, or ≥ 5 when considering symmetry). The length of the model should at least extend over Lpp. The mass model should reflect the steel weight distribution and the distribution of cargo both in vertical, longitudinal and transverse directions.

The fatigue damage should be calculated so that the effects of all the main load conditions are accounted for. For tankers, the ballast condition and fully loaded condition are normally sufficient. A vessel speed set to 2/3 of the service speed in full load and ballast condition should be applied in the modelling.

For load effects which are unsymmetrical with respect to the ship’s centreline (e.g. torsion induced stresses of container ships), the fatigue damage must be determined for both ship halves. The fatigue damage of any members due to un-symmetrical load effect may then be determined as the mean value of fatigue damages calculated for port and starboard side members.

5.1.4

In the evaluation of the ship response due to external wave induced loading, the effect of wave diffraction and radiation should be accounted for.

5.2 The long-term distribution

5.2.1

The long-term distribution of load responses for fatigue analyses may be estimated using the wave climate, represented by the distribution of Hs and Tz, as described in Table 5.1, representing the North Atlantic (Marsden squares 8, 9 and 15, [1]), or Table 5.2 for world wide operation. As a guidance to the choice between these data sets one should consider the average wave environment the vessel is expected to encounter during its design life. The world wide sailing routes will therefore normally apply. For shuttle tankers and vessels that will sail frequently on the North Atlantic, or in other harsh environments, the wave data given in Table 5.1 should be applied, if not otherwise specified.

The scatter diagrams are equal for all wave directions and specified at class midpoint values.

TZ(s) / Hs (m)	3.5	4.5	5.5	6.5	7.5	8.5	9.5	10.5	11.5	12.5	13.5	14.5	15.5	16.5	17.5	Sum
1.0	0	72	1416	4594	4937	2590	839	195	36	5	1	0	0	0	0	14685
2.0	0	5	356	3299	8001	8022	4393	1571	414	87	16	3	0	0	0	26167
3.0	0	0	62	1084	4428	6920	5567	2791	993	274	63	12	2	0	0	22196
4.0	0	0	12	318	1898	4126	4440	2889	1301	445	124	30	6	1	0	15590
5.0	0	0	2	89	721	2039	2772	2225	1212	494	162	45	11	2	1	9775
6.0	0	0	1	25	254	896	1482	1418	907	428	160	50	14	3	1	5639
7.0	0	0	0	7	85	363	709	791	580	311	131	46	14	4	1	3042
8.0	0	0	0	2	27	138	312	398	330	197	92	35	12	3	1	1547
9.0	0	0	0	1	8	50	128	184	171	113	58	24	9	3	1	750
10.0	0	0	0	0	3	17	50	80	82	59	33	15	6	2	1	348
11.0	0	0	0	0	1	6	18	33	37	29	17	8	3	1	0	153
12.0	0	0	0	0	0	2	7	13	15	13	8	4	2	1	0	65
13.0	0	0	0	0	0	1	2	5	6	6	4	2	1	0	0	27
14.0	0	0	0	0	0	0	1	2	2	2	2	1	1	0	0	11
15.0	0	0	0	0	0	0	0	1	1	1	1	0	0	0	0	4
16.0	0	0	0	0	0	0	0	0	0	1	0	0	0	0	0	1
Sum	0	77	1849	9419	20363	25170	20720	12596	6087	2465	872	275	81	20	6	100000

Table 5.1 Scatter diagram for the North Atlantic

TZ(s) / Hs (m)	3.5	4.5	5.5	6.5	7.5	8.5	9.5	10.5	11.5	12.5	13.5	14.5	15.5	16.5	17.5	Sum
1.0	311	2734	6402	7132	5071	2711	1202	470	169	57	19	6	2	1	0	26287
2.0	20	764	4453	8841	9045	6020	3000	1225	435	140	42	12	3	1	0	34001
3.0	0	57	902	3474	5549	4973	3004	1377	518	169	50	14	4	1	0	20092
4.0	0	4	150	1007	2401	2881	2156	1154	485	171	53	15	4	1	0	10482
5.0	0	0	25	258	859	1338	1230	776	372	146	49	15	4	1	0	5073
6.0	0	0	4	63	277	540	597	440	240	105	39	13	4	1	0	2323
7.0	0	0	1	15	84	198	258	219	136	66	27	10	3	1	0	1018
8.0	0	0	0	4	25	69	103	99	69	37	17	6	2	1	0	432
9.0	0	0	0	1	7	23	39	42	32	19	9	4	1	1	0	178
10.0	0	0	0	0	2	7	14	16	14	9	5	2	1	0	0	70
11.0	0	0	0	0	1	2	5	6	6	4	2	1	1	0	0	28
12.0	0	0	0	0	0	1	2	2	2	2	1	1	0	0	0	11
13.0	0	0	0	0	0	0	1	1	1	1	0	0	0	0	0	4
14.0	0	0	0	0	0	0	0	0	1	0	0	0	0	0	0	1
Sum	331	3559	11937	20795	23321	18763	11611	5827	2480	926	313	99	29	9	0	100000

Table 5.2 Scatter diagram for the World Wide trade

5.2.2

The environmental wave spectrum for the different sea states can be defined applying the Pierson Moskowitz wave spectrum,

$$S_\eta(\omega|H_s,T_z) = \frac{H_s^2}{4\pi}\left(\frac{2\pi}{T_z}\right)^4 \omega^{-5} \exp\left(-\frac{1}{\pi}\left(\frac{2\pi}{T_z}\right)^4 \omega^{-4}\right), \qquad \omega > 0$$

5.2.3

The response spectrum of the ship based on the linear model is directly given by the wave spectrum, when the relation between unit wave height and stresses, the transferfunction $H_\sigma(\omega|\theta)$, is established as

$$S_\sigma(\omega|H_s,T_z,\theta) = \left|H_\sigma(\omega|\theta)\right|^2 \cdot S_\eta(\omega|H_s,T_z)$$

5.2.4

The spectral moments of order *n* of the response process for a given heading may described as

$$m_n = \int_{\omega} \omega^n \cdot S_\sigma(\omega \mid H_s, T_z, \theta) d\omega$$

The spectral moments may include wave spreading as :

$$m_n = \int_{\omega} \sum_{\theta-90^o}^{\theta+90^o} f_s(\theta) \omega^n \cdot S_\sigma(\omega \mid H_s, T_z, \theta) d\omega$$

using a spreading function $f(\theta) = k\cos^n(\theta)$, where k is selected such that $\sum_{\theta-90^o}^{\theta+90^o} f(\theta) = 1$,
and normally applying n=2.

5.2.5

The stress range response for ship structures can be assumed to be Rayleigh distributed within each short term condition. The stress range distribution for a given sea state *i* and heading direction *j* is then,

$$F_{\Delta\sigma ij}(\sigma) = 1 - \exp\left(-\frac{\sigma^2}{8m_{0ij}}\right)$$

where m_0 is the spectral moment of order zero.

5.2.6

In order to establish the long-term distribution of stress ranges, the cumulative distribution may be estimated by a weighted sum over all sea states and heading directions. The long-term stress range distribution is then calculated from,

$$F_{\Delta\sigma}(\sigma) = \sum_{\substack{i=1 \\ j=1}}^{\substack{\text{all seastates} \\ \text{all headings}}} r_{ij} \cdot F_{\Delta\sigma ij}(\sigma) \cdot p_{ij}$$

where:

p_{ij}	is the probability of occurrence of a given sea state i combined with heading j
$r_{ij} = \frac{\nu_{ij}}{\nu_0}$	is the ratio between the response crossing rates in a given sea state and the average crossing rate.
$\nu_0 = \sum p_{ij} \cdot \nu_{ij}$	is the average crossing rate.
$\nu_{ij} = \frac{1}{2\pi}\sqrt{\frac{m_{2ij}}{m_{0ij}}}$	is the response zero-crossing rate in sea state i and heading j.

5.2.7

In derivation of the accumulated fatigue damage, the estimated long-term stress range distribution can be applied. A Weibull distribution is found to describe the long-term stress range distribution well, having shape parameter h and scale parameters q. The fitting of the Weibull distribution to the sum of Rayleigh distributions in 5.2.6 should preferably be based on a least square technique for a number of stress ranges σ. The Weibull distribution is described as:

$$F_{\Delta\sigma}(\sigma) = 1 - \exp\left(-\left(\frac{\sigma}{q}\right)^h\right)$$

As a guidance to define the Weibull distribution parameters, the stress levels corresponding to a cumulative probability of 95% and 99% will approximately divide the fatigue damage in three equal part-damages, indicating the most important range of the response distribution.

The parameters q and h of the fitted long-term Weibull distribution is applied in the calculation of the accumulated fatigue damage, see Section 2.1.2.

5.2.8

As an alternative to derive the accumulated fatigue damage based on the fitted long-term Weibull distribution, a summation of the fatigue damage within each sea-state and heading direction can be applied, where the stress range distribution within each short-term condition is Rayleigh distributed, see Section 2.1.3.

5.3 Transfer functions

5.3.1

The transfer function (frequency response function) H(ω,θ), representing the response to a sinusoidal wave with unit amplitude for different frequencies ω and wave heading directions θ, can be obtained applying linear potential theory and the equation of motions of the ship, (see 5.1.4 above).

5.3.2

The vertical bending moment may be estimated by making a hydrodynamic model of a vessel including mass distribution data and by running a wave load program that determines the response for a set of wave frequencies and heading directions. The vertical bending moment transfer function is computed as the vertical bending moment $M_v(\omega,\theta)$ per unit wave amplitude (H/2).

$$H_v(\omega \mid \theta) = \frac{M_v(\omega \mid \theta)}{H / 2}$$

5.3.3

The horizontal bending moment transfer function, $H_h(\omega,\theta)$, is to be determined similarly to the vertical bending moment transfer function with consistent phase relations.

5.3.4

The external pressures are to be determined similarly to the vertical bending moment with consistent phase relations. In the waterline region, a reduction of the pressure range apply due to intermittent wet or dry surfaces [3].

5.3.5

The internal tank pressures may be obtained by combining the accelerations described in Section 4.5, substituting the given acceleration estimates with those obtained from computations with combined transfer functions for motions and accelerations relative to the ship axis system. The largest pressure induced by vertical, horizontal and longitudinal acceleration should be applied in determining the pressure amplitude.

5.3.6

A consistent representation of phase and amplitude for the transfer functions are required in order to achieve a correct modelling of the combined local stress response.

5.4 Combination of transfer functions

5.4.1

The combined stress response may be determined by a linear complex summation of stress transfer functions.The combined local stress transfer functions may be found by combining the complex response transfer function for the loading as

$$H_\sigma(\omega|\theta)=A_1H_v(\omega|\theta)+A_2H_h(\omega|\theta)+A_3H_t(\omega|\theta)$$

$$+A_4H_p(\omega|\theta)+A_5H_c(\omega|\theta)$$

where:

A_1	=	stress per unit vertical bending moment
A_2	=	stress per unit horizontal bending moment
A_3	=	stress per unit torsional bending moment
A_4	=	stress per unit relative lateral external pressure load
A_5	=	stress per unit relative lateral internal pressure load
$H_\sigma(\omega\| \theta)$		transfer function for combined local stress.
$H_v(\omega\| \theta)$		transfer function for vertical bending moment at a representative section.
$H_h(\omega\| \theta)$		transfer function for horizontal bending moment.
$H_t(\omega\| \theta)$		transfer function for torsional bending moment. Only relevant for vessels with large hatch openings in the deck.
$H_p(\omega\| \theta)$		transfer function for external pressure in centre of the considered panel.
$H_c(\omega\| \theta)$		transfer function for liquid cargo pressure in centre of the considered panel

A_k is the local stress response in the considered detail due to a unit sectional load for load component k. The factors A_k may be determined by FEM analyses or alternatively by a simplified method as described in Chapter 3, replacing the described loads by unit loads. Note that it is important to ensure compatibility between the reference (co-ordinate) systems used in the load model and the stress analysis model.

5.4.2

When the stress analysis extends over several hull sections it may be necessary to select load transfer functions for specific points or sections in order to determine the factors describing the stress per unit load, A_k, in 5.4.1.

As a further simplification the factors A_k may be determined for one specific wave heading and/or wave frequency and assumed constant for all other headings/frequencies.

When the hull pressure distribution is determined from a wave loading program, the factors A_k may be determined by adding unit sectional loads at the considered sections, to determine the effect of each individual load component.

5.4.3

In the waterline the stress range is equal to the pressure amplitude, as negative pressures may not occur (intermittent wet and dry surfaces). The effective stress range for longitudinals in the waterline region may be estimated using the reduction factor, r_p, as described in 4.3.1. Alternatively, the stress range distribution may be determined from the pressure ranges by integration of pressures in each wave height (or sea state) in the long-term environmental distribution,[3].

5.4.4

Non-linear effects due to large amplitude motions and large waves can be neglected in the fatigue assessment analysis since the stress ranges at lower load levels (intermediate wave amplitudes) contribute relatively more to the cumulative fatigue damage. In cases where linearization is required, e.g. in order to determine the roll damping, it is recommended that the linearization is performed at a load level representative for the stress ranges that contribute most to fatigue damage. I.e. stresses at probability level of exceedance between 10^{-2} to 10^{-4} .

5.5 Design wave approach

5.5.1

As a simplification to the frequency domain analysis in Sections 5.2 and 5.3, a design wave approach may be applied. In this simplified approach, the extreme load response effect over a specified number of load cycles, e.g. $n_o = 10^4$, is determined. The resulting stress range, $\Delta\sigma$, is then representative for the stress at probability level of exceedance of 10^{-4} per cycle.

The derived extreme stress response is combined with an assumed Weibull shape parameter h to define the long-term stress range distribution. The Weibull shape parameter for the stress response can be determined from the long-term distribution of the dominating load according to the procedure described in 5.2.7. Alternatively, the Weibull shape parameters specified in 3.2.2 may be applied, if a long-term load response analysis is not available.

The design wave may be chosen according to the following procedure:

1) The linear wave load corresponding to a $1/n_o$ probability level per cycle, e.g. midship bending moment, is determined by a long-term distribution with all headings included.
2) The maximum value of the transfer function is chosen for the worst heading and frequency for the wave load of interest.
3) The equivalent wave amplitude is determined by dividing the wave load corresponding to a $1/n_o$ probability level per cycle with the transfer function value from 2)
4) The wave steepness is checked such that it does not in any case exceed 1/7.
   For blunt (not peaked) transfer functions the wave steepness should normally not be taken less than 1/10. If the wave steepness is too high, the wave frequency in 2) is lowered somewhat and the procedure is repeated. This may sometimes be necessary for blunt transfer functions.
5) With the determined wave amplitude, frequency and heading the stress range during one wave cycle is determined by combining the resulting stresses from the real and imaginary components of the local stress or by time-stepping the wave through one wave cycle.
6) The total stress range due to hull girder bending and due to plate and/or stiffener bending associated with local pressure loads, is determined by combining the sums of the resulting real and imaginary component notch stress. Alternatively, the stress range may be obtained by time stepping the wave through one wave cycle, while determining the combined hull girder and local stress for each time step.

Note: In the waterline region, the negative sea pressure load should never be taken larger than the static pressure at the location considered.

5.5.2

The selection of wave height and wave periods should in general aim at determining the load response effect at a $1/n_o$ probability level of exceedance per cycle. This may also be determined by choosing the $1/n_o$ combination of wave height and period that gives the most sincere load response effect.

5.6 Stress component based stochastic analysis

5.6.1

For longitudinal elements in the cargo area a stress component based stochastic fatigue evaluation procedure may be employed. The load transfer functions calculated by the wave load program are then to be transferred to stress transfer functions. The load transfer functions normally include:

- Global vertical hull girder bending moments and shear forces
- Global horizontal bending moment
- Vessel motions in six d.o.f.
- Pressures for all panels of the 3-D diffraction model

The stress transfer functions are combined to a total stress transfer function as described in Section 5.4 and a stochastic fatigue evaluation is performed. Hence, the simultaneous occurrence of the different load effects is preserved.

The stress response factors A_k may in an initial phase be based on simplified formulas. After the global and local FE analyses have been carried out the stress factors A_k are to be updated and the fatigue evaluation repeated. The factors A_k are to include all relevant stress concentration factors either as tabulated values found in Chapter 10 or as the results of detailed FE stress concentration analyses using very fine mesh stress concentration models as described in Section 6.6.

5.6.2

The stochastic fatigue evaluation may be performed by calculating the part fatigue damage for each cell in the wave scatter diagram based on the applied wave spectrum, wave spreading function, ship heading and S/N data etc. The total damage is then a sum of all the part fatigue damages.

5.6.3

Alternatively, an equivalent long term stress distribution may be calculated from the applied wave spectrum and wave spreading function using a summation over each wave period/ship heading for each cell in the wave scatter diagram. In this way the Weibul parameter for the equivalent long term stress distribution can be determined and used for the fatigue damage calculation.

5.7 Full stochastic analyses

5.7.1

A local stress concentration model is used for the analysis. For these details mesh size is to be in the order of the plate thickness. Hence, all load effects, global and local, are taken care of in addition to the geometric stress concentration. 8-noded shell or 20-noded solid elements are used for this purpose. Typical details selected for the fully stochastic analyses are; discontinuous panel knuckles, bracket terminations of the main girder system and stiffeners subjected to large relative deflections. These are typical fatigue prone areas.

5.7.2

The global FE analysis is run for all wave load cases, i.e. 12 headings and 20-25 wave periods per heading, amounting to 240-300 load cases for each basic loading condition and ship speed. For each load case the deformations of the global FE model are automatically transferred to the local FE model as boundary displacements. In addition the local internal and external hydrodynamic pressures need to be automatically transferred to the local FE model by the wave load program. The part fatigue damage from each cell in the wave scatter diagram is then to be calculated based on the principal stresses from the local FE model extrapolated to the hotspot, the wave spectrum, wave spreading function, S/N data etc.

6. Finite Element Analysis

6.1 Finite element models

6.1.1

The main aim of applying a finite element model in the fatigue analysis is to obtain a more accurate assessment of the stress response in the hull structure. Several types or levels of Finite Element models are to be used in the analyses. Most commonly, five levels of finite element models are referred to:

1) *Global stiffness model*. A relatively coarse mesh is to be used to represent the overall stiffness and global stress distribution of the primary members of the hull. Typical models are shown in Figures 6.2-3.
2) *Cargo hold model*. The model is used to analyse the deformation response and nominal stresses of the primary members of the midship area. The model will normally cover ½+1+½ cargo hold length in the midship region. Typical models are shown in Figures 6.4-5.
3) *Frame and girder models* are to be used to analyse stresses in the main framing/girder system. The element mesh is to be fine enough to describe stress increase in critical areas (such as bracket with continuos flange). Typical models are:
   - Web frame at mid-tank and at the transverse bulkhead in the midship area and in the forebody, Fig. 6.6a.
   - Transverse bulkhead stringers with longitudinal connection, Fig. 6.6b.
   - Longitudinal double bottom girders and side stringers.
4) *Local structure models* are used to analyse stresses in stiffeners subjected to large relative deformation. Areas which normally are considered are:
   - Side, bottom and inner bottom longitudinals at the intersection to transverse bulkheads, Fig. 6.7.
   - Vertical stiffeners at transverse bulkhead, Fig. 6.7.
   - Horizontal longitudinals on longitudinal bulkheads at the connection to horizontal stringer levels at the transverse bulkheads, Fig. 6.6b.
5) *Stress concentration models* are used for fully stochastic fatigue analyses and for simplified fatigue analyses for details were the geometrical stress concentration is unknown. Typical details to be considered are:
   - Discontinuous panel knuckles, Fig. 6.8.
   - Bracket and flange termination's of main girder system.

6.1.2

All FE models are to be based on *reduced scantlings*, i.e. corrosion additions t_k, are to be deducted as given in the Rules [1].

6.1.3

Effects from all stress raisers that are not implicitly included in fatigue test data and corresponding S-N curves must be taken into account in the stress analysis. In order to correctly determine the stresses to be used in fatigue analyses, it is important to note the definition of the different stress categories:

– Nominal stresses are those derived from beam element models, 6.4, or from coarse mesh FEM models of type 2 and type 3 as defined above. Stress concentrations resulting from the gross shape of the structure, e.g. shear lag effects, are included in the nominal stresses derived from coarse mesh FEM models
– Geometric stresses includes nominal stresses and stresses due to structural discontinuities and presence of attachments, but excluding stresses due to presence of welds. Stresses derived from fine mesh FEM models (type 5) are geometric stresses. Effects caused by fabrication imperfections as e.g. misalignment of structural parts, are however normally not included in FEM analyses, and must be separately accounted for. The greatest value of the extrapolation to the weld toe of the geometric stress distribution immediately outside the region effected by the geometry of the weld, is commonly denoted hot spot stress.
– Notch stress is the total stress at the weld toe (hot spot location) and includes the geometric stress and the stress due to the presence of the weld.

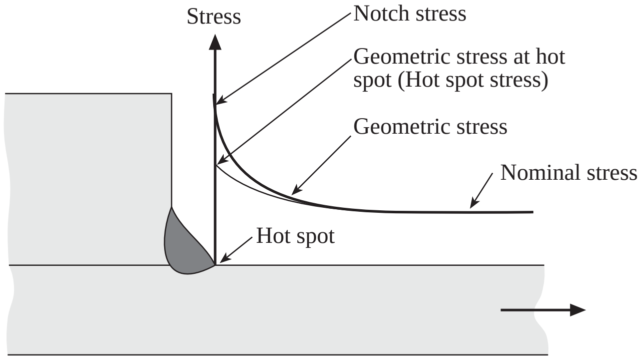

Figure 6.1 Definition of stress categories

6.2 Global hull analysis

6.2.1

The purpose of the global hull analysis is to obtain a reliable description of the overall stiffness and global stress distribution in the primary members in the hull. The following effects should be taken into account:

– vertical hull girder bending including shear lag effects
– vertical shear distribution between ship side and bulkheads
– horizontal hull girder bending including shear lag effects
– torsion of the hull girder (if open hull type)
– transverse bending and shear

6.2.2

The extent of the model is dependent on the type of response to be considered and the structural arrangement of the hull. In cases where the response within the region considered is dependent on the stiffness variation of the hull over a certain length, the finite element model is generally required to extend over minimum the same length of the hull.

Thus for determination of the torsional response as well as the horizontal bending response of the hull of an open type ship it is generally required that the model extent covers the complete hull length, depth and breadth (a half breadth model may be used if the structure is symmetric, or can with sufficient accuracy be modelled as being symmetric, and antisymetric boundary condition is assumed at the centreline). A complete finite element model may also be necessary for the evaluation of the vertical hull girder bending of ships with a complex arrangement of superstructures (e.g. passenger ships), and for ships of complex cross-section (e.g. catamarans). For car carriers and Ro-Ro ships, the transverse deformation- and stress response due to rolling may also require a model extending over the complete vessel length to be applied.

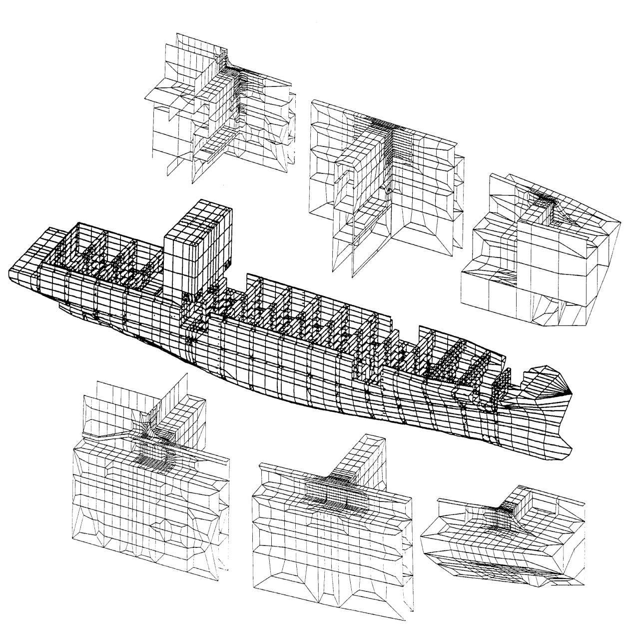

Figure 6.2 Global hull model of container vessel

6.2.3

The *loads* can be produced by direct computation of hydrodynamic pressures and motions in accordance with Chapter 5. Simplified load models (pressures / line loads) producing specified hull girder loads, as outlined in Chapter 4 and/or based on the Rules as described in Appendix C may also be applied.

6.2.4

The *global analysis* may be carried out with a relatively coarse mesh. Stiffened panels may be modelled by means of anisotropic elements. Alternatively, a combination of plate elements and beam elements, may be used. It is important to have a good representation of the overall membrane panel stiffness in the longitudinal/transverse directions and for shear.

Examples showing global finite element models for torsional analysis of a container vessel and global analysis of an oil tanker are shown in Figs. 6.2 and 6.3 respectively. The models may also be used to calculate nominal global (longitudinal) stresses away from areas with stress concentrations. In areas where local stresses in web frames, girders or other areas (as hatch corners) are to be considered (see Section 6.4-6) fine mesh areas may be modelled directly into the coarser model using suitable element transitions meshes to come down from coarse meshes to finer meshes. This approach leads to a fairly large set of equations to be solved simultaneously. An example of this is the container vessel shown in Figure 6.2 where the six hatch corner models initially were put directly into the global model and analysed together in order to determine hot-spot stresses in the hatch corners.

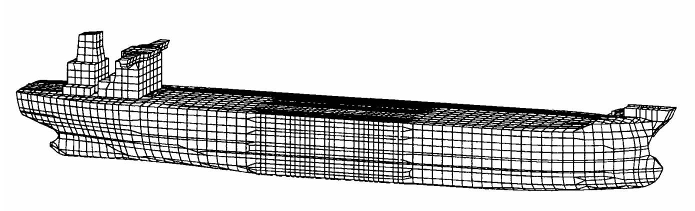

Figure 6.3 Global hull model of shuttle tanker

6.2.5

In general the various mesh models have to be "compatible" meaning that the coarser models are to have meshes producing deformations and/or forces applicable as boundary conditions for the finer mesh models. If super-element techniques are available, the model for local stress analysis may be applied as lower level super-elements in the global model.

6.2.6

Fine mesh models may be solved separately by transferring boundary deformations/ boundary forces and local internal loads to the local model. This load transfer can be done either manually or, if sub-modelling facilities are available, automatically by the computer programme. The finer mesh models are usually referred to as sub-models. The advantage of a sub-model or an independent local model is that the analysis is carried out separately on the local model. In this way less computer recourses are necessary and a controlled step by step analysis procedure can be carried out.

6.2.7

When the models are not compatible, deformations obtained in the coarser models cannot be applied directly in the finer mesh models. In such cases forces should preferably be transferred from the coarse model to the more detailed model rather than forced deformations.

6.2.8

Refined mesh models, when subjected to boundary forces or forced deformation from the coarser models, shall be checked to give comparable deformations and/or boundary forces as obtained from the coarse mesh model. Furthermore, it is important that the extent of the fine mesh model is sufficiently large to prevent that boundary effects due to prescribed forces and/or deformations on the model boundary affects the stress response in the areas of particular interest.

6.3 Cargo hold analysis

6.3.1

The cargo hold/tank analysis is used to analyse deformation response and nominal stresses of the primary hull structural members in the midship area. This model also provides boundary conditions for frame and girder analysis models.

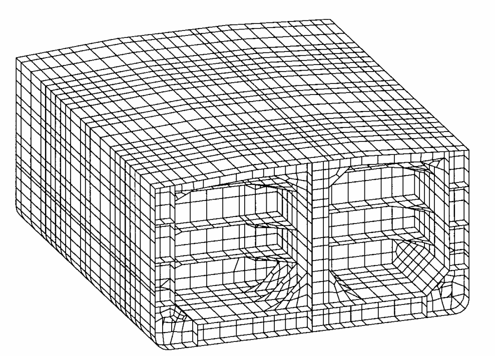

a) 8-noded shell/composite elements

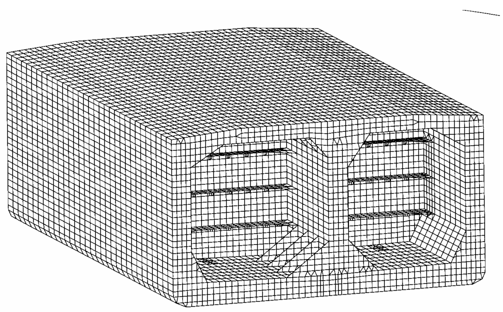

b) 4-noded shell elements

Figure 6.4 Cargo hold models of shuttle tanker (midship area)

6.3.2

Cargo hold model. The finite element model is normally to cover the considered tank/hold, and in addition one half tank/hold outside each end of the considered tank/hold, i.e. the model extent is ½ + 1 + ½ hold or tank. If there is symmetry in structure and loading, a model covering the half breadth of the ship may be used. If there is a symmetry plane at the half-length of the considered tank/hold, the extent of the model may be taken as one half tank/hold on each side of the transverse bulkhead. Figs. 6.4 and 6.5 shows typical cargo hold midship models for a tanker and a container vessel respectively.

Note that for ships which give rise to warping response, a coarse mesh finite element model of the entire ship hull length may be required for torsional response calculations.

6.3.3

Load application. Two alternative ways of applying the loads are described here depending on whether or not simplified calculation of loads as outlined in Chapter 4, or wave loads by direct computation (Chapter 5) has been carried out.

In both cases lateral loads from sea pressure, cargo etc. are to be applied along the model. The longitudinal hull girder loads, however, have to be treated differently.

a) *Simplified loads:*
Hull girder loads, moments and shear forces, are to be applied to the ends of the model and analysed as *separate* load conditions. The shear forces are to be distributed in the cross-sections according to a shear flow analysis. Then, the hull girder response and the response from the lateral load distribution can be combined as outlined in Section 3.4.
Using this option, vertical load balance for the lateral load case will not be achieved and it will be important to use boundary conditions that minimise the effects of the unbalance.

b) *Loads by direct load computations:*
A consistent set of lateral loads along the model and hull girder loads at the model ends can be applied simultaneously to the model. This will automatically take care of the load combination issue, as loads based on direct hydrodynamic analysis will be simultaneously acting loads.

In this case the combined set of loads will approach a balance (equilibrium) such that a minimum of reaction forces at the supports should be present. In any case the boundary conditions should be arranged such as to minimise the effects of possible unbalances. The loads and boundary conditions in the hull cross section at each end of the model should be evaluated carefully when modelling only a part of the hull in order to avoid unrealistic stiffness from the forebody/aftbody.

6.3.4

Boundary conditions are closely related to how the loads are being applied to the FEM model. If the model covers one half breadth of the vessel, symmetry conditions are to be applied in the centreline plane.

In order to cover the lateral load response associated with *case a)* “simplified load application” above, the model is to be supported vertically by distributed springs at the intersections of the transverse bulkheads with ship sides and the longitudinal bulkheads. The spring constants are to be calculated for the longitudinal bulkheads and the ship sides based on actual bending and shear stiffnesses and for a model length of three cargo holds. In addition, symmetry conditions at the model ends are to be applied. In this way no hull girder loads enter into the model. To account for the hull girder loads cases (moments & shear) the symmetry conditions at the ends have to be removed and the loads applied at the ends as described above applying the loads one at the time as separate load cases.

In cases where reduced models spanning ½ hold on each side of the transverse bulkhead is used the model can be fixed along the intersection between ship sides and transverse bulkheads.

To cater for *case b)* “ loads by direct computations” the same spring system as in case a) can be applied, but all load components (lateral, moment and shear) are to be applied as a consistent set of simultaneously acting loads as produced by the hydrodynamic analysis.

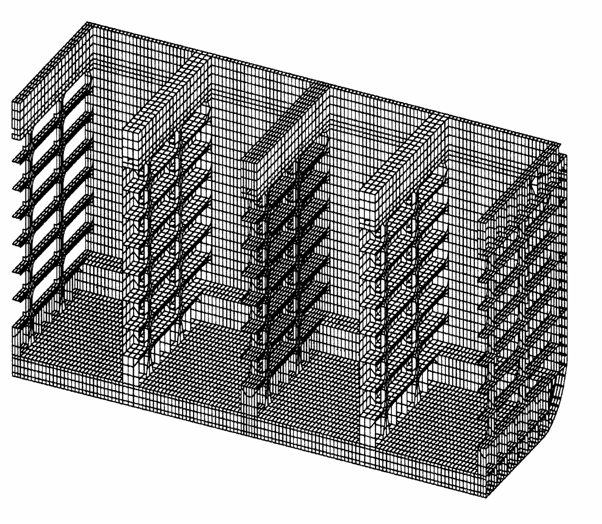

Figure 6.5 Cargo hold model of container vessel

6.3.5

Finite element mesh. The mesh fineness of the cargo hold/tank analysis is to be decided based on the method of load application and type of elements used.

The element mesh of the cargo hold/tank model shall represent the deformation response and be fine enough to enable analysis of nominal stress variations in the main framing/girder system. The following may be considered as a guidance:

- A minimum of 3 elements (4-noded shell/ membrane elements) over the web height will be necessary in areas where stresses are to be derived. With 8-noded elements, 2 elements over the web/girder height will normally be sufficient. Fig. 6.4 illustrates these two alternatives for possible mesh subdivisions in a double skin tanker. An additional example for the cellular cargo area of a container vessel is shown in Fig. 6.5 using 4-noded shell elements.
- For the tanker model shown in Fig. 6.4a, the general element length is equal to the web frame spacing. This implies that the effective flange/shear lag effect of the plate flanges (transverse web frames) will not be properly represented in this model, and that the mesh is not suitable for representation of stresses in way of stress concentrations as knuckles and bracket terminations.
- The mean girder web thickness in way of cut-outs may generally be taken as follows;

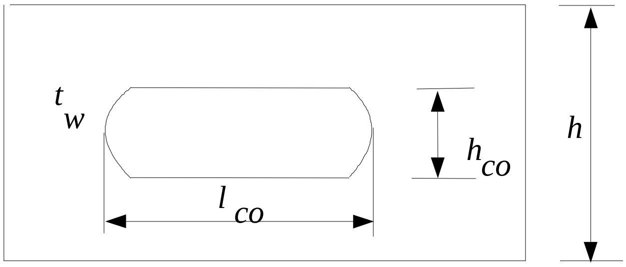

$$t_{mean} = \frac{h - h_{co}}{h r_{co}} t_w$$

where

t_w = web thickness

$$r_{co} = 1 + \frac{l_{co}^2}{2.6(h - h_{co})^2}$$

l_{co} = length of cut-out

h_{co} = height of cut-out

h = girder web height

For large values of r_{co} (> 2.0), geometric modelling of the cut-out is advisable.

6.4 Frame and girder models

6.4.1

Frame and girder models shall be capable of analysing deformations as well as stresses in the framing/girder system. Typical results derived will be membrane stresses caused by bending, shear and torsion for example in a double skin construction.

6.4.2

This model may be included in the cargo hold/tank analysis model, or run separately with prescribed boundary deformations/forces, ref. 6.2.6. However, provided sufficient computer capacity is available, it will in most cases be convenient to combine the two analyses into one model. The mesh density of the frame and girder model may then be used for the full extension of the cargo hold/tank FE model. Examples of such models are given in Figs. 6.4b and 6.5.

6.4.3

Finite element mesh. The element mesh should be fine enough to describe stress increase in critical areas (such as brackets with continuos flange). Typical local frame/girder models are given in Fig. 6.6. The following may be considered as a guidance:

- Normally element sizes equal to the stiffener spacing will be acceptable.
- In the longitudinal direction 3 elements between transverse frames is recommended for 4-noded elements. For 8-noded elements 2 elements is considered acceptable.
- A minimum of 3 elements (4-noded shell/ membrane elements) over the web and girder heights will be necessary in areas where stresses are to be derived, see for example Fig. 6.4b showing the framing system in a double skin tanker with 4-noded elements. With 8-noded elements, 2 elements over the web/girder height will normally be sufficient, Fig. 6.4a.
- If cut-outs are not modelled, the mean girder web thickness in way of cut-outs may generally be taken as in 6.3.5 above.
- To the extent that reduced effectivity of flanges, webs etc. are not represented by the element formulation itself; the reduced effectivity may be defined by assigning reduced thickness of plate elements or cross-sectional areas of area elements. Efficiency of girder and frame flanges may be calculated by formulae given in Design Principles in the Rules [1]. However, care should be exercised in reducing thicknesses, as the effective flange for bending is different from the effective flange for membrane response. It will therefore not be possible to satisfy both conditions with the same model. Hence, an appropriately fine mesh able to capture the shear lag effect of girders and the warping effect of unsymmetrical members is recommended.

6.4.4

The model for analysis of frames and girders should be compatible with the cargo hold model if forced deformations are applied. If a separate analysis of frames and girders is carried out without any finite element calculation of the global stress response, the extent of the model, boundary conditions and load distribution should be carefully evaluated in order to obtain an acceptable global support and stiffness for the frame/girder model.

Similarly to the cargo hold model, the frame/girder model may be used for calculation of nominal stresses. For the models shown in Fig. 6.4b, 6.5 and 6.6a, the notch stresses at bracket toe terminations and panel knuckles have to be calculated using additional K-factors (K_g and K_w).

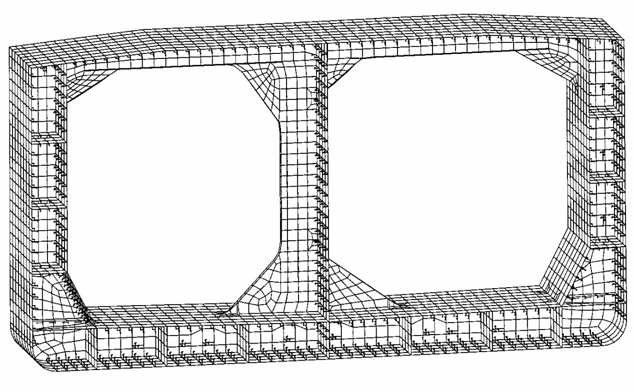

a) Local web frame model

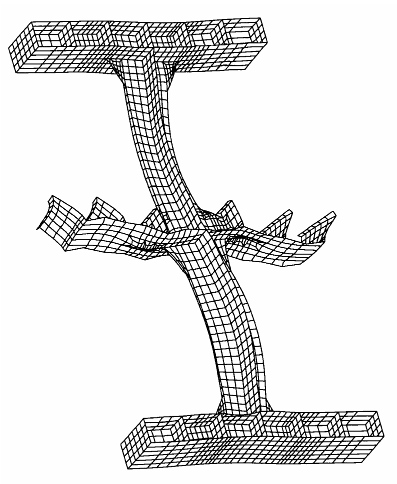

b) Stringer frame model

Figure 6.6 Frame and girder models

6.4.5

Local beam- and finite element analysis are utilised for determination of nominal stresses in frames, stringers and girders, and for determination of the deflection at supports of e.g. side and bottom longitudinal stiffeners.

Dependent on the complexity of the structure and the type of response investigated, alternative 3-D and 2-D analyses may be considered.

The Classification Notes for strength analysis of different types of ships, i.e. tankers and bulk carriers, give examples of beam and finite element modelling including calculation of efficient flanges, rigid element ends, boundary conditions and spring supports.

Global hull girder stresses shall be calculated based on actual thicknesses. Local stresses shall be calculated based on reduced scantlings, i.e. newbuilding scantlings minus corrosion addition t_k as given in Table 2.4

For simplified analyses, loads are generally to be determined in accordance with Section 4, and the external- and internal loads shall generally be considered as separate load cases. The combined stress response shall be determined in accordance with 3.4.5.

Direct hydrodynamic load analyses are to be carried out as outlined in Chapter 5.

Unless a fine mesh finite element analysis is carried out, only nominal stresses will be derived. This implies that relevant K-factors has to be used for calculation of notch stresses, see also Chapter10.

6.4.6

For calculation of nominal stresses in a web frame/ girder/ stringer system a 3-D beam or finite element model may be applied.

The longitudinal model extent shall be sufficient to obtain realistic boundary conditions. A model length extending from the middle of one hold to the middle of the adjacent hold is sufficient provided symmetry planes at the half lengths of the adjacent holds exist.

As the external and internal loads are analysed as separate load cases, the applied loads for each load case are generally unbalanced, and realistic support conditions must be defined.

6.4.7

When calculating nominal stresses in a simple frame or in a well defined grillage systems, a 2-D model may be applied.

Typical 2-D models are:

- one transverse web frame supported by side, girders, deck and bottom
- double bottom grillage, including floors and girders
- side construction including web, frames and stringers

For 2-D models the sensitivity of the assumed boundary conditions and support definition should be evaluated.

6.5 Local structure models

6.5.1

The local structure analyses are used to analyse stresses in local areas. Stresses in laterally loaded local plates and stiffeners subjected to large relative deformations between girders/frames and bulkheads may be necessary to investigate along with stress increase in critical areas (such as brackets with continuous flanges). Local structure models may also be used to determine the edge stress in way of critical hatch corner openings in, e.g. container vessels. In such cases the mesh fineness (i.e. the element length along the critical edge) is not to be larger than 0.2 R where R is the radius of curvature of the hatch corner. If 4-noded elements are used fictitious bar elements are to be applied at the free edge in order to facilitate a precise and straight forward read-out of the critical edge stress to be used in the fatigue analysis.

The model may be included in the 3-D cargo hold/tank analysis model of the frame and girder system, but may also be run separately with prescribed boundary deformations/forces from the frame and girder model. Note that local lateral pressure loads must be applied to the local model (if of relevance for the response).

6.5.2

Areas to model. As an example the following structures of a tanker are normally to be considered:

- Longitudinals in double bottom and adjoining vertical bulkhead members. See Fig. 6.7, which shows a model with 8-noded shell elements.
- Deck longitudinals and adjoining vertical bulkhead members.
- Double side longitudinals and adjoining horizontal bulkhead members.

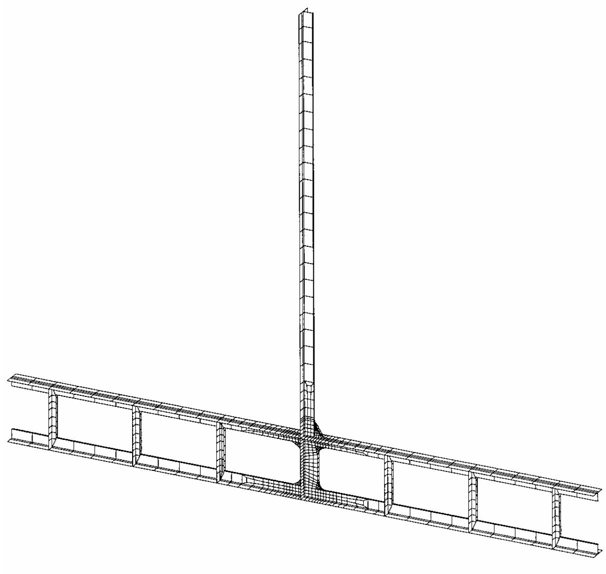

Figure 6.7 Stiffener transition at transverse bulkhead

6.5.3

As a simplified approach local structure stiffener models may be modelled with beam elements in order to establish a simple basis for *nominal stress* to be applied in conjunction with established stress concentration factors as given in Chapter 10. It should be noted, however, that the K_g factors are derived on the basis of the simplified stress analysis procedure in Chapter 3 using the effective stiffener flanges given in 3.5.7.

6.5.4

Finite element mesh. Normally three (3) 8-noded elements are to be used over the height (web) of the stiffeners. Corresponding element sizes are to be used for the stiffener flange and the plate, noting that the plate mesh should be fine enough to pick up the shear lag effect. It is especially important to model unsymmetrical stiffeners correctly in order to capture the skew bending effect. In a model like the one in Fig. 6.7 the best strategy will be to combine the local structure stiffener model with the mesh fineness as described here with a *stress concentration model* (Section 6.6) in order to get a good description of the stress concentration in the bracket as basis for fatigue analysis. In a stochastic fatigue analysis procedure this is the preferred way of modelling.

6.6 Stress concentration models

6.6.1

Local finite element analyses may be used for calculation of local geometric stresses at the hot spots and for determination of associated K-factors. These analyses involve use of fine element mesh models of details such as bracket connections, stiffener to web frame connections or local design of frames/girders. For this purpose it is important to note the definition of the K-factors and their relation to the S-N curve (see also 10.1.2).

6.6.2

It is normally appreciated that it may be a considerable task to derive notch stresses directly from finite element analysis. This is due to:

- The local geometry has to be included in the finite element model in order to obtain stresses that account for this geometry. Thus in order to include the effect of the weld joint its geometry has to be included by three-dimensional elements. This may imply a rather large computer model.
- If a finite element mesh having zero radius models the hot spot region at corner details, the calculated stress will approach infinity as the element size is decreased to zero. Thus, a radius at such regions has to be assumed in order to obtain reliable results. The modelling of a relevant radius requires a very fine element mesh increasing the size of the computer model.

Hence, for design analysis a simplified numerical procedure is used in order to reduce the demand for large fine mesh models for the calculation of *K*-factors. The *K*-factor is calculated in two steps, $K = K_g \cdot K_w$

1) By means of a fine mesh model using shell elements (or alternatively solid elements) the stress concentration due to the geometry effect of the actual detail is calculated resulting in a K_g - factor.
2) The stress concentration due to the weld itself, K_w-factor, may be based on standard values from Table 10.4 or 10.6 or direct finite element calculations with very fine mesh of solid elements (weld radius has to be modelled).

6.6.3

The aim of the finite element analysis is normally not to calculate directly the notch stress at a detail but to calculate the geometric stress distribution in the region of the hot spot such that these stresses can be used either directly in the fatigue assessment of given details or as a basis for derivation of stress concentration factors. Reference is made to Fig. 6.10 as an example showing the stress distribution in front of an attachment (A-B) welded to a plate with thickness *t*. The notch stress is due to the presence of the attachment and the weld. The aim of the finite element analysis is to calculate the stress at the weld toe (hot spot) due to the presence of the attachment, denoted geometric stress, σ_g. The stress concentration factor due to this geometry effect is defined as,

$$K_g = \frac{\sigma_g}{\sigma_{nominal}}$$

The stress concentration factor due to the weld itself may be taken from Table 10.4 for butt-welds, K_w. Also, with reference to Fig. 6.10, the resulting stress concentration factor is defined as

$$K = \frac{\sigma_{notch}}{\sigma_{nominal}}$$

With the following definition of the stress concentration factor due to the weld only,

$$K_w = \frac{\sigma_{notch}}{\sigma_g}$$

The resulting stress concentration factor is obtained as

$$K = K_g \cdot K_w$$

Thus the main emphasis of the finite element analysis is to make a model that will give stresses with sufficient accuracy at a region outside that effected by the weld. For sufficiently accurate calculation of K_g the model should have a fine mesh for extrapolation of stresses back to the weld toe

6.6.4

Changes in the density of the element mesh, where local stresses are to be analysed, should be avoided. The geometry of the elements should be evaluated carefully in order to avoid errors due to deformed elements (for example corner angles between 60° and 120° and length/breadth ratio less than 5).

The size of the model should be so large that the calculated results are not significantly affected by assumptions made for boundary conditions and application of loads. If the local stress model is to be given forced deformations from a coarser model (global model, frame/girder model or local structure model) the models have to be compatible as described in 6.2.5. If the models do not satisfy this requirement, forced deformations cannot be applied, and forces and simplified boundary conditions have to be modelled.

6.6.5

Elements size for stress concentration analysis. FEM stress concentration models are generally very sensitive to element type and mesh size. By decreasing the element size the FEM stresses at discontinuities will in the limit approach infinity. It is therefore necessary to set a lower bound for element size and use an extrapolation procedure to the hot spot to have a uniform basis for comparison of results from different computer programs and users. On the other hand, in order to properly pick up the geometric stress increase it is important that the stress reference points in t/2 and 3t/2 (Fig. 6.10) are not inside the same element. This implies that element sizes in the order of the plate thickness are to be used for the modelling. If solid modelling is used, the element size in way of the hot spot may have to be reduced to half the plate thickness in case the overall geometry of the weld is included in the model representation, Fig. 6.11.

It is recommended that shell elements are used as the standard element type and that solid elements are used on a comparative basis to investigate K_g factors in special areas.

Fig. 6.8 shows an example of a hopper tank knuckle in a tanker in which shell elements were used for the coarser models and solid elements for the fine mesh stress concentration model in order to directly determine the geometric stress at the knuckle line σ_g and hence the geometric stress concentration factor K_g directly.

For this case the nominal stress is defined as the average element stress one half longitudinal spacing from the knuckle line. This is referring to a frame and girder analysis model in which the element width is equal to the spacing between the longitudinals.

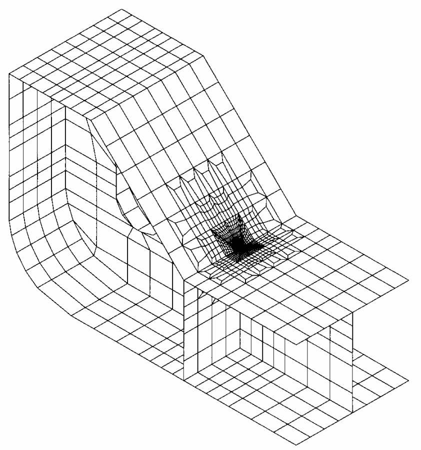

Figure 6.8 SCF model of hopper tank knuckle

6.6.6

Element stresses are normally derived at the gaussian integration points. Depending on element type it may be necessary to perform several extrapolations in order to determine the stress at the location representing the weld toe. In order to determine the proper principal stress direction, the information on the direction stresses shall be preserved.

6.6.7

Hot spot point. When shell elements are used for the modelling and the overall geometry of the weld is not included in the model, the extrapolation shall be performed to the element intersection lines (in order to get results that corresponds to tests in general). However, for the hopper tank knuckle, the hot spot stress depends on the global geometry of the weld. The weld toe distance, x_{wt}, is defined as the distance from the weld toe to the intersection between the hopper plate surface and the inner bottom surface, see Figure 6.9. The extrapolation may be performed to a point x_{wt} from the element intersection lines when surface stresses are extrapolated. (This is to get correspondence with measured values on an actual geometry).

If the (overall) weld geometry is included in the model, the extrapolation is related to the weld toe as shown in Fig. 6.10.

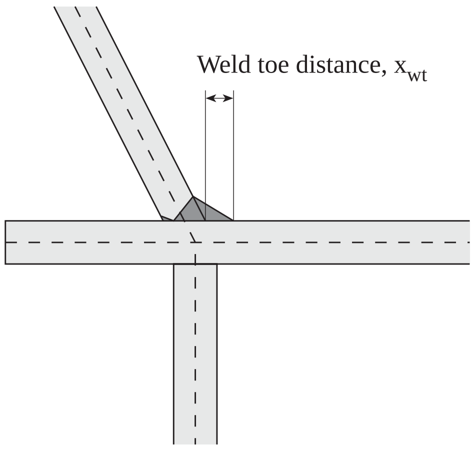

Figure 6.9 Hopper tank knuckle

6.6.8

Stress extrapolation procedure. First stresses are extrapolated from the gaussian integration points to the plate surface through the plate thickness. Then a further extrapolation to the line A - B is conducted. The final extrapolation of component stresses are carried out as a linear extrapolation of surface stresses along line A - B at a distance t/2 and 3t/2 from the weld toe, alternatively the element intersection line (where t denotes the plate thickness). Having determined the extrapolated stress components at the hot spot, the principal stresses are to be calculated and used for the fatigue evaluation.

The stress extrapolation procedure may be tested for similar cases based on laboratory testing and/or where results have been presented in the literature.

This procedure has been tested against known target values for a plate with a non load carrying attachment and a cut-out in a web for longitudinal transfer. Acceptable results have been achieved using 8-node shell elements and 20 node volume elements with size equal the thickness. However, this methodology is experience based and one should be cautious to use it for details very different from what it has been calibrated for. The results may also be dependent on the finite element program. It is therefore recommended that the analysis program with proposed element mesh is tested against a well known detail prior to use for fatigue assessment.

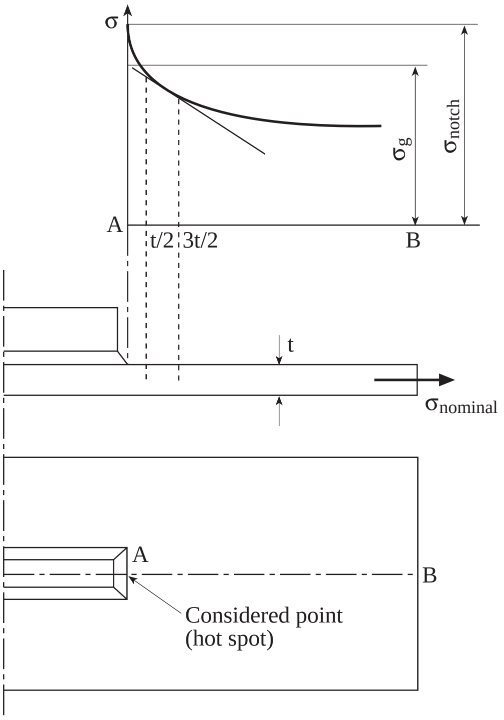

Figure 6.10 Stress distribution at an attachment and extrapolation of stresses

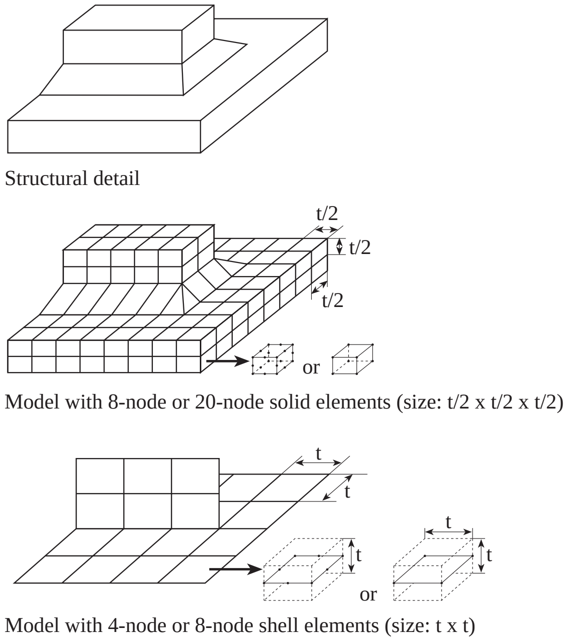

Figure 6.11 Examples of modelling

7. Fatigue Analysis of Oil Tankers

7.1 Where to analyse

7.1.1

Fatigue damages are known to occur more frequently for some ship types and categories of hull structure elements. The fatigue life is in particular related to the magnitude of the dynamic stress level, the corrosiveness of the environment and the magnitude of notch- and stress concentration factors of the structural details, which all vary depending on ship type and structure considered. The importance of a possible fatigue damage is related to the number of potential damage points of the considered type for the ship or structure in question and to its consequences.

7.1.2

A major fraction of the total number of fatigue damages on ship structures occurs in panel stiffeners on the ship side and bottom and on the tank boundaries of ballast- and cargo tanks. However, the calculated fatigue life depends on the type of stiffeners used, and the detail design of the connection to supporting girder webs and bulkheads. In general un-symmetrical profiles will have a reduced fatigue life compared to symmetrical profiles unless the reduced effectiveness of the un-symmetrical profile is compensated by an improved design for the attachment to transverse girder webs and bulkhead structures.

7.1.3

Structural elements in the cargo area being of possible interest for fatigue evaluation are listed in Table 7.1

Structure member	*Structural detail*	*Load type*
Side-, bottom- and deck plating and longitudinals	Butt joints, deck openings and attachment to transverse webs, transverse bulkheads, hopper knuckles and intermediate longitudinal girders	Hull girder bending, stiffener lateral pressure load and support deformation
Transverse girder and stringer structures	Bracket toes, girder flange butt joints, curved girder flanges, knuckle of inner bottom and sloped hopper side and other panel knuckles including intersection with transverse girder webs. Single lug slots for panel stiffeners, access and lightening holes	Sea pressure load combined with cargo or ballast pressure load
Longitudinal girders of deck and bottom structure	Bracket termination's of abutting transverse members (girders, stiffeners)	Hull girder bending, and bending / deformation of longitudinal girder and considered abutting member

Table 7.1 Tankers

7.2 Fatigue analysis

7.2.1

Depending on the required accuracy of the fatigue evaluation it may be recommended to divide the design life into a number of time intervals due to different loading conditions and limitations of durability of the corrosion protection. For example, the design life may be divided into one interval with good corrosion protection and one interval where the corrosion protection is more questionable for which different S-N data should be used, see Section 2.3. Each of these intervals should be divided into that of loaded and ballast conditions. The following guidance may be applied:

7.2.2

For vessels intended for normal, world wide trading, the fraction of the total design life spent at sea, should not be taken less than 0.85. The fraction of design life in the fully loaded cargo and ballast conditions, p_n, may be taken from Table 7.2;

Vessel type	Tankers
Loaded conditions	0.45
Ballast conditions	0.40

Table 7.2 Fraction of time at sea in loaded, ballast condition, p_n respectively

7.2.3

For preliminary calculations and as an rough approximation of relative deflection between transverse bulkheads and adjacent web frames in ship side of <u>double hull</u> tankers, the following values, at the probability level of 10^{-4}, may be used:

$$\delta = (1-(1-2z/D)^2)\,\delta_m \quad \text{(mm)}$$

where

$$\delta_m = \frac{0.3 S l_s^2 D}{E\sqrt{i_a i_b}\sqrt{1+N_S}} \cdot p$$

for designs with side stringers

$$\delta_m = \frac{110 l_s^3 D^2}{E I_b \sqrt{1+N_s}} \cdot p \quad \text{for designs without side stringers}$$

z = vertical distance from baseline to considered longitudinal (m)

l_s = distance between bulkhead and transverse frame

D = depth of ship (m)

p = dynamic pressure, p_e, for external pressure load

= pressure due to transverse acceleration for internal pressure load

S = sum of plate flange width on each side of the horizontal stringer

i_a = I_a / S

i_b = I_b / l_s

I_a = moment of inertia for the longitudinal stringer

I_b = moment of inertia for the. transverse frame

N_S = number of cross ties

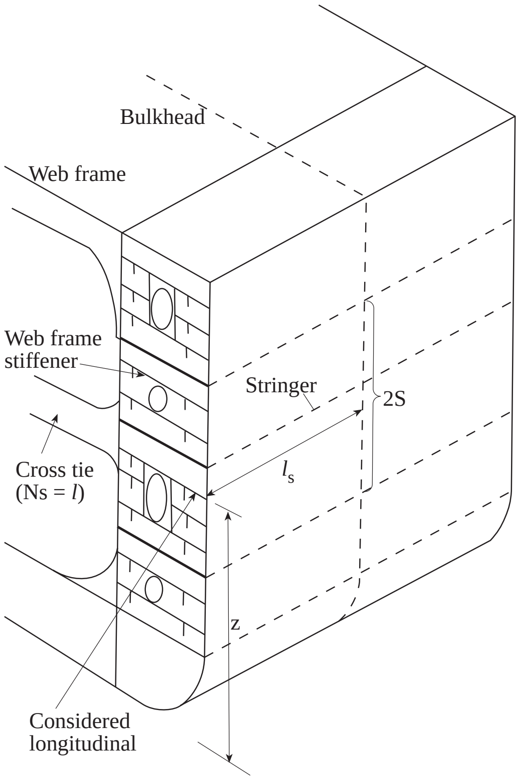

Figure 7.1 Relative deflections- definitions

7.2.4

For similar tank filling conditions on both sides of a bulkhead, e.g. for a bulkhead between two cargo tanks, the following apply;

a) the effect of vertical acceleration is cancelled and may be set to zero
b) the pressures due to motion are added for bulkheads normal to the direction (plane) of the motions.

The net pressure range may be taken as:

p_i = 2 p_2 for longitudinal bulkheads between cargo tanks and,

p_i = 2 p_3 for transverse bulkheads between cargo tanks,

(Note that $\Delta p = 2\ p_i$ when liquid on both sides).

7.2.5

As a simplification, sloshing pressures may normally be neglected in fatigue computations. However, if sloshing is to be considered, the sloshing pressures in partly filled tanks may be taken as given in the Rules [1], Pt.3 Ch.1 Sec. 4, C306. The pressure amplitude is defined at the probability level of 10^{-4}. In case of partly filled tanks on both sides of a bulkhead, the pressure range may be taken as the sum of the pressure amplitudes in the two tanks. Otherwise the range may be taken equal to the amplitude.

Unless otherwise specified, it may be assumed that tanks (in tankers) are partly filled 10% of the vessels design life.

7.3 Example of application (Simplified methods example)

7.3.1 Introduction

In this Appendix an example of the fatigue assessment of a welded connection between a longitudinal and a bracket in the shipside is considered. Before starting to calculate the stresses it may be of relevance to decide what loads and load conditions and the level of detail shall be considered for the calculation of stresses. The following observations have implication on how the calculations are made.

A) The analysis is to be performed according to simplified procedure, see Figure 1.1. The loads may be taken in accordance with Chapter 4. The local and global loads are based on the main dimensions of the vessel given in Table 7.3. Further, the Rules [1] describes what loading conditions to be considered and minimum requirements to the corrosive environment.

B) The considered detail is the termination of a bracket on top of a longitudinal. The simplified stress calculation procedure as defined in Chapter 3 is normally sufficient. In this example, the connection between a longitudinal and a frame in the shipside is considered, using the simplified method.

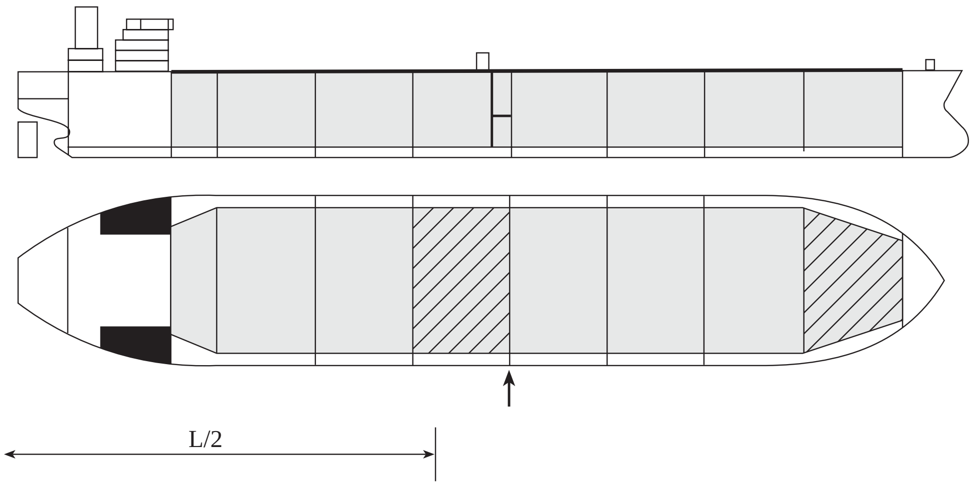

Figure 7.2 View of ship and location of detail in ship

Length of ship	L	=	221	m
Breadth of ship	B	=	42	m
Block coefficient	C_B	=	0.83	
Design speed	V	=	13	knots
Depth of ship	D	=	20.3	m
Vertical Sectional modulus at deck line	Z_v	=	23.1	m^3
Neutral axis above keel	n_0	=	8.2	m
Horizontal sec. modulus in ship side	Z_h	=	40.1	m^3

Table 7.3 The example ship's main dimensions

7.3.2 Geometry of longitudinal and bracket termination.

For different load conditions it is normally only the loads that change for each load condition. It may therefore be practical to calculate the stresses per unit bending moment and per unit lateral pressure and scale these with relevant values for each load condition. It is primarily the calculation of stresses due to lateral pressures that will be simplified by such an approach. For a bracket termination on top of a stiffener, the stresses to be considered related to lateral pressure are due to

– stiffener bending (Figure 7.4)
– relative deflection between bulkhead and first frame (Figure 7.5)
– double hull bending (Figure 7.6)

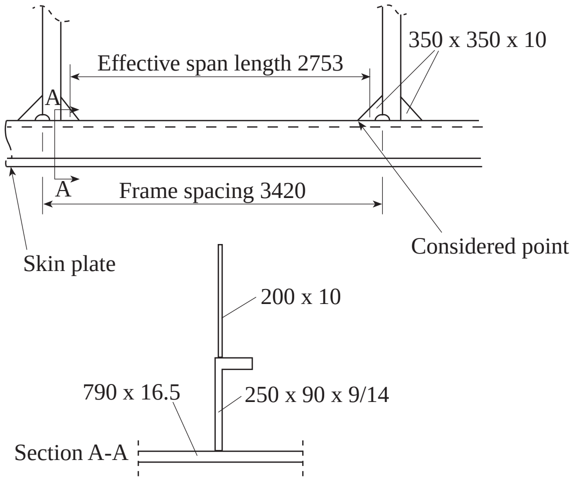

Figure 7.3 Description on detail

Stiffener sectional modulus at top of flange	Z_s	=	$0.461\ 10^{-3}$	m^3
Distance above keel	z	=	13.06	m
Effective span length as defined in Figure 3.4	l	=	2753	mm
Length of bracket side	b	=	350	mm
Distance from end of stiffener to hot spot	x = b/3	=	116.7	mm
Web frame spacing	l_s	=	3420	mm
Stiffener spacing	s	=	790	mm
Thickness of plate	t_p	=	16.5	mm
Height of stiffener	h	=	250	mm
Thickness of web	t_w	=	9	mm
Width of flange	b_f	=	90	mm
Thickness of flange	t_f	=	14	mm
Thickness of bracket	t_b	=	10	mm
Thickness of transverse frame plating	t_{fr}	=	14	mm
Distance from neutral axis to top flange	z_{01}	=	222.6	mm

Table 7.4 Geometry of stiffener considered

The stresses are to be calculated based on the reduced scantlings. Here it is assumed that the corrosion allowance is subtracted, and the dimensions given in Table 7.4 are net scantling values. The stresses are to be calculated at the considered point on the weld connection of bracket and longitudinal stiffener as shown in Figure 7.3

7.3.3 K-factors

An important parameter in the fatigue analysis is the stress concentration factor. The stress concentration factor describes the increase in notch stress due to local geometry, weld geometry and workmanship. The value of the K-factor has to be decided for the considered detail before the notch stresses can be calculated. Reference is made to Chapter 10.

The considered geometry is an unsymmetrical L-profile exposed to lateral loading in combination with global bending moments. For unsymmetrical stiffeners there is an additional stress concentration compared to nominal stresses from symmetrical beam results when subjected to lateral pressure loads.

For the weld at the end of a triangular bracket welded on top of the stiffener flange, the K-factor for axial stresses (related to global loads) is taken according to Table 10.2

K_{axial} = $K_g\ K_w$ = $\underline{2.1}$

and K-factor for local stiffener bending stresses (induced by lateral pressure)

$K_{lateral}$ = $K_g\ K_w\ K_{n2} = 2.1 \cdot K_{n2} = 2.1 \cdot 1.485$ = $\underline{3.119}$

The factor K_{n2} due to unsymmetrical cross section is given in 10.2.13 as

K_{n2} = $(1 + \gamma\beta^2)/(1 + \gamma\beta^2\psi)$ = 1.485

where

β = $1 - t_w/b_f$ = 0.9

ψ = $(h-t_f)^2 t_w/(4Z_s)$ = 0.272

γ = $3(1-(\mu/280))/(1+(\mu/40))$ (Table10.10) = 1.004

μ = $l^4/(b_f^3 t_f\ h^2\ (4h/t_w^3 + s/t^3)$ = 138.583

Comment to derivation of K-factor

K_w = 1.5 due to weld geometry given in 10.1.2

K_g = $2.1/K_w$ = 1.40 may be compared with fine mesh FEM for axial load

$K_g \cdot K_{n2}$ = 2.08 may be compared with fine mesh FEM for lateral pressure load

7.3.4 Calculation of stresses due to lateral pressure

7.3.4.1 General

The stresses to be considered due to lateral pressure are according to 3.5.4 and 11.2.1

$$\sigma_{2A} = K_{lateral}\frac{M}{Z_S} + K_{axial}\frac{m_\delta E I}{l^2\ Z_S} r_\delta\ \delta = \sigma_{2A}{}' + \sigma_\delta$$

$$\sigma_2 = K_{axial}\frac{K_b p_e b^2 r_a}{\sqrt{i_a i_b}}$$

where

σ_{2A}' is stress due to stiffener bending (7.3.4.2)

σ_{δ} is stress caused by relative deflection between frame and bulkhead (7.3.4.3)

σ_2 is stress caused by bending of double hull (7.3.4.4)

The main dimensions of the ship and the geometry of the stiffener are given in Tables 7.3 and 7.4, respectively. Values concerning frame and girder geometry are contained in Table 7.5. When using values not defined in either of the tables the values will be stated. When calculating the stresses and deflections, the unit lateral pressure, p_e, is 1 kN/m^2 and Young's modulus, E, is $2.1 \cdot 10^5$ N/mm^2.

Sum of plate flange width on each side of the horizontal stringer nearest to D/2	S	=	7000	mm
Thickness of inner side	t_{p2}	=	16	mm
Area of stiffeners of inner side	Al_2	=	4000	mm^2
Longitudinal moment of inertia about the transverse frame	I_a	=	$6.42 \cdot 10^{11}$	mm^4
Transverse moment of inertia about the longitudinal axis	I_b	=	$2.82 \cdot 10^{11}$	mm^4
Smeared out stiffness about longitudinal stringer, $i_a=I_a/S$	i_a	=	$91.71 \cdot 10^6$	mm^3
Smeared out stiffness about transverse frame, $i_b=I_b/l_s$	i_b	=	$82.46 \cdot 10^6$	mm^3
Distance from weld to neutral axis in double hull	r_a	=	1245	mm
Longitudinal length of double skin panel of considered Section. The tank length.	a	=	22500	mm
Transverse width of double skin panel of considered section. The distance from deck line to double bottom	b	=	19500	mm
Number of struts	N_S	=	0	
Breadth of wing tank	h_{db}	=	3000	mm

Table 7.5 Frame and girder geometry

7.3.4.2 Calculation of stresses due to stiffener bending.

The stress due to stiffener bending is calculated as described in 3.5.4, accounting for the effective span of the longitudinal and the reduction of the effective bending moment at the weld toe.

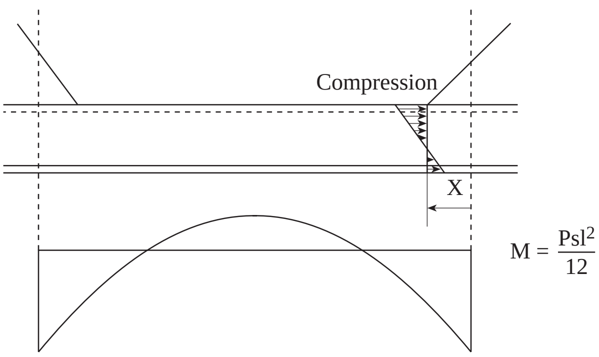

Figure 7.4 Stress due to stiffener bending for external pressure load

The stress per unit lateral pressure (1 kN/m^2) is

$$\sigma_{2A}' = K_{lateral} \frac{M}{Z_S}$$

where

M = $\frac{psl^2}{12} r_p$ (bending moment at the considered point)

$$r_p = 6\left(\frac{x}{l}\right)^2 - 6\left(\frac{x}{l}\right) + 1.0$$ (reduction in bending moment)

$$r_p = 6\left(\frac{116.7}{2753}\right)^2 - 6\left(\frac{116.7}{2753}\right) + 1.0 = 0.756 = 0.756$$

$$\sigma_{2A}' = K_{lateral} \frac{psl^2}{12 Z_S} r_p$$

$$\sigma_{2A}' = 3.119 \frac{10^{-3} \cdot 790 \cdot 2753^{\ 2}}{12 \cdot 0.461 \cdot 10^6} 0.756 = \underline{2.552 \text{ N/mm}^2}$$

To determine the stresses from stiffener bending in the relevant loading conditions the bending stress is to be multiplied with the relevant dynamic pressure. For an external pressure load there will be a compression at the considered point, as described in Figure 7.4.

7.3.4.3 Relative deflection between frame and bulkhead

Stresses may also be induced due to relative deflections between the transverse framing and the bulkhead. In order to determine the correct magnitude of the deflection, a finite element analysis is required. For a more detailed analysis (FEM) of double hull vessel the deflection should be seen in connection with the double hull bending stresses. As an approximation, however, the relative deflection may be taken according to the simplified formula in 7.2.3.

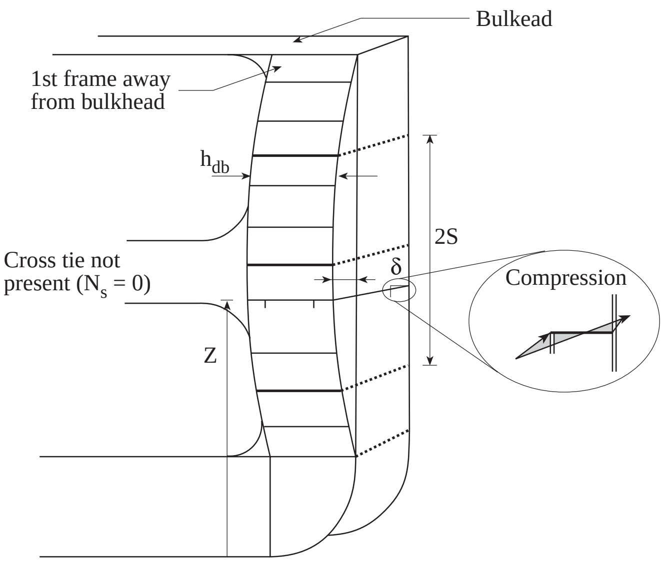

Figure 7.5 Stress due to relative deflection between frame and bulkhead

The stress due to the relative deflection is calculated for a unit pressure, to be

$$\sigma_\delta = K_{axial} \frac{m_\delta EI}{l^2 Z_S} r_\delta \cdot \delta$$

where

$r_\delta = 1 - 2\left(\frac{x}{l}\right)$ (reduction factor for the moment at the hotspot)

$\delta = \left(1 - \left(1 - \frac{2z}{D}\right)^2\right)\delta_m$ (simplified calculation of deflection at considered point considered according to 7.2.3)

$\delta_m = \frac{0{,}3 S l_S{}^2 D}{E\sqrt{i_a i_b}\sqrt{1+N_S}} p_e$ (for designs with side stringers)

$Z_S = I/z_{01}$

$m_\delta = 4.4$ (moment factor due to relative deflection according to 3.5.4)

$$r_\delta = 1 - 2\left(\frac{116.7}{2753}\right) = 0.915$$

$$\delta = \frac{0{,}3 \cdot 7000 \cdot 3420^2 \cdot 20.3}{2.1 \cdot 10^5 \sqrt{82.46 \cdot 10^6 \cdot 91.71 \cdot 10^6}\sqrt{1+0}} 10^{-3} = 0.027 \text{ mm}$$

$$\delta = \left(1 - \left(1 - \frac{2 \cdot 13.06}{20.3}\right)^2\right) 0.0273 = 0.025 \text{ mm}$$

$$\sigma_\delta = K_{axial} \frac{m_\delta E z_{01}}{l^2} \cdot r_\delta \cdot \delta$$

$$\sigma_\delta = 2.1 \frac{4.4 \cdot 2.1 \cdot 10^5 \cdot 222.6}{2753^2} \cdot 0.915 \cdot 0.0251 = \underline{1.31 \text{ N/mm}^2}$$

To determine the stresses from relative deflection in the relevant loading conditions the deflection stress is to be multiplied with the relevant dynamic pressure. The external pressure at the height of the stiffener is applied to determine these stresses, as the vessel has horizontal frames in the shipside. For internal pressures the net outward pressure is applied.

It is seen from Figure 7.5 that the bending of the stiffener is resulting in compression at the considered point for external pressure loads. Assuming tension stress positive, a negative stress is the result in the hot spot when exposed to external lateral pressure.

7.3.4.4 Double hull stresses

The longitudinal secondary stresses in the double hull panels at the intersection with the transverse bulkhead can be assessed applying 3-d frame or finite element analyses.

In this example the stress caused by double hull bending is calculated according to the simplified procedure in Chapter 11.

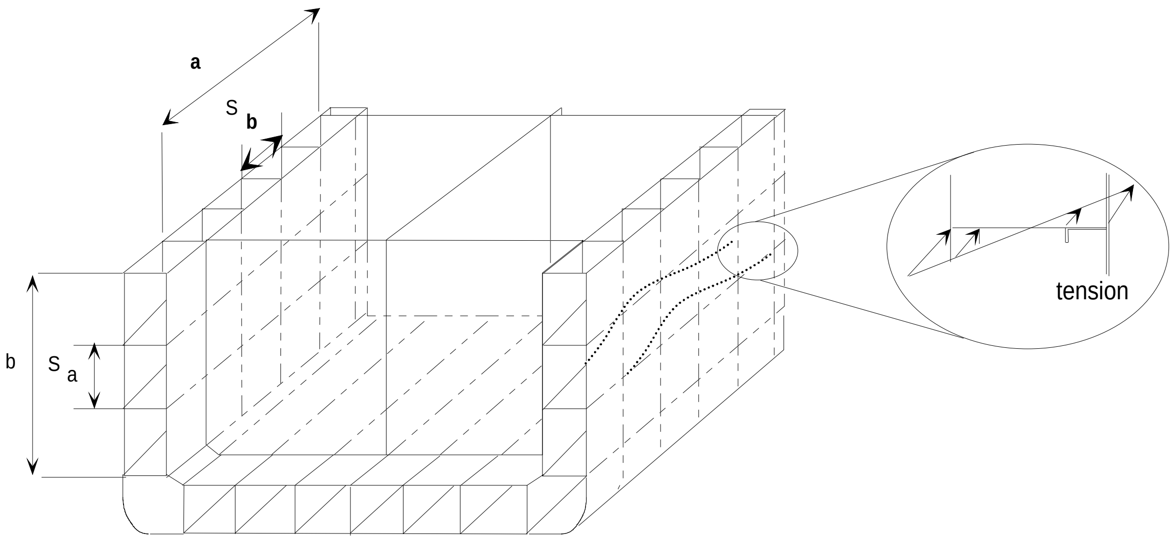

Figure 7.6 Double hull stress due to external pressure

Unit lateral pressure at the shipside result in deformation of the double hull as indicated in Figure 7.6. The stress in the flange of the stiffener considered is according to 11.2.1

$$\sigma_2 = K_{axial} \frac{K_b p_e b^2 r_a}{\sqrt{i_a i_b}}$$ (double bottom longer than wide)

$$\rho = \frac{a}{b} \sqrt[4]{\frac{i_b}{i_a}}$$ (aspect ratio, factor used to estimate the K_b coefficient)

where

$I_a = 6.42 \cdot 10^{11}$ mm^4 (sectional moment of inertia of the longitudinal stringer)

$I_b = 2.82 \cdot 10^{11}$ mm^4 (sectional moment of inertia of the transverse frame)

$i_a = I_a / S = 6.42 \cdot 10^{11}/7000$ $= 91.71 \cdot 10^6$ mm^3

$i_b = I_b / l_s = 2.82 \cdot 10^{11}/3420$ $= 82.46 \cdot 10^6$ mm^3

$K_b = 0.088$ (support bending stress coefficient from Table 11.1, case no. 1. Assumed simply supported in deck and bottom. Linear interpolation of ρ at the η = 1.0 column.)

$$\rho = \frac{22500}{19500} \sqrt[4]{\frac{82.46 \cdot 10^6}{91.71 \cdot 10^6}} = 1.124$$

$$\sigma_2 = 2.1 \frac{0.088 \cdot 10^{-3} \cdot 19500^2 \cdot 1245}{\sqrt{91.71 \cdot 10^6 \cdot 82.46 \cdot 10^6}} = \underline{1.01 \text{ N/mm}^2}$$

To determine the stresses from the double hull bending in the relevant loading conditions the bending stress is to be multiplied with the relevant dynamic pressure. When using the simplified formulas of Chapter 11, the effective pressure to be applied is the average pressure over the double hull panel. The average pressure is calculated as the dynamic pressure amplitude, reduced according to the exposed underwater area

$P_{eff,dh} = P_e T_{act} / D$

It is seen from Figure 7.6 that the bending of the stiffener is resulting in tension at the considered point of the stiffener. Assuming tension stress positive, a positive stress is the result in the hot spot when exposed to external lateral pressure.

7.3.5 Load conditions

The load conditions to be considered are normally given in the Rules [1] for the specific ship types. For the considered tanker for oil, two load conditions have been used

1) Fully loaded, with a fraction of time $p_n = 0.45$ and

2) Ballast with a fraction of time $p_n = 0.40$.

The load conditions should be defined in terms of draughts T_{act} and GM and KR (or period of Roll, T_R) as given in Table 7.6 for the considered vessel. Guidance for choice of these values is given in Section 4.5. The internal and external pressure loads are dependent on the load condition. Data for the present vessel is given in Table 7.6.

	Fully loaded			*Ballast*		
Draught	T_f	=	14.20 m	T_b	=	7.20 m
Metacentric height	GM	=	5.04 m	GM	=	13.86 m
Roll radius of gyration	K_R	=	16.38 m	K_R	=	16.38 m
Part of time in load condition	p_n	=	0.45	p_n	=	0.4
Density	ρ_{cargo}	=	1000 kg/m^3	ρ_{Water}	=	1025 kg/m^3

Table 7.6 Definition of load conditions

7.3.6 Refining fatigue calculation parameters

7.3.6.1 SN-curve and corrosion protection

The detail is located in a coated ballast tank with cathodic protection. According to the Rules at least 5 years of corrosive environment should be applied. For a vessel with a minimum fatigue life of 20 years this implies that the S-N curve of Type I in air is applied for the first 15 years (equivalent to efficient coating lifetime of 10 years) and the curve of Type II applies for the remainder of the time. This will result in scaling factor as in 2.5.1 $\chi = 1.3$, when the calculated life is equal to the design life.

7.3.6.2 The environmental correction factor f_e

The vessel will trade in on world wide operation and thus the environmental correction factor $f_e = 0.8$ may be applied as described in 3.4.3.

7.3.6.3 The effects of mean stress

The mean stress is to be calculated based on the mean stress in each load condition. In this example the approach is simplified by assuming that the mean stress on the average is zero (half the time in compression and half the time in tension) and using $f_m = 0.85$. This may be detailed by calculating the mean stress at the notch from still water load and determining f_m from 2.2.3 or 2.3.4 for the relevant load condition.

7.3.7 Calculation for Load condition - Fully loaded (FL)

7.3.7.1 Internal pressure loads

The longitudinal is located in a ballast tank with no local bending in the fully loaded condition due to internal pressure loads. The loads due to cargo pressures will, however, act on the double hull and cause double hull stresses and frame deflections. The accelerations and pressures are calculated according to 4.4.1 for the cargo tank as

a_v = 2.43 m/s^2

a_t = 3.74 m/s^2

a_l = 1.08 m/s^2

h_s = 7.235 m

y_s = 9.00 m

x_s = 11.25 m

p_1 = 17.58 kN/m^2

p_2 = 33.66 kN/m^2

p_3 = 12.15 kN/m^2

The effective net pressure outward from the cargo is resulting in double hull bending between bulkheads. The lateral pressure caused by the transverse acceleration, a_t, scaled to the 10^{-4} level, is according to 4.4.1

$p_{i,dh} = f_a\, \rho\, a_t\, |y_s|$

where

f_a = $0.5^{1/h}$ (scaling factor to transform the load effect to probability level 10^{-4}, when the acceleration is specified at 10^{-8} level)

h = $2.26 – 0.54 \log_{10}(L)$ (the Weibull shape parameter)

h = 2.26-0.54 log(221) = 0.994

f_a = $0.5^{1/0.994} = 0.4979$

$p_{i,dh}$ = 0.4979·1.00·3.74·9.00 = <u>16.76kN/m^2</u>

7.3.7.2 External sea pressure loads

The sea pressure is calculated according to 4.3.1

$p_e = r_p p_d$

where

$$p_d = 10\left[|y|\frac{\phi}{2} + C_B \frac{|y| + k_f}{16}\left(0.7 + 2\frac{z_w}{T_{act}}\right)\right]$$ (dynamic pressure amplitude below the waterline dominated by roll motion)

$$r_p = \frac{T_{act} + z_{wl} - z}{2 z_{wl}}$$ (reduction of pressure amplitude to the considered point in the wave zone)

$\phi = 50\, c / (B + 75)$ (maximum roll angle as described in 4.5.1)

$c = (1.25 – 0.025\, T_R)\, k$

$T_R = 2\, k_R / \sqrt{GM}$ (period of roll, maximum 30 (s))

$z_{wl} = \frac{3}{4}\frac{p_{dT}}{\rho g}$ (distance from actual water line. It is assumed that the external sea pressure above $T_{act} + z_{wl}$ will not contribute to fatigue damage)

$z_w = z$ (vertical distance from the baseline to the load point)

$p_{dt} = p_d$ at $z_w = T_{act}$

$k = 1.0$ (for ship with bilge keel)

$f = 6.10$ m (vertical distance from the waterline to the top of the ship's side)

$k_f = \min\begin{cases} T_{act} \\ f \end{cases}$ (the smallest of T_{act} and $f = 6.10$)

$y = 9.00$ m (horizontal distance from the centre line to the loadpoint)

$T_R = 2 \cdot 16.38 / \sqrt{5.04} = 14.59$ sec.

$c = (1.25 - 0.025 \cdot 14.59)\, 1.0 = 0.885$

$\phi = 50 \cdot 0.885 / (42 + 75) = 0.378$

$$p_d = 10\left[|\,21.00\,|\frac{0.378}{2} + 0.83\frac{|\,21.00\,| + 6.10}{16}\left(0.7 + 2\frac{13.06}{14.20}\right)\right] = 75.39 \text{ kN/m}^2$$

$$p_{dt} = 10\left[|\,21.00\,|\frac{0.378}{2} + 0.83\frac{|\,21.00\,| + 6.10}{16}\left(0.7 + 2\frac{14.20}{14.20}\right)\right] = 77.65 \text{ kN/m}^2$$

$z_{wl} = 3 \cdot 77.65 / (4 \cdot 1.025 \cdot 9.81) = 5.79$ m

$$r_p = \frac{14.20 + 5.79 - 13.06}{2 \cdot 5.79} = 0.598$$

$p_e = 0.598 \cdot 75.39 = \underline{45.08 \text{ kN/m}^2}$

The pressure $p_\delta = p_e$ is applied in the evaluation of relative deflection. The effective "smeared out" double hull pressure is estimated as

$p_{e,dh} = p_e\ T_{act} / D = 45.08 \cdot 14.20/20.3 = \underline{31.53 \text{ kN/m}^2}$

7.3.7.3 Combination of stress components

The stress amplitudes due to internal and external pressures are combined considering the sign. Positive stress is defined as tension at the location of the weld

Stresses due to external pressure loads

+ Stiffener bending (p_e= 45.08 kN/m^2)	$c \cdot 45.08 \cdot 2.552$:	-115.04	N/mm^2
+ Relative deflection ($p_{e,\delta} = p_e$= 45.08 kN/m^2)	$c \cdot 45.08 \cdot 1.309$:	-59.01	N/mm^2
+ Double hull bending ($p_{e,dh}$ = 31.53 kN/m^2)	$t \cdot 31.53 \cdot 1.006$:	31.72	N/mm^2
= Stresses from external sea pressure loads	σ_e=	-142.33	N/mm^2

Stresses due to internal pressure loads

+ Stiffener bending ($p_i = 0$)		0	N/mm^2
+ Relative deflection ($p_{i,\delta}$ = 16.76 kN/m^2)	t·16.76·1.309:	21.94	N/mm^2
+ Double hull bending ($p_{i,dh}$ = 16.76 kN/m^2)	c·16.76·1.006:	-16.86	N/mm^2
= Stresses from internal pressure loads	σ_i=	5.08	N/mm^2

t = 1 tension

c = -1 compression

The combined local stress range is determined according to 3.4.5 as

$$\Delta\sigma_l = 2\sqrt{\sigma_e^2 + \sigma_i^2 + 2\rho_p \sigma_e \sigma_i}$$

$$\rho_p = \frac{1}{2} - \frac{z}{10T_{act}} + \frac{|x|}{4L} + \frac{|y|}{4B} - \frac{|x| \cdot z}{5LT_{act}} \qquad z \leq T_{act}$$

where

x, y and z are the coordinates of the load point, according to the coordinate system described in 3.4.5 with origo = (midship, centreline, baseline)

x = 0 m

y = 21.00 m

z = 13.06 m

$$\rho_p = \frac{1}{2} - \frac{13.06}{10 \cdot 14.2} + \frac{|0|}{4 \cdot 221} + \frac{|21.00|}{4 \cdot 42} - \frac{|0| \cdot 13.06}{5 \cdot 221 \cdot 14.20} = 0.533$$

$$\Delta\sigma_l = 2\sqrt{(-142.33)^2 + 5.08^2 + 2 \cdot 0.533 \cdot (-142.33) \cdot 5.08} = \underline{279.38\ kN/m^2}$$

7.3.7.4 Global hull bending moments

The vertical wave bending moments are computed according to 4.2.1 as

$M_{wo,h} = -0.11 \cdot f_r\ k_{wm} \cdot C_w \cdot L^2 \cdot B \cdot (C_B + 0.7)$ (sagging moment)

$M_{wo,s} = 0.19 \cdot f_r\ k_{wm} \cdot C_w \cdot L^2 \cdot B \cdot C_B$ (hogging moment)

The horizontal wave bending moment is calculated according to 4.2.2 as

$M_H = 0.22\ f_r\ L^{9/4}\ (T_{act} + 0.30\ B)\ C_B\ (1-\cos(2\pi x/L))$

where

C_w = 10.75 – [(300-L) / 100]3/2 (wave coefficient)

$f_r = 0.5^{1/h0}$ (factor to transform the load from 10^{-8} to 10^{-4} probability level)

h_0 = 2.21 – 0.54 log(L) (long term Weibull shape parameter)

x = L/2 (distance from A.P to considered point)

k_{wm} = 1.0 (moment distribution factor)

C_w	$= 10.75 - [(300 - 221) / 100]3/2$	=	10.05
h_0	$= 2.21 - 0.54 \log(221)$	=	0.944
f_r	$= 0.5^{1/0,944}$	=	0.4799
For f_r	$= 1.0$ (10^{-8} probability level)		
$M_{w0,s}$	$= - 0.11 \cdot 1.0 \cdot 1.0 \cdot 10.05 \cdot 221^2 \cdot 42 \cdot (0.83 + 0.7)$	=	$-3469.6 \cdot 10^3$ kNm
$M_{w0,h}$	$= 0.19 \cdot 1.0 \cdot 1.0 \cdot 10.05 \cdot 221^2 \cdot 42 \cdot 0.83$	=	$3251.1 \cdot 10^3$ kNm
M_H	$= 0.22 \cdot 1.0 \cdot 221^{9/4} \cdot (14.20 + 0.30 \cdot 42)\ 0.83\ (1-\cos(\pi))$	=	$1843.1 \cdot 10^3$ kNm
For f_r	$= 0.4799$ (10^{-4} probability level)		
$M_{w0,s}$	$= - 0.11 \cdot 0.4799 \cdot 1.0 \cdot 10.05 \cdot 221^2 \cdot 42 \cdot (0.83 + 0.7)$	=	$-1665.1 \cdot 10^3$ kNm
$M_{w0,h}$	$= 0.19 \cdot 0.4799 \cdot 1.0 \cdot 10.05 \cdot 221^2 \cdot 42 \cdot 0.83$	=	$1560.2 \cdot 10^3$ kNm
M_H	$= 0.22 \cdot 0.4799 \cdot 1.0 \cdot 221^{9/4} \cdot (14.20 + 0.30 \cdot 42)\ 0.83\ (1-\cos(\pi))$	=	$884.5 \cdot 10^3$ kNm

7.3.7.5 Stresses from global loads

The vertical and horizontal bending moments results in the following stress ranges, according to 3.5.1 and 3.5.2 at the 10^{-4} level

$$\Delta\sigma_v = K_{axial}\left(M_{Wo.h} - M_{Wo.s}\right) 10^{-3} \frac{(z - n_0)}{I_N}$$ (vertical global stress range)

$$\Delta\sigma_{hg} = 2 K_{axial} M_H\ 10^{-3} \frac{|y|}{I_C}$$ (horizontal global stress range)

$$\Delta\sigma_g = \sqrt{\Delta\sigma_V{}^2 + \Delta\sigma_g{}^2 + 2\rho_{vh}\Delta\sigma_V\Delta\sigma_{hg}}$$ (combined global stress range)

where

I_N	$= Z_v\ (D-n_0)$	(moment of inertia of hull cross section)
I_C	$= Z_h\ B/2$	(moment of inertia about the vertical neutral axis)
y	$= B/2 - (h+t_p)$	(distance in m from vertical neutral axis to considered member)
ρ_{vh}	$= 0.1$	(average correlation between vertical and horizontal wave induced bending stress from 3.4.4)

y $= 42/2 - (0.25+0.0165)$ = 20.73 m

$$\Delta\sigma_v = 2.1(1560.2 \cdot 10^3 - (-1665.1 \cdot 10^3)) \frac{|13.06 - 8.2|}{23.1 \cdot (20.3 - 8.2)} = 117.77\ \text{N/mm}^2$$

$$\Delta\sigma_{hg} = 2.1 \cdot 2 \cdot 884.5 \cdot 10^3 \frac{|20.73|}{40.1 \cdot 21.00} = 91.45\ \text{N/mm}^2$$

$$\Delta\sigma_g = \sqrt{117.77^2 + 91.45^2 + 2 \cdot 0.1 \cdot 117.77 \cdot 91.45} = \underline{156.16\ \text{N/mm}^2}$$

7.3.7.6 Combined hot-spot stresses

The combined stress range is corrected for an assumed zero mean stresses level, f_m = 0.9, and assumed world wide trading routes, f_e = 0.8. The combined hot spot stress at the 10^{-4} level is then calculated to be

$$\Delta\sigma = f_e \max\begin{cases}\Delta\sigma_g + b\cdot\Delta\sigma_l \\ a\cdot\Delta\sigma_g + \Delta\sigma_l\end{cases}$$ (the combined global and local stress range)

where

a, b Load combination factors, accounting for the correlation between the wave induced local and global stress range equal 0.6

$$\Delta\sigma = 0.8 \max\begin{cases}156.16 + 0.6\cdot 279.38 \\ 0.6\cdot 156.16 + 279.38\end{cases}$$

$\Delta\sigma$ = 298.46 N/mm^2

With a correction for mean stress according to 2.2.4 assuming zero mean stress, the stress range to be used in fatigue calculations becomes

$\Delta\sigma_o = f_m \cdot \Delta\sigma$

$\Delta\sigma_o = 0.85 \cdot 298.46 = \underline{253.69 \text{ N/mm}^2}$

7.3.7.7 Long term distribution

The period of roll is found to be T_R = 14.59 sec. Using this roll period the Weibull shape parameter for the location of considered detail is calculated according to 3.2.2

$h = h_0 + h_a z/T_{act} - 0.005(T_{act} - z)$ (for ship side below the water line)

$h_0 = 2.21 - 0.54 \log(L)$

where

$h_a = 0.0$ (factor depending on the motion response period)

$h_0 = 2.21 - 0.54 \log(221) = 0.944$

$h = 0.944 + 0.00 - 0.005(14.20 - 13.06) = \underline{0.938}$

(A possible check is here to consult Table 2.8 using the above Weibull parameter, h, and stress range, $\Delta\sigma_o$.)

7.3.7.8 Fatigue part damage

The part damage in the fully loaded condition over 20 years design life is calculated according to 2.1.2, for the one slope in Air curve to be

$$D = \frac{\nu_0 T_d}{\bar{a}} p_{full} q_{full}{}^m \Gamma\left(1 + \frac{m}{h}\right)$$

where

$$\nu_0 T_d = \frac{20\cdot 365\cdot 24\cdot 3600}{4Log_{10}(L)}$$ (the number of cycles during 20 years)

$\Gamma(1 + \frac{m}{h})$ (the value of the gamma function from Table 2.7)

$q_{full} = \frac{\Delta\sigma_0}{(\ln n_0)^{1/h}}$ (the Weibull scale parameter)

$n_0 = 10^4$ (total number of cycles associated with the probability level 10^{-4} and the $\Delta\sigma_0$)

$p_n = 0.45$ (part of time fully loaded)

$\Delta\sigma_0 = 253.69$ N/mm^2 (considered stress range)

$h = 0.938$ (the Weibull shape parameter)

$\bar{a} = 5.75 \cdot 10^{12}$ (S-N Curve parameter for the curve Ib)

$m = 3.0$ (S-N Curve parameter for the curve Ib)

$\nu_0 T_d = \frac{20 \cdot 365 \cdot 24 \cdot 3600}{4 Log_{10}(221)} = 6.7 \cdot 10^7$

$\Gamma(1+\frac{m}{h}) = 8.024 - 8 \cdot (8.024-7.671)/10 = 7.742$

$q_{full} = \frac{253.69}{(\ln 10^4)^{1/0.938}} = 23.78$ N/mm^2

$D_n = \frac{6.7 \cdot 10^7}{5.75 \cdot 10^{12}} 0.45 \cdot 23.78^{3.0} \cdot 7.742 = \underline{0.546} = \underline{0.546}$

or calculated with the two slope curve D_n = $\underline{0.601}$

7.3.8 Calculation for Load condition - Ballast (BL)

7.3.8.1 Internal pressure loads

The longitudinal is located in a ballast tank using density of water, 1.025 tonn/m^3. The accelerations and pressures are calculated according to 4.4.1 for the ballast tank as

a_v = 4.96 m/s^2

a_t = 4.57 m/s^2

a_l = 1.13 m/s^2

h_s = 7.24 m

y_s = 1.50 m

x_s = 11.25 m

p_1 = 36.81 kN/m^2

p_2 = 7.02 kN/m^2

p_3 = 12.71 kN/m^2

The local internal pressure amplitude at the 10^{-4} probability level is then calculated according to 4.4 as

$$p_i = f_a \max \begin{cases} p_1 = \rho a_v \, h_s \\ p_2 = \rho a_t \, |y_s| \\ p_3 = \rho a_l \, |x_s| \end{cases}$$

where

$f_a = 0.4979$ (from fully loaded condition in 7.3.7.1)

$$p_i = 0.497 \max \begin{cases} p_1 = 1.025 \cdot 4.96 \cdot 7.24 \\ p_2 = 1.025 \cdot 4.57 \cdot |1.50| \\ p_3 = 1.025 \cdot 1.13 \cdot |11.25| \end{cases}$$

p_i = $\underline{18.33 \text{ kN/m}^2}$

The effective net pressure outwards for calculation of double hull bending is taken from the transverse acceleration according to 7.2.4 (the pressures p_1 and p_3 do not contribute to double hull bending since they act on both inner and outer hull).

$p_{i,dh} = 2\ p_2 = 2\ f_a\ \rho\ a_t |y_s|$

$p_{i,dh} = 2 \cdot 0.4979 \cdot 1.025 \cdot 4.57 \cdot 1.5 = \underline{7.00 \text{ kN/m}^2}$

The above pressure is also applied for the stresses from relative deflection between the bulkhead and the frame as the vessel has horizontal framing in the double hull. ($p_{i,\delta} = p_{i,dh}$)

7.3.8.2 External sea pressure loads

The sea pressure is calculated according to 4.3.1

$p_e = r_p p_d$

where

$$p_d = 10\left[|y|\frac{\phi}{2} + C_B \frac{|y| + k_f}{16}\left(0.7 + 2\frac{z_w}{T_{act}}\right)\right]$$ (dynamic pressure amplitude below the waterline dominated by roll motion)

$$r_p = \frac{T_{act} + z_{wl} - z}{2 z_{wl}}$$ (reduction of pressure amplitude to the considered point in the wave zone)

ϕ = 50 c / (B + 75) (maximum roll angle as described in 4.5.1)

c = (1.25 – 0.025 T_R) k

$T_R = 2\ k_R / \sqrt{GM}$ (period of roll, maximum 30 (s))

$z_{wl} = \frac{3}{4}\frac{p_{dT}}{\rho g}$ (distance from actual water line. It is assumed that the external sea pressure above $T_{act} + z_{wl}$ will not contribute to fatigue damage)

z_w = z Maximum T_{act} (vertical distance from the baseline to the load point)

$p_{dt} = p_d$ at $z_w = T_{act}$

k = 1.0 (for ship with bilge keel)

f = 13.10 m (vertical distance from the waterline to the top of the ship's side)

$$k_f = \min\begin{cases} T_{act} \\ f \end{cases}$$ (the smallest of T_{act} and f = 7.2 m)

y = 21.00 m (horizontal distance from the centre line to the loadpoint)

$z_w = T_{act} = 7.2$ m

$T_R = 2 \cdot 16.38 / \sqrt{13.86}$. $= 8.80$ sec

$c = (1.25 - 0.025 \cdot 8.80) \, 1.0$ $= 1.03$

$\phi = 50 \cdot 1.03 / (42 + 75)$ $= 0.440$

$$p_d = 10\left[|\,21.00\,| \frac{0.440}{2} + 0.83 \frac{|\,21.00\,| + 7.20}{16}\left(0.7 + 2\frac{7.20}{7.20}\right)\right] = 85.70 \text{ kN/m}^2$$

$p_{dt} = p_d = 85.70$ kN/m^2 $(z_w = T_{act})$

$z_{wl} = 3 \cdot 85.70 / (4 \cdot 1.025 \cdot 9.81) = 6.39$ m

$r_p = \dfrac{7.20 + 6.39 - 13.06}{2 \cdot 6.39}$ $= 0.041$

$p_e = 0.041 \cdot 85.70$ $=$ <u>3.51 kN/m^2</u>

The pressure $p_\delta = p_e$ is applied in the evaluation of relative deflection as the hull has horizontal frames.

The effective "smeared out" double hull pressure is estimated as

$p_{e,dh} = p_e \; T_{act} / D = 3.51 \cdot 7.20/20.3$ $=$ <u>1.24 kN/m^2</u>

7.3.8.3 Combination of stress components

The stress amplitudes due to internal and external pressures are combined considering the sign. Positive stress is defined as tension at the location of the weld

Stresses due to external pressure loads

+ Stiffener bending (p_e = 3.51 kN/m^2)	$c \cdot 3.51 \cdot 2.552$:	-8.96 N/mm^2
+ Relative deflection ($p_{e,\delta}$ = 3.51kN/m^2)	$c \cdot 3.51 \cdot 1.309$:	-4.59 N/mm^2
+ Double hull bending ($p_{e,dh}$ = 1.24 kN/m^2)	t $1.24 \cdot 1.006$:	<u>1.25 N/mm^2</u>
= Stresses from external sea pressure loads	σ_e =	<u>-12.30 N/mm^2</u>

Stresses due to internal pressure loads

+ Stiffener bending (p_i = 18.33 kN/m^2)	$t \cdot 18.33 \cdot 2.552$:	46.78 N/mm^2
+ Relative deflection ($p_{i,\delta}$= 7.00 kN/m^2)	t $7.00 \cdot 1.309$:	9.16 N/mm^2
+ Double hull bending ($p_{i,dh}$= 7.00 kN/m^2)	c $7.00 \cdot 1.006$:	<u>- 7.04 N/mm^2</u>
= Stresses from internal pressure loads	σ_i =	<u>48.90 N/mm^2</u>

t = 1 tension

c = -1 compression

The combined local stress is determined according to 3.4.5 as

$$\Delta\sigma_l = 2\sqrt{\sigma_e^2 + \sigma_i^2 + 2\rho_p \sigma_e \sigma_i}$$

$$\rho_p = \frac{1}{2} - \frac{z}{10T_{act}} + \frac{|x|}{4L} + \frac{|y|}{4B} - \frac{|x| \cdot z}{5LT_{act}}$$

where

x, *y* and *z* are the coordinates of the load point, according to the coordinate system described in 3.4.5 with origo = (midship, centreline, baseline)

$x = 0$ m

$y = 21.00$ m

$z = T_{act} = 7.20$ m (z > T_{act})

$$\rho_p = \frac{1}{2} - \frac{7.20}{10 \cdot 7.20} + \frac{|0|}{4 \cdot 221} + \frac{|21.00|}{4 \cdot 42} - \frac{|0| \cdot 7.20}{5 \cdot 221 \cdot 7.20} \qquad = 0.525$$

$$\Delta\sigma_l = 2\sqrt{(-12.30)^2 + 48.90^2 + 2 \cdot 0.525 \cdot (-12.30) \cdot 48.90} \qquad = \underline{87.43\ \text{kN/m}^2}$$

7.3.8.4 Global hull bending moments

The vertical wave wave bending moments are computed according to 4.2.1 as

$M_{wo,h} = -0.11 \cdot f_r \cdot k_{wm} \cdot C_w \cdot L^2 \cdot B \cdot (C_B + 0.7)$ (sagging moment)

$M_{wo,s} = -0.19 \cdot f_r \cdot k_{wm} \cdot C_w \cdot L^2 \cdot B \cdot C_B$ (hogging moment)

The horizontal wave bending moment is calculated according to 4.2.2 as

$M_H = 0.22\ f_r\ L^{9/4}\ (T_{act} + 0.30\ B)\ C_B\ (1-\cos(2\pi x/L))$

where

$x = L/2$ (distance from A.P to considered point)

$f_r = 0.5^{1/0,944} = 0.4799$ (calculated in 7.3.7.4)

The vertical bending moments for the 10^{-4} level are the same as calculated for the fully loaded condition in 7.3.7.4

For $f_r = 1.0$ (10^{-8} probability level)

$M_{w0,s}$	$= -0.11 \cdot 1.0 \cdot 1.0 \cdot 10.05 \cdot 221^2 \cdot 42 \cdot (0.83 + 0.7)$	$=-3469.6 \cdot 10^3$kNm
$M_{w0,h}$	$= 0.19 \cdot 1.0 \cdot 1.0 \cdot 10.05 \cdot 221^2 \cdot 42 \cdot 0.83$	$=3251.1 \cdot 10^3$ kNm
M_H	$= 0.22 \cdot 1.0 \cdot 221^{9/4} \cdot (7.20 + 0.30 \cdot 42)\ 0.83\ (1-\cos(\pi))$	$=1361.7 \cdot 10^3$ kNm

For $f_r = 0.4799$ (10^{-4} probability level)

$M_{w0,s}$	$= -0.11 \cdot 0.4799 \cdot 1.0 \cdot 10.05 \cdot 221^2 \cdot 42 \cdot (0.83 + 0.7)$	$=-1665.1 \cdot 10^3$kNm
$M_{w0,h}$	$= 0.19 \cdot 0.4799 \cdot 1.0 \cdot 10.05 \cdot 221^2 \cdot 42 \cdot 0.83$	$=1560.2 \cdot 10^3$ kNm
M_H	$= 0.22 \cdot 0.4799 \cdot 1.0 \cdot 221^{9/4} \cdot (7.20 + 0.30 \cdot 42)\ 0.83\ (1-\cos(\pi))$	$= 653.5 \cdot 10^3$ kNm

7.3.8.5 Stresses from global loads

The vertical and horizontal bending moments results in the following stress ranges, according to 3.5.2 and 3.5.3 at the 10^{-4} level

$$\Delta\sigma_v = K_{axial}(M_{Wo.h} - M_{Wo.s})\frac{(z - n_0)}{I_N} \qquad \text{(vertical global stress range)}$$

$\Delta\sigma_{hg} = 2\,K_{axial} M_H \; 10^{-3} \dfrac{|y|}{I_C}$ (horizontal global stress range)

$\Delta\sigma_g = \sqrt{\Delta\sigma_V{}^2 + \Delta\sigma_{hg}{}^2 + 2\rho_{vh}\Delta\sigma_V\Delta\sigma_{hg}}$ (combined global stress range)

where

I_N = Z_v (D-n_0) (moment of inertia of hull cross section)

I_C = Z_h B/2 (moment of inertia about the vertical neutral axis)

y = B/2 – (h+t_p) (distance in m from vertical neutral axis to considered member)

ρ_{vh} = 0.1 (taken from 7.3.7.5)

y = 42/2 – (0.25+0.0165) = 20.73 m

$\Delta\sigma_v = 2.1(1560.2\cdot 10^3 - (-1665.1\cdot 10^3))\dfrac{|13.06-8.2|}{23.1\cdot(20.3-8.2)}$ = 117.77 N/mm^2

$\Delta\sigma_{hg} = 2.1\cdot 2\cdot 653.5\cdot 10^3 \dfrac{|20.73|}{40.1\cdot 21.00}$ = 67.57 N/mm^2

$\Delta\sigma_g = \sqrt{117.77^2 + 67.57^2 + 2\cdot 0.1\cdot 117.77\cdot 67.57}$ = 141.52 N/mm^2

7.3.8.6 Combined hot-spot stresses

The combined stress range is corrected for an assumed zero mean stresses level, f_m = 0.9, and assumed world wide trading routes, f_e = 0.8. The combined hot spot stress at the 10^{-4} level is then calculated to be

$\Delta\sigma = f_e \max\begin{cases}\Delta\sigma_g + b\cdot\Delta\sigma_l \\ a\cdot\Delta\sigma_g + \Delta\sigma_l\end{cases}$ (the combined global and local stress range)

where

a, b Load combination factors, accounting for the correlation between the wave induced local and global stress range = 0.6

$\Delta\sigma = 0.8 \max\begin{cases}141.52 + 0.6\cdot 87.43 \\ 0.6\cdot 141.52 + 87.43\end{cases}$

$\Delta\sigma$ = 155.18 N/mm^2

With a correction for mean stress according to 2.2.4 assuming zero mean stress, the stress range to be used in fatigue calculations becomes

$\Delta\sigma_o = f_m \cdot \Delta\sigma$

$\Delta\sigma_o = 0.85 \cdot 155.18 =$ 131.9 N/mm^2

7.3.8.7 Long term distribution

The period of roll is found to be T_R = 8.80 sec. Using this roll period, the Weibull shape parameter at the considered location is, according to 3.2.2

h = $h_0 + h_a(D-z)/(D-T_{act})$ (for ship side above the water line)

h_0 = 2.21 – 0.54 log(L)

where

h_a = 0.05 (factor depending on the motion response period)

h_0 = 2.21 – 0.54 log(221) = 0.944

h = 0.944 + 0.05(20.3 – 13.06)/(20.3-7.20) = <u>0.972</u>

A possible check is here to consult Table 2.8 using the above Weibull parameter, h, and stress range, $\Delta\sigma_o$.

7.3.8.8 Fatigue part damage

The part damage in the ballasted condition over 20 years design life is calculated according to 2.1.2, for the one slope in Air curve to be

$$D = \frac{\nu_0 T_d}{\bar{a}} p_{ballast} q_{ballast}^m \Gamma\left(1+\frac{m}{h}\right)$$

where

$$\nu_0 T_d = \frac{20 \cdot 365 \cdot 24 \cdot 3600}{4 Log_{10}(L)}$$ (the number of cycles during 20 years)

$\Gamma(1+\frac{m}{h})$ (the value of the gamma function from Table 2.7)

$$q_{ballast} = \frac{\Delta\sigma_0}{(\ln n_0)^{1/h}}$$ (the Weibull scale parameter)

$n_0 = 10^4$ (total number of cycles associated with the probability level 10^{-4} and the $\Delta\sigma_0$)

p_n =0.40 (part of time ballasted)

$\Delta\sigma_0$ = 131.9 N/mm^2 (considered stress range)

h = 0.972 (the Weibull shape parameter)

$\bar{a}$ = $5.75 \cdot 10^{12}$ (S-N Curve parameter for the curve Ib)

m = 3.0 (S-N Curve parameter for the curve Ib)

$$\nu_0 T_d = \frac{20 \cdot 365 \cdot 24 \cdot 3600}{4 Log_{10}(221)} = 6.7 \cdot 10^7$$

$$\Gamma(1+\frac{m}{h}) = 6.750 - 2 \cdot (6.750-6.483)/10 = 6.697$$

$$q_{ballasted} = \frac{131.9}{(\ln 10^4)^{1/0.972}} = 13.43 \text{ N/mm}^2$$

$$D_n = \frac{6.7 \cdot 10^7}{5.75 \cdot 10^{12}} 0.40 \cdot 13.43^{3.0} \cdot 6.697 = \underline{0.0757}$$

or calculated with the two slope curve D_n = <u>0.052</u>

7.3.9 Fatigue life calculated from the one slope S-N Curve Ib

The total fatigue damage during 20 years is found by summing the part damage from each of the loading, and checking the damage up against the criteria in 2.1.2

$$D = \frac{\nu_0 T_d}{\bar{a}} \sum_{n=1}^{N_{load}} p_n q_n^m \Gamma(1 + \frac{m}{h_n}) = \sum_{n=1}^{N_{load}} D_n \le \eta$$

Where η is the usage factor. If the criteria is fulfilled the fatigue damage is considered acceptable. Using the estimated values from the S-N Curve Ib

$D = 0.546 + 0.076 = \underline{0.622}$

When considering the corrosive environment the χ- factor from 2.5.1 increased fatigue damage

$D = 0.622\ \chi = 0.622 \cdot 1.3 = 0.809$

If the usage factor η = 1.0, the life of the considered part is

$T_{life} = 20 / 0.809 = \underline{24.7 \text{ years}}$.

The most exactly calculated values are from the two slope S-N Curve I. The complete calculation of fatigue life in 7.3.10 is calculated based on these values.

7.3.10 Fatigue life calculated from the two slope S-N Curve I

The total fatigue damage during 20 years is found by summing the part damages from each load condition. The accumulated fatigue is then checked against the criteria in Section 2.1. Using the In-Air, curve I, the damage is

$$D = \frac{\nu_0 T_d}{\bar{a}} \sum_{n=1}^{N_{load}} p_n q_n^m \Gamma(1 + \frac{m}{h_n}) = \sum_{n=1}^{N_{load}} D_n = 0.601 + 0.052 = \underline{0.653}$$

When considering the corrosive environment after the 15 years of efficient corrosion protection, the factor χ = 1.3, may as a simplification be used to estimate fatigue life as

$D_{cor} = 0.653 \cdot 1.3 = 0.849$

$T_{life} = 20 / 0.849 = 23.6$ years

A more direct approach, is to scale the damage after the efficient life of the coating, $T_{coating}$ + 5 years = 15 years , has passed by the difference between the In-air and corrosive environment SN-curves, which is commonly set to a factor of 2.3. In this case the difference between the in-air and corrosive SN-curves I and II are calculated to be a factor of 2.24

$T_{life\_in\_air} = 20 / 0.653 = 30.6$ years

$T_{life} = T_{coating} + (T_{life\_in\_air} - T_{coating})/2.24 = 15 + (30.6 - 15)/2.24 = \underline{22 \text{ years}}$

$D_{corr} = 20 / 22 = 0.91$

Further, a direct account for the mean stress level according to 2.2.4 would give a more favourable life estimate, as the detail in this example, is under static compression in the most severe condition - the fully loaded. The resulting mean stress factors would be $f_m = 0.74$ for the fully loaded and $f_m = 1.00$ for the ballast conditions. This will result in a fatigue life of 26.3 years and will thus be acceptable by a small margin.

The conclusion is that the detail has an acceptable fatigue life.

8. Fatigue analysis of bulk carriers

8.1 Where to analyse

8.1.1

Fatigue damages are known to occur more frequently for some ship types and categories of hull structure elements. The fatigue life is in particular related to the magnitude of the dynamic stress level, the corrosiveness of the environment and the magnitude of notch- and stress concentration factors of the structural details, which all vary depending on ship type and structure considered. The importance of a possible fatigue damage is related to the number of potential damage points of the considered type for the ship or structure in question and to its consequences.

Structure member	*Structural detail*	*Load type*
Hatch corners	Hatch corner	Hull girder bending, hull girder torsional deformation
Hatch side coaming	Termination of end bracket	Hull girder bending
Main frames	End bracket terminations, weld of main frame web to shell for un-symmetrical main frame profiles	External pressure load, ballast pressure load as applicable
Longitudinals of hopper tank and top wing tank	Connection to transverse webs and bulkheads	Hull girder bending, sea- and ballast pressure load
Double bottom longitudinals[1)]	Connection to transverse webs and bulkheads	Hull girder bending stress, double bottom bending stress and sea-, cargo- and ballast pressure load
Transverse webs of double bottom, hopper and top wing tank	Slots for panel stiffener including stiffener connection members, knuckle of inner bottom and sloped hopper side including intersection with girder webs (floors). Single lug slots for panel stiffeners, access and lightening holes	Girder shear force, and bending moment, support force from panel stiffener due to sea-,cargo- and ballast pressure load

1) The fatigue life of bottom and inner bottom longitudinals of bulk carriers is related to the combined effect of axial stress due to hull girder- and double bottom bending, and due to lateral pressure load from sea or cargo.

Table 8.1 Bulk Carriers

8.1.2

A major fraction of the total number of fatigue damages on ship structures occurs in panel stiffeners on the ship side and bottom and on the tank boundaries of ballast- and cargo tanks. However, the calculated fatigue life depends on the type of stiffeners used, and the detail design of the connection to supporting girder webs and bulkheads. In general un-symmetrical profiles will have a reduced fatigue life compared to symmetrical profiles unless the reduced efficiency of the un-symmetrical profile is compensated by an improved design for the attachment to transverse girder webs and bulkhead structures.

8.1.3

Structural elements in the cargo area being of possible interest for fatigue evaluation are listed in Tables 8.1 and 8.2.

Structure member	*Structural detail*	*Load type*
Upper deck plating	Hatch corners and side coaming terminations	Hull girder bending
Side-, bottom- and deck longitudinals	Butt joints and attachment to transverse webs, transverse bulkheads, hatch opening corners and intermediate longitudinal girders	Hull girder bending, stiffener lateral pressure load and support deformation
Transverse girder and stringer structures	Bracket toes, girder flange butt joints, curved girder flanges, panel knuckles at intersection with transverse girder webs etc. Single lug slots for panel stiffeners, access and lightening holes	Sea pressure load combined with cargo or ballast pressure load
Transverse girders of wing tank[1)]	Single lug slots for panel stiffeners	Sea pressure load (in particular in ore loading condition)

1) The transverse deck-, side- and bottom girders of the wing tanks in the ore loading condition are generally subjected to considerable dynamic shear force- and bending moment loads due to large dynamic sea pressure (in rolling) and an increased vertical racking deflection of the transverse bulkheads of the wing tank. The rolling induced sea pressure loads in the ore loading condition will normally exceed the level in the ballast (and a possible oil cargo) condition due to the combined effect of a large GM-value and a small rolling period. The fatigue life evaluation must be considered with respect to the category of the wing tank considered (cargo oil tank, ballast tank or void). For ore-oil carriers, the cargo oil loading condition should be considered as for tankers.

Table 8.2 Ore Carriers

8.2 Fatigue analysis

The procedure below may be applicable to the simplified fatigue analysis of bulk carriers.

8.2.1

The internal loads will be calculated according to 4.4.1. It is noted that for bulk and ore cargoes, only p_1 need to be considered. The appropriate density and pressure height for bulk cargoes should specially be considered to give a hold mass according to Table 8.3.

	Ore holds	*Empty holds*
Alternate condition	M_{HD} or M_{Full} according to Pt.5 Ch.2 Sec.5	Zero
Homogenous condition	M_H according to Rules Pt.5 Ch.2 Sec.5	M_H according to Rules Pt.5 Ch.2 Sec.5

Table 8.3 Hold mass

If masses specified in the submitted loading conditions are greater than those in Table 8.3, the maximum masses shall be used for fatigue strength calculations.

The external loads shall be taken according to 4.3.1. The draught for the loaded conditions shall be taken as the scantling draught. The draught for the ballast condition shall be taken as the ballast draught given in the loading manual, or 0.35T if the loading manual is not available. (Where T is scantling draught).

Hull girder bending moments shall be calculated according to 4.2.1.

For vessels intended for normal trading the fraction of the total design life spent at sea, should not be taken less than 0.85. The fraction of the design life in the fully loaded and ballast conditions, p_n, may be taken from Table 8.4.

Vessel type	*Bulk carriers larger than Panamax (*)*	*Panamax bulk carriers and smaller (*)*	*Vessels intend to carry ore cargoes mostly*
Alternate condition	0.25	0	0.5
Homogenous condition	0.25	0.5	0
Ballast condition	0.35	0.35	0.35

(*) Panamax vessel as defined in Classification Note 31.1 Sec.1.2.1

Table 8.4 Fraction of time at sea, p_n

8.2.2

Stresses due to stiffener bending shall be taken according to 3.5.4.

For bottom and inner bottom longitudinals the effect of relative deflections shall be taken into account at locations where this effect is significant. The relative deformations is to be obtained by a direct strength analysis (Classification Note 31.1 show modelling examples).

Local secondary double bottom stresses according to 3.5.3 shall be taken into account.

The local stress ranges shall be combined according to 3.4.5.

Stress concentration factors shall be taken according to Chapter 10.

8.2.3

Global stress ranges shall be calculated according to 3.5.1 and 3.5.2

The global stress ranges shall be combined according to 3.4.4.

8.2.4

The local and global stress ranges shall be combined according to 3.4.3 taking into account the reduction factor, f_e in 3.4.3 and mean stress reduction factor, f_m in 2.2.3 or 2.2.4.

Calculate the fatigue damage according to 2.1.2 for all the fatigue load cases. For effective corrosion protection periods, see 2.4.

8.3 Example of Application, Bulk Carrier (Simplified methods example)

8.3.1 Introduction

In this Appendix an example of the fatigue assessment of welded connection between a longitudinal and a flat bar in the inner bottom is considered. Before starting to calculate the stresses it may be of relevance to decide what loads and load conditions and the level of detail shall be considered for the calculation of stresses. The following observations have implications on how the calculations are made.

A) The analysis is to be performed according to the simplified procedure, see Figure 1.1, with some additional input from finite element analysis. The loads may be taken in accordance with Chapter 4. The local and global loads are based on the main dimensions of the vessel given in Table 8.5. Further the Rules [1] describes minimum requirements to the corrosive environment. Special consideration should be given to Section 8.2.

B) The considered detail is a termination of a web stiffener on top of a longitudinal. The simplified stress calculation procedure as defined in Chapter 3 is normally sufficient (reference is also made to Section 8.2). In this example, the connection between a longitudinal and a transverse floor in the ships inner bottom is considered, using the simplified method.

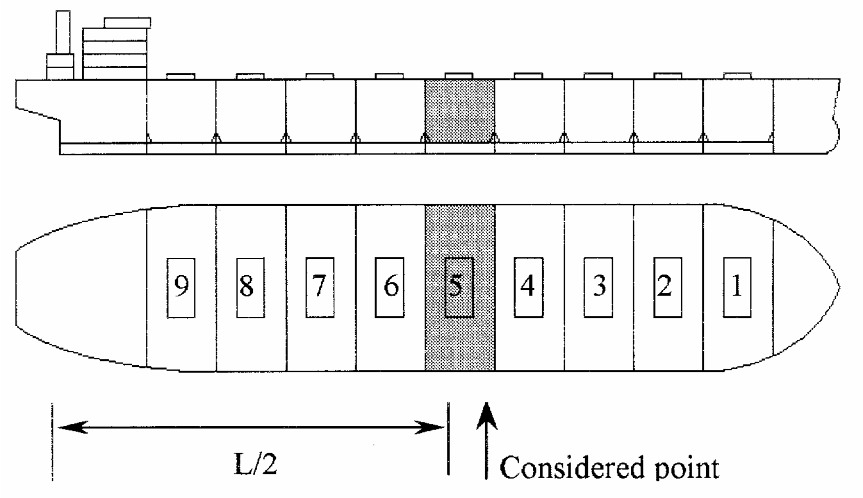

Figure 8.1 View of ship and location of detail in ship

Length of ship	L	=	275	m
Breadth of ship	B	=	45	m
Depth of ship	D	=	24.1	m
Block coefficient	C_B	=	0.85	
Design speed	V	=	15	knots
Vertical section modulus at deck line	Z_N	=	40.79	m^3
Neutral axis above keel	n_0	=	10.59	m
Horizontal section modulus in ships side	Z_C	=	62.66	m^3
Total deadweight capacity		=	150000	t
Total hold volume		=	174420	m^3
Volume hold 5	V_H	=	18410	m^3
Maximum homogenous mass in hold 5	M_H	=	15833	t
Maximum alternate mass in hold 5	M_{HD}	=	28350	t
Ore holds		1, 3, 5, 7, 9		
Empty holds		2, 4, 6, 8		
Ballast hold		6		
Class notation		**+1A1** Bulk Carrier **BC-A**		
Target fatigue life		20 years		

Table 8.5 The example ship's main dimensions

8.3.2 Geometry of longitudinal and bracket termination

It may be practical to calculate the stress per unit bending moment and per unit lateral pressure and scale these with the relevant values for each load condition. It is primarily the calculation of stresses due to lateral pressure that will be simplified by such an approach. For a web stiffener termination on top of a stiffener, the stresses to be considered related to lateral pressure are due to

- stiffener bending
- relative deflection between the two floors
- double hull bending

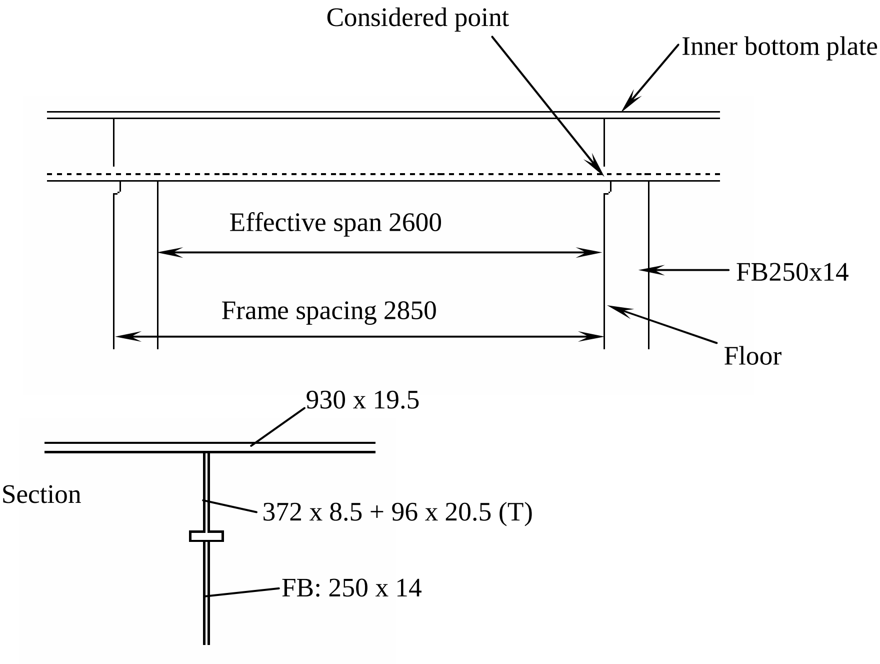

Figure 8.2 Description of the considered detail

Stiffener section modulus at top flange	Z_s	=	$0.921\ 10^{-3}$	m^3
Distance above keel	z	=	2.088	m
Effective span as defined in Figure 3.4	l	=	2600	mm
Height of stiffener on top	b	=	250	mm
Distance from end of stiffener to hot spot	x	=	0	mm
Web frame spacing	l_s	=	2850	mm
Breadth of plating	s	=	930	mm
Thickness of plate	t_p	=	19.5	mm
Height of stiffener	h	=	372	mm
Thickness of web	t_w	=	8.5	mm
Width of flange	b_f	=	96	mm
Thickness of flange	t_f	=	20.5	mm
Distance from neutral axis to top of flange	Z_{01}	=	233.5	mm

Table 8.6 Geometry of stiffener considered, T-profile

The stresses are to be calculated based on reduced scantlings. Here it is assumed that the corrosion addition is subtracted, and the dimensions given in Table 8.6 are reduced scantling values. The stresses are calculated at the considered point on the weld connection of stiffener on top and longitudinal stiffener as shown in Figure 8.2.

8.3.3 Load conditions

The load conditions to be considered are given in 8.2. For the considered vessel, i.e. a 'Capesized' bulk carrier, three load cases have been taken into account.

1) Alternate loaded, with fraction of time $p_n = 0.25$
2) Homogeneously loaded, with fraction of time $p_n = 0.25$
3) Ballast, with fraction of time $p_n = 0.35$

The load conditions should be defined in terms of draughts, GM and K_R as given in Table 8.7 for the considered vessel. Guidance for choice of these values is given in Sections 4.5 and 8.2.

The density and corresponding filling height are calculated according to 8.2.1.

$h_s = 26.3$ m (Filling to top of coaming)

$V_H = 18410$ m^3 (No 5 cargo hold volume to top of hatch)

$M_{HD} = 28350$ t (Maximum mass in hold no 5 in alternate condition)

$M_H = 15833$ t (Maximum mass in hold no 5 in homogenous condition)

Homogenous condition:

$M_H = 15833$ t (homogenous mass)

This mass will give the following filling height and density

$h_s = 26.3$ m ρ 15833/18410 = 0.86 t/m^3

Alternate condition:

This vessel has **BC-A** notation

$M_{HD} = 28350$ t (rules defined alternate mass)

This mass will give the following filling height and density:

$h_s = 26.3$ m $\rho = 28350 / 18410 = 1.54$ t/m^3

		Alternate	*Homogenous*	= *Ballast*
Draught	T_f	17.78 m	17.78 m	7.16 m
Metacentric height	GM	9.51 m	9.51 m	14.67 m
Roll gyradius	K_R	17.55 m	17.55 m	17.55 m
Part time in condition	p_n	0.25	0.25	0.35
Density	ρ	1.54 t/m^3	0.86 t/m^3	1.025 t/m^3
Filling height	h_s	26.3 m	26.3 m	24.7 m

Table 8.7 Definition of load conditions

8.3.4 K-factors

An important parameter in fatigue analysis is the stress concentration factor. The stress concentration factor describes the increase in notch stress due to local geometry, weld geometry and workmanship. The value of the K-factor has to be decided for the considered detail before the notch stresses can be calculated. Reference is made to Chapter 10.

For the weld at the end of a flat bar stiffener on top of the stiffener flange, the K-factor for axial stress (related to global loads) is taken according to Table 10.2.

$K_{axial} = K_g K_w = 2.1$

and K-factor for local stiffener bending stresses (induced by lateral pressure)

$K_{lateral} = K_g K_w = 2.4$

8.3.5 Calculation of stresses due to lateral pressure

8.3.5.1 General

The stresses to be considered due to lateral pressure are according to 3.5.4

$$\sigma_{2A} = K_{lateral} \frac{M}{Z_s} + K_{axial} \frac{m_\delta EI}{l^2 Z_s} r_\delta \cdot \delta = \sigma_{2A}' + \sigma_\delta$$

$$\sigma_2 = K_{axial} \cdot \sigma_{DB}$$

where

σ_{2A}' is stresses due to stiffener bending (8.3.5.2)

σ_δ is stresses caused by relative deflection between two adjacent frames (8.3.5.3)

σ_2 is stresses caused by bending of double hull (8.3.5.4)

The main particulars of the ship and the geometry of the stiffener are given in Tables 8.5 and 8.6 respectively. When using values not defined in either of the tables the values will be stated. When calculating the stresses and deflections, the unit lateral pressure, p_e, is 1 kN/m^2 and Young's modulus, E, is 2.1x10^5 N/mm^2.

8.3.5.2 Calculation of stresses due to stiffener bending

The stress due to stiffener bending is calculated as described in 3.5.5, accounting for the effective span of the longitudinal and the reduction of the effective bending moment at the weld toe.

The stress per unit lateral pressure (1 kN/m^2) is

$$\sigma_{2A}' = K_{lateral} \frac{M}{Z_s}$$

where

$M = \frac{psl^2}{12} r_p$ (bending moment at the considered point)

$r_p = 6\left(\frac{x}{l}\right)^2 - 6\left(\frac{x}{l}\right) + 1$ (reduction in bending moment)

$$r_p = 6\left(\frac{0}{2600}\right)^2 - 6\left(\frac{0}{2600}\right) + 1 = 1$$

$$\sigma_{2A}' = K_{lateral} \frac{psl^2}{12 Z_s} r_p$$

$$\sigma_{2A}' = 2.4 \frac{10^{-3} \cdot 930 \cdot 2600^2}{12 \cdot 0.921 \cdot 10^6} 1.0 = 1.365 \text{ N/mm}^2$$

To determine the stresses from the stiffener bending in the relevant loading conditions the bending stress is to be multiplied with the relevant dynamic pressure. For pressure load from cargo in hold there will be compression at the considered point and for pressure load from ballast there will be tension.

8.3.5.3 Relative deflection between frame and bulkhead

Stresses may also be induced due to relative deflections between the two adjacent frames. In order to determine the correct magnitude of the deflection, a finite element analysis is required. For a more detailed analysis of double hull vessel the relative deflection should be seen in connection with the double hull bending stresses.

$$\sigma_\delta = K_{axial} \frac{m_\delta EI}{l^2 Z_s} r_\delta \cdot \delta$$

where

$r_\delta = 1 - 2\left(\frac{x}{l}\right)$ (reduction factor for the moment at hotspot)

$$r_\delta = 1 - 2\left(\frac{0}{2600}\right) = 1$$

δ (relative deflection between the frames, taken from finite element analysis)

$\delta_{alternate,external}$ = +0.55 mm (Alternate condition, see 8.3.3)

$\delta_{homogenous,external}$ = +0.55mm (Homogenous condition, see 8.3.3)

$\delta_{ballast,external}$ = +0.29 mm (Ballast condition, see 8.3.3)

$\delta_{alternate,internal}$ = -1.93 mm (Alternate condition, see 8.3.3)

$\delta_{homogenous,internal}$ = -1.08 mm (Homogenous condition, see 8.3.3)

$\delta_{ballast,internal}$ = +0.00 mm (Ballast condition, see 8.3.3)

$$I = Z_s \cdot z_{01}$$

$$\sigma_\delta = K_{axial} \frac{m_\delta E z_{01}}{l^2} r_\delta \cdot \delta$$

$$\sigma_\delta = 2.1 \frac{4.4 \cdot 2.1 \cdot 10^5 \cdot 233.5}{2600^2} 1.0 \cdot \delta$$

$\sigma_{\delta,alternate,external}$ = +36.86 N/mm^2 (Tension)

$\sigma_{\delta,homogenous,external}$ = +36.86 N/mm^2 (Tension)

$\sigma_{\delta,ballast,external}$ = +19.44 N/mm^2 (Tension)

$\sigma_{\delta,alternate,internal}$ = -129.36 N/mm^2 (Compression)

$\sigma_{\delta,homogenous,internal}$ = -72.39 N/mm^2 (Compression)

$\sigma_{\delta,ballast,internal}$ = +0.00 N/mm^2

Since the deflection values are taken from a finite element analysis these stresses are reflecting the relevant dynamic pressure and are not based on 1 kN/m^2.

8.3.5.4 Double hull stresses

The longitudinal secondary stresses in the double bottom can be assessed by applying 3-D frame or finite element analyses. In this case the values are taken from the cargo hold finite element analysis.

$\sigma_{DB,alternate,external}$ = -2.91 N/mm^2 (Compression)

$\sigma_{DB,homogenous,external}$ = -2.91 N/mm^2 (Compression)

$\sigma_{DB,ballast,external}$ = -1.72 N/mm^2 (Compression)

$\sigma_{DB,alternate,internal}$ = +3.28 N/mm^2 (Tension)

$\sigma_{DB,homogenous,internal}$ = +2.54 N/mm^2 (Tension)

$\sigma_{DB,ballast,internal}$ = +0.00 N/mm^2

This gives us the following notch stresses:

$\sigma_{2,alternate,external}$ = -2.91 K_{axial} = -6.11 N/mm^2 (Compression)

$\sigma_{2,homogenous,external}$ = -2.91 K_{axail} = -6.11 N/mm^2 (Compression)

$\sigma_{2,ballast,external}$ = -1.72 K_{axial} = -3.61 N/mm^2 (Compression)

$\sigma_{2,alternate,internal}$ = +3.28 K_{axial} = +6.89 N/mm^2 (Tension)

$\sigma_{2,homogenous,internal}$ = +2.54 K_{axail} = +5.33 N/mm^2 (Tension)

$\sigma_{2,ballast,internal}$ = +0.00 K_{axial} = +0.00 N/mm^2

Since the double bottom stress values are taken from a finite element analysis these stresses are reflecting the relevant dynamic pressure and are not based on 1 kN/m^2.

8.3.6 Refining fatigue calculation parameters

8.3.6.1 SN-curve and corrosion protection

The detail is located in a coated ballast tank with cathodic protection. For a vessel with a minimum fatigue life of 20 years this implies that the SN-curve of Type I in air is applied for the first 15 years and the curve of Type II applies for the remainder of the time. This will result in a scaling of, χ = 1.3, when the calculated life is equal to the design life.

8.3.6.2 The environmental factor f_e

The vessel will trade in world wide operation and thus the environmental correction factor f_e = 0.8 may be applied as described in 3.4.3.

8.3.6.3 The effects of mean stress

The mean stress is to be calculated based on the mean stress of each load condition. In this example the approach is simplified by assuming that the stress is tension over the whole cycle for the ballast condition, f_m = 1.0, and compression for the loaded conditions, f_m = 0.7. This may be detailed by calculating the mean stress at the notch from still water loads and determining f_m from 2.2.3 or 2.3.4 for the relevant load condition.

8.3.7 Calculation for Load condition - Alternate

8.3.7.1 Internal pressure loads

Since the longitudinal is positioned in the double bottom ballast tank, which is empty in the loaded conditions, there will be no pressure from the ballast tank, giving rise to stiffener bending. The cargo in the hold will however cause local bending of the longitudinal. The accelerations and pressures are calculated according to 4.4.1 for the cargo hold.

For bulk and ore cargoes, only p_1 need to be considered this means that only vertical accelerations are of interest.

a_v = 2.43 m/s^2

h_s = 26.3 m

ρ = 1.54 t/m^3

p_1 = 94.42 kN/m^2

The lateral pressure caused by the vertical acceleration, a_v, scaled to the 10^{-4} level , is according to 4.4.1

$$p_i = f_a \rho a_v h_s$$

where

$f_a = 0.5^{1/h}$ (scaling factor to transform the load effect from probability level 10^{-4}, when the acceleration is specified at 10^{-8} level)

$h = h_0 + h_a$ (Weibull shape parameter, the shape parameter for bulkheads are used since this is an internal member)

$$h_0 = 2.21 - 0.54\log_{10}(L)$$

$$h_0 = 2.21 - 0.54\log_{10}(275) = 0.893$$

$$h = 0.893 + 0.05 = 0.943$$

$$f_a = 0.5^{1/0.943} = 0.479$$

$$p_i = 0.479 \cdot 1.54 \cdot 2.43 \cdot 26.3 = 47.14$$

8.3.7.2 External sea pressure loads

Since the considered longitudinal is an internal member there will be no contribution from seapressure.

8.3.7.3 Combination of stress components

The stress amplitude due to internal pressures is combined considering the sign. Positive stress is defined as tension at the location of the weld

Stresses due to external pressure loads

+ Stiffener bending	(p_e=0)		=	0 N/mm^2
+Relative deflection			=	+36.86 N/mm^2
+Double hull bending			=	-6.11 N/mm^2
= Stresses from external sea loads		σ_e	=	+30.75 N/mm^2

Stresses due to internal pressure loads

+ Stiffener bending	(p_i=47.14)	cx47.14x1.365	=	-65.35 N/mm^2
+ Relative deflection			=	-129.36 N/mm^2
+ Double hull bending			=	+6.88 N/mm^2
= Stresses from internal pressure loads		σ_i	=	-186.83 N/mm^2

t = 1 tension

c = -1 compression

The combined local stress range is determined according to 3.4.5 as

$$\Delta\sigma_l = 2\sqrt{\sigma_e^2 + \sigma_i^2 + 2\rho_p \sigma_e \sigma_i}$$

$$\rho_p = \frac{1}{2} - \frac{z}{10T_{act}} + \frac{|x|}{4L} + \frac{|y|}{4B} - \frac{|x| \cdot z}{5LT_{act}} \qquad z \le T_{act}$$

where

x, y and z are the co-ordinates for the load point, according to the co-ordinate system described in 3.4.5 with origo = (midship, centreline, baseline)

x= 23.75 m

y= 3.72 m

z= 2.088 m

$$\rho_p = \frac{1}{2} - \frac{2.088}{10 \cdot 17.78} + \frac{|23.75|}{4 \cdot 275} + \frac{|3.72|}{4 \cdot 45} - \frac{|23.75| \cdot 2.088}{5 \cdot 275 \cdot 17.78} = 0.528$$

$$\Delta\sigma_l = 2\sqrt{(+30.75)^2 + (-186.83)^2 + 2 \cdot 0.526 \cdot 30.75 \cdot (-186.83)} = 345.16 \text{ kN/mm}^2$$

8.3.7.4 Global hull bending moments

The vertical wave bending moment are computed according to 4.2.1 as

$$M_{wo,s} = -0.11 \cdot f_r \cdot k_{wm} \cdot C_w \cdot L^2 \cdot B \cdot (C_B + 0.7) \qquad \text{(Sagging)}$$

$$M_{wo,h} = 0.19 \cdot f_r \cdot k_{wm} \cdot C_w \cdot L^2 \cdot B \cdot C_B \qquad \text{(Hogging)}$$

The horizontal wave bending moment is calculated according to 4.2.2 as

$$M_H = 0.22 \cdot f_r \cdot L^{9/4} (T_{act} + 0.30B) C_B (1 - \cos(2\pi x / L))$$

where

$C_w = 10.75 - [(300 - L)/100]^{3/2}$ (wave coefficient)

$f_r = 0.5^{1/h0}$ (factor to transform from 10^{-8} to 10^{-4} probability level)

$h_0 = 2.21 - 0.54 \log_{10}(L)$ (long term Weibull shape parameter)

x = 161.25 (distance from AP to considered point)

k_{wm} = 1.0 (moment distribution factor)

$C_w = 10.75 - [(300 - 275)/100]^{3/2}$ = 10.625

$h_0 = 2.21 - 0.54 \log_{10}(275)$ = 0.893

$f_r = 0.5^{1/0.893}$ = 0.4601

$M_{wo,s} = -0.11 \cdot 0.4601 \cdot 1.0 \cdot 10.625 \cdot 275^2 \cdot 45 \cdot (0.85 + 0.7)$ = -2836.2 10^3 kNm

$M_{wo,h} = 0.19 \cdot 0.4601 \cdot 1.0 \cdot 10.625 \cdot 275^2 \cdot 45 \cdot 0.85$ = 2686.5 10^3 kNm

$M_H = 0.22 \cdot 0.4601 \cdot 275^{9/4} (17.78 + 0.30 \cdot 45) 0.85 (1 - \cos(2\pi 161.25/275))$ = 1538.4 10^3 kNm

8.3.7.5 Stresses from global loads

The vertical and horizontal bending moments result in the following stress ranges, according to 3.5.2 and 3.5.3 at the 10^{-4} level

$$\Delta\sigma_v = K_{axial}\left(M_{WO,h} - M_{WO,s}\right)\frac{(z-n_0)}{I_N}$$ (vertical global stress range)

$$\Delta\sigma_{hg} = K_{axial}\,2M_H\,\frac{|y|}{I_C}$$ (horizontal global stress range)

$$\Delta\sigma_g = \sqrt{\Delta\sigma_v^2 + \Delta\sigma_{hg}^2 + 2\rho_{vh}\Delta\sigma_v\Delta\sigma_{hg}}$$ (combined global stress range)

where

$I_N = Z_N\left(D - n_0\right)$ (moment of inertia of hull cross section)

$I_C = Z_C\; B/2$ (moment of inertia about the vertical neutral axis)

$\rho_{vh} = 0.1$ (average correlation between vertical and horizontal wave induced bending stress from 3.4.4)

$$\Delta\sigma_v = 2.1\left(2686.5\cdot 10^3 - \left(-2836.2\cdot 10^3\right)\right)\frac{|2.088-10.59|}{40.79(24.1-10.59)} = 178.93\ \text{N/mm}^2$$

$$\Delta\sigma_{hg} = 2.1\cdot 2\cdot 1538.4\cdot 10^3\ \frac{3.72}{62.66\cdot 45/2} = 17.05\ \text{N/mm}^2$$

$$\Delta\sigma_g = \sqrt{178.93^2 + 17.05^2 + 2\cdot 0.1\cdot 178.93\cdot 17.05} = 181.43\ \text{N/mm}^2$$

8.3.7.6 Combined hot spot stresses

The combined stress range is corrected for an assumed zero mean stress level, f_m = 0.7, and assumed world wide trading routes, f_e = 0.8. The combined hot spot stress at the 10^{-4} level is then calculated to be

$$\Delta\sigma = f_e\ \max\begin{cases}\Delta\sigma_g + b\cdot\Delta\sigma_l \\ a\cdot\Delta\sigma_g + \Delta\sigma_l\end{cases}$$ (the combined global and local stress range)

where

a, b Load combination factors, accounting for the correlation between the wave induced local and global stress range equal 0.6

$$\Delta\sigma = 0.8\max\begin{cases}181.43 + 0.6\cdot 345.16 = 388.53 \\ 0.6\cdot 181.43 + 345.16 = 454.02\end{cases}$$

$$\Delta\sigma = 363.21\ \text{N/mm}^2$$

With a correction for mean stress according to 2.2.4 assuming compression over the whole cycle, the stress range to be used in fatigue calculations become.

$$\Delta\sigma_o = f_m\cdot\Delta\sigma$$

$$\Delta\sigma_o = 0.7\cdot 363.21 = 254.25\ \text{N/mm}^2$$

8.3.7.7 Long term distribution

The Weibull shape parameter for the location of the considered detail is calculated according to 3.2.2

$$h = h_0 + h_a$$

$$h_0 = 2.21 - 0.54\log_{10}(L)$$

$$h_0 = 2.21 - 0.54\log_{10}(275) = 0.893$$

$$h = 0.893 + 0.05 = 0.943$$

(A possible check is here to consult Table 2.8 using the above Weibull parameter, h, and the stress range, $\Delta\sigma_o$.)

8.3.7.8 Fatigue part damage

The part damage in the alternate condition over 20 years fatigue life is calculated according to 2.1.2, for the one slope in Air curve to be

$$D_{alternate} = \frac{v_0 T_d}{\bar{a}} p_{alternate} \cdot q^m_{alternate} \cdot \Gamma\left(1+\frac{m}{h}\right)$$

where

$v_0 T_d = \dfrac{20\cdot 365\cdot 24\cdot 3600}{4Log_{10}(L)}$ (the number of cycles during 20 years)

$\Gamma\left(1+\dfrac{m}{h}\right)$ (the value of the gamma function from table 2.7)

$$q_{alternate} = \frac{\Delta\sigma_o}{(\ln n_0)^{1/h}}$$

$n_0 = 10^4$ (the total number of cycles associated with 10^{-4} level and stress range)

$p_n = 0.25$ (part of time alternate)

$\Delta\sigma_o = 254.25$ N/mm^2

h = 0.943

$\bar{a} = 5.75\cdot 10^{12}$ (SN Curve parameter for the curve Ib)

m = 3.0 (SN Curve parameter for the curve Ib)

$$v_0 T_d = \frac{20\cdot 365\cdot 24\cdot 3600}{4Log_{10}(275)} = 6.46\cdot 10^7$$

$$\Gamma\left(1+\frac{m}{h}\right) = 7.671 - 3(7.671 - 7.342)/10 = 7.572$$

$$q_{alternate} = \frac{254.25}{\left(\ln 10^4\right)^{1/0.943}} = 24.12 \text{ N/mm}^2$$

$$D_{alternate} = \frac{6.46\cdot 10^7}{5.75\cdot 10^{12}} 0.25\cdot 234.12^3 \cdot 7 - 572 = 0.299$$

8.3.8 Calculation for Load condition - Homogenous

8.3.8.1 Internal pressure loads

Since the longitudinal is positioned in the double bottom ballast tank, which is empty in the loaded conditions, there will be no pressure from the ballast tank, giving rise to stiffener bending. The cargo in the hold will however cause local bending of the longitudinal. The accelerations and pressures are calculated according to 4.4.1 for the cargo hold.

For bulk and ore cargoes, only p_1 need to be considered this means that only vertical accelerations are of interest.

a_v = 2.43 m/s^2

h_s = 26.3 m

ρ = 0.86 t/m^3

p_1 = 54.96 kN/m^2

The lateral pressure caused by the vertical acceleration, a_v, scaled to the 10^{-4} level , is according to 4.4.1

$p_i = f_a \rho a_v h_s$

where

$f_a = 0.5^{1/h}$ (scaling factor to transform the load effect from probability level 10^{-4}, when the acceleration is specified at 10^{-8} level)

$h = h_0 + h_a$ (Weibull shape parameter)

$h_0 = 2.21 - 0.54\log_{10}(L)$

$h_0 = 2.21 - 0.54\log_{10}(275) = 0.893$

$h = 0.893 + 0.05 = 0.943$

$f_a = 0.5^{1/0.943} = 0.479$

$p_i = 0.479 \cdot 0.86 \cdot 2.43 \cdot 26.3 = 26.33$

8.3.8.2 External sea pressure loads

Since the considered longitudinal is an internal member there will be no contribution from sea pressure.

8.3.8.3 Combination of stress components

The stress amplitude due to internal pressures is combined considering the sign. Positive stress is defined as tension at the location of the weld

Stresses due to external pressure loads

+ Stiffener bending (p_e=0)		=	0 N/mm^2
+Relative deflection		=	+36.86 N/mm^2
+Double hull bending		=	-6.11 N/mm^2
= Stresses from external sea loads	σ_e	=	+30.75 N/mm^2

Stresses due to internal pressure loads

+ Stiffener bending (p_i=26.33)	cx26.33x1.365	=	-35.94 N/mm^2
+ Relative deflection		=	-72.39 N/mm^2
+ Double hull bending		=	+5.33 N/mm^2
= Stresses from internal pressure loads	σ_i	=	-103.0 N/mm^2

t=1 tension

c=-1 compression

The combined local stress range is determined according to 3.4.5 as

$$\Delta\sigma_l = 2\sqrt{\sigma_e^2 + \sigma_i^2 + 2\rho_p \sigma_e \sigma_i}$$

$$\rho_p = \frac{1}{2} - \frac{z}{10T_{act}} + \frac{|x|}{4L} + \frac{|y|}{4B} - \frac{|x| \cdot z}{5LT_{act}} \qquad z \le T_{act}$$

where

x, y and z are the co-ordinates for the load point, according to the co-ordinate system described in 3.4.5 with origo = (midship, centreline, baseline)

x= 23.75 m

y= 3.72 m

z= 2.088 m

$$\rho_p = \frac{1}{2} - \frac{2.088}{10 \cdot 17.78} + \frac{|23.75|}{4 \cdot 275} + \frac{|3.72|}{4 \cdot 45} - \frac{|23.75| \cdot 2.088}{5 \cdot 275 \cdot 17.78} = 0.528$$

$$\Delta\sigma_l = 2\sqrt{(+30.75)^2 + (-103)^2 + 2 \cdot 0.528 \cdot 30.75 \cdot (-103)} = 181.22 \text{ kN/mm}^2$$

8.3.8.4 Global hull bending moments

The vertical wave bending moment are computed according to 4.2.1 as, same as for alternate condition

$$M_{wo,s} = -0.11 \cdot f_r \cdot k_{wm} \cdot C_w \cdot L^2 \cdot B \cdot (C_B + 0.7) \qquad \text{(Sagging)}$$

$$M_{wo,h} = 0.19 \cdot f_r \cdot k_{wm} \cdot C_w \cdot L^2 \cdot B \cdot C_B \qquad \text{(Hogging)}$$

The horizontal wave bending moment is calculated according to 4.2.2 as

$$M_H = 0.22 \cdot f_r \cdot L^{9/4} (T_{act} + 0.30B) C_B (1 - \cos(2\pi x / L))$$

where

$C_w = 10.75 - [(300 - L)/100]^{3/2}$ (wave coefficient)

$f_r = 0.5^{1/h0}$ (factor to transform from 10^{-8} to 10^{-4} probability level)

$h_0 = 2.21 - 0.54 \log_{10}(L)$ (long term Weibull shape parameter)

x = 161.25 (distance from AP to considered point)

k_{wm} = 1.0 (moment distribution factor)

$C_w = 10.75 - [(300 - 275)/100]^{3/2}$ = 10.625

$h_0 = 2.21 - 0.54 \log_{10}(275)$ = 0.893

$f_r = 0.5^{1/0.893}$ = 0.4601

$M_{wo,s} = -0.11 \cdot 0.4601 \cdot 1.0 \cdot 10.625 \cdot 275^2 \cdot 45 \cdot (0.85 + 0.7)$ = -2836.2 10^3 kNm

$M_{wo,h} = 0.19 \cdot 0.4601 \cdot 1.0 \cdot 10.625 \cdot 275^2 \cdot 45 \cdot 0.85$ = 2686.5 10^3 kNm

$M_H = 0.22 \cdot 0.4601 \cdot 275^{9/4} (17.78 + 0.30 \cdot 45) 0.85 (1 - \cos(2\pi 161.25/275))$ = 1538.4 10^3 kNm

8.3.8.5 Stresses from global loads

The vertical and horizontal bending moments result in the following stress ranges, according to 3.5.2 and 3.5.3 at the 10^{-4} level

$$\Delta\sigma_v = K_{axial} (M_{WO,h} - M_{WO,s}) \frac{(z - n_0)}{I_N} \qquad \text{(vertical global stress range)}$$

$$\Delta\sigma_{hg} = K_{axial}\, 2M_H \frac{|y|}{I_C}$$ (horizontal global stress range)

$$\Delta\sigma_g = \sqrt{\Delta\sigma_v^2 + \Delta\sigma_{hg}^2 + 2\rho_{vh}\Delta\sigma_v\Delta\sigma_{hg}}$$ (combined global stress range)

where

$$I_N = Z_N\left(D - n_0\right)$$ (moment of inertia of hull cross section)

$$I_C = Z_C\; B/2$$ (moment of inertia about the vertical neutral axis)

$\rho_{vh} = 0.1$ (average correlation between vertical and horizontal wave induced bending stress from 3.4.4)

$$\Delta\sigma_v = 2.1\left(2686.5\cdot 10^3 - \left(-2836.2\cdot 10^3\right)\right)\frac{|2.088 - 10.59|}{40.79(24.1 - 10.59)} = 178.93\ \text{N/mm}^2$$

$$\Delta\sigma_{hg} = 2.1\cdot 2\cdot 1538.4\cdot 10^3\ \frac{3.72}{62.66\cdot 45/2} = 17.05\ \text{N/mm}^2$$

$$\Delta\sigma_g = \sqrt{178.93^2 + 17.05^2 + 2\cdot 0.1\cdot 178.93\cdot 17.05} = 181.43\ \text{N/mm}^2$$

8.3.8.6 Combined hot spot stresses

The combined stress range is corrected for an assumed zero mean stress level, $f_m = 0.7$, and assumed world wide trading routes, $f_e = 0.8$. The combined hot spot stress at the 10^{-4} level is then calculated to be

$$\Delta\sigma = f_e\ \max\begin{cases}\Delta\sigma_g + b\cdot\Delta\sigma_l \\ a\cdot\Delta\sigma_g + \Delta\sigma_l\end{cases}$$ (the combined global and local stress range)

where

a, b Load combination factors, accounting for the correlation between the wave induced local and global stress range equal 0.6

$$\Delta\sigma = 0.8\max\begin{cases}181.43 + 0.6\cdot 181.22 = 290.16 \\ 0.6\cdot 181.43 + 181.22 = 290.08\end{cases}$$

$$\Delta\sigma = 232.11\ \text{N/mm}^2$$

With a correction for mean stress according to 2.2.4 assuming compression over the whole cycle, the stress range to be used in fatigue calculations become.

$$\Delta\sigma_o = f_m\cdot\Delta\sigma$$

$$\Delta\sigma_o = 0.7\cdot 232.11 = 162.48\ \text{N/mm}^2$$

8.3.8.7 Long term distribution

The Weibull shape parameter for the location of the considered detail is calculated according to 3.2.2

$$h = h_0 + h_a$$

$$h_0 = 2.21 - 0.54\log_{10}(L)$$

$$h_0 = 2.21 - 0.54\log_{10}(275) = 0.893$$

$$h = 0.893 + 0.05 = 0.943$$

(A possible check is here to consult Table 2.8 using the above Weibull parameter, h, and the stress range, $\Delta\sigma_o$.)

8.3.8.8 Fatigue part damage

The part damage in the homogenous condition over 20 years fatigue life is calculated according to 2.1.2, for the one slope in Air curve to be

$$D_{homogenous} = \frac{v_0 T_d}{\bar{a}} p_{homogenous} \cdot q_{homogenous}^m \cdot \Gamma\left(1+\frac{m}{h}\right)$$

where

$v_0 T_d = \dfrac{20 \cdot 365 \cdot 24 \cdot 3600}{4 Log_{10}(L)}$ (the number of cycles during 20 years)

$\Gamma\left(1+\dfrac{m}{h}\right)$ (the value of the gamma function from table 2.7)

$$q_{homogenous} = \frac{\Delta\sigma_o}{(\ln n_0)^{1/h}}$$

$n_0 = 10^4$ (the total number of cycles associated with 10^{-4} level and stress range)

$p_n = 0.25$ (part of time homogenous)

$\Delta\sigma_o = 162.48$ N/mm^2

h = 0.943

$\bar{a} = 5.75 \cdot 10^{12}$ (SN Curve parameter for the curve Ib)

m = 3.0 (SN Curve parameter for the curve Ib)

$$v_0 T_d = \frac{20 \cdot 365 \cdot 24 \cdot 3600}{4 Log_{10}(275)} = 6.46 \cdot 10^7$$

$$\Gamma\left(1+\frac{m}{h}\right) = 7.671 - 3(7.671 - 7.342)/10 = 7.572$$

$$q_{homogenous} = \frac{162.48}{(\ln 10^4)^{1/0.943}} = 15.42 \text{ N/mm}^2$$

$$D_{homogenous} = \frac{6.46 \cdot 10^7}{5.75 \cdot 10^{12}} 0.25 \cdot 15.42^3 \cdot 7.572 = 0.078$$

8.3.9 Calculation for Load condition - Ballast

8.3.9.1 Internal pressure loads

In this load case the ballast water will cause the internal loads. The accelerations and pressures are calculated according to 4.4.1 for the cargo hold.

a_v = 2.43 m/s^2

a_t = 5.54 m/s^2

a_l = 1.25 m/s^2

h_s = 24.1 m

y_s = 12.68 m

x_s = 0 m

ρ = 1.025 t/m^3

The local internal pressure pressure amplitude at the 10^{-4} probability level level is then calculated according to 4.4 as

$$p_i = f_a \max \begin{cases} p_1 = \rho \cdot a_v \cdot h_s \\ p_2 = \rho \cdot a_t |y_s| \\ p_3 = \rho \cdot a_l |x_s| \end{cases}$$

where

$f_a = 0.5^{1/0.943} = 0.479$ (From 8.3.7.3)

$$p_i = 0.479 \max \begin{cases} p_1 = 1.025 \cdot 2.43 \cdot 24.1 = 60.03 \\ p_2 = 1.025 \cdot 5.54 \cdot 12.68 = 72.00 \\ p_3 = 1.025 \cdot 1.25 \cdot 0 = 0 \end{cases}$$

$p_i = 34.49$ kN/m^2

8.3.9.2 External sea pressure loads

Since the considered longitudinal is an internal member there will be no contribution from sea pressure.

8.3.9.3 Combination of stress components

The stress amplitude due to internal pressures is combined considering the sign. Positive stress is defined as tension at the location of the weld

Stresses due to external pressure loads

+ Stiffener bending	(p_e=0)		=	0 N/mm^2
+Relative deflection			=	+19.44 N/mm^2
+Double hull bending			=	-3.61 N/mm^2
= Stresses from external sea loads		σ_e	=	+15.83 N/mm^2

Stresses due to internal pressure loads

+ Stiffener bending	(p_i=34.49)	tx34.49x1.365	=	+47.08 N/mm^2
+ Relative deflection			=	0 N/mm^2
+ Double hull bending			=	0 N/mm^2
= Stresses from internal pressure loads		σ_i	=	+47.08 N/mm^2

t=1 tension

c=-1 compression

The combined local stress range is determined according to 3.4.5 as

$$\Delta\sigma_l = 2\sqrt{\sigma_e^2 + \sigma_i^2 + 2\rho_p \sigma_e \sigma_i}$$

$$\rho_p = \frac{1}{2} - \frac{z}{10T_{act}} + \frac{|x|}{4L} + \frac{|y|}{4B} - \frac{|x| \cdot z}{5LT_{act}} \qquad z \le T_{act}$$

where

x, y and z are the co-ordinates for the load point, according to the co-ordinate system described in 3.4.5 with origo = (midship, centreline, baseline)

x= 23.75 m

y= 3.72 m

z= 2.088 m

$$\rho_p = \frac{1}{2} - \frac{2.088}{10 \cdot 17.78} + \frac{|23.75|}{4 \cdot 275} + \frac{|3.72|}{4 \cdot 45} - \frac{|23.75| \cdot 2.088}{5 \cdot 275 \cdot 7.16} = 0.525$$

$$\Delta\sigma_l = 2\sqrt{(+15.83)^2 + (+47.08)^2 + 2 \cdot 0.525 \cdot 15.83 \cdot 47.08} = 113.57 \text{ kN/mm}^2$$

8.3.9.4 Global hull bending moments

The vertical wave bending moment are computed according to 4.2.1 as

$$M_{wo,s} = -0.11 \cdot f_r \cdot k_{wm} \cdot C_w \cdot L^2 \cdot B \cdot (C_B + 0.7) \qquad \text{(Sagging)}$$

$$M_{wo,h} = 0.19 \cdot f_r \cdot k_{wm} \cdot C_w \cdot L^2 \cdot B \cdot C_B \qquad \text{(Hogging)}$$

The horizontal wave bending moment is calculated according to 4.2.2 as

$$M_H = 0.22 \cdot f_r \cdot L^{9/4} (T_{act} + 0.30B) C_B (1 - \cos(2\pi x / L))$$

where

$C_w = 10.75 - [(300 - L)/100]^{3/2}$ (wave coefficient)

$f_r = 0.5^{1/h0}$ (factor to transform from 10^{-8} to 10^{-4} probability level)

$h_0 = 2.21 - 0.54 \log_{10}(L)$ (long term Weibull shape parameter)

x = 161.25 (distance from AP to considered point)

k_{wm} = 1.0 (moment distribution factor)

$C_w = 10.75 - [(300 - 275)/100]^{3/2}$ = 10.625

$h_0 = 2.21 - 0.54 \log_{10}(275)$ = 0.893

$f_r = 0.5^{1/0.893}$ = 0.4601

The vertical bending moments are the same as calculated for the loaded conditions

$M_{wo,s} = -0.11 \cdot 0.4601 \cdot 1.0 \cdot 10.625 \cdot 275^2 \cdot 45 \cdot (0.85 + 0.7)$ = -2836.2 10^3 kNm

$M_{wo,h} = 0.19 \cdot 0.4601 \cdot 1.0 \cdot 10.625 \cdot 275^2 \cdot 45 \cdot 0.85$ = 2686.5 10^3 kNm

$M_H = 0.22 \cdot 0.4601 \cdot 275^{9/4} (7.16 + 0.30 \cdot 45) 0.85 (1 - \cos(2\pi 161.25/275))$ = 1016.1 10^3 kNm

8.3.9.5 Stresses from global loads

The vertical and horizontal bending moments result in the following stress ranges, according to 3.5.1 and 3.5.2 at the 10^{-4} level

$$\Delta\sigma_v = K_{axial}\left(M_{WO,h} - M_{WO,s}\right)\frac{(z-n_0)}{I_N}$$ (vertical global stress range)

$$\Delta\sigma_{hg} = K_{axial}\,2M_H\,\frac{|y|}{I_C}$$ (horizontal global stress range)

$$\Delta\sigma_g = \sqrt{\Delta\sigma_v^2 + \Delta\sigma_{hg}^2 + 2\rho_{vh}\Delta\sigma_v\Delta\sigma_{hg}}$$ (combined global stress range)

where

$I_N = Z_N\left(D-n_0\right)$ (moment of inertia of hull cross section)

$I_C = Z_C\ B/2$ (moment of inertia about the vertical neutral axis)

$\rho_{vh} = 0.1$ (average correlation between vertical and horizontal wave induced bending stress from 3.4.4)

$$\Delta\sigma_v = 2.1\left(2686.5\cdot10^3 - \left(-2836.2\cdot10^3\right)\right)\frac{|2.088-10.59|}{40.79(24.1-10.59)} = 178.93\ \text{N/mm}^2$$

$$\Delta\sigma_{hg} = 2.1\cdot2\cdot1016.1\cdot10^3\ \frac{3.72}{62.66\cdot45/2} = 11.26\ \text{N/mm}^2$$

$$\Delta\sigma_g = \sqrt{178.93^2 + 11.26^2 + 2\cdot0.1\cdot178.93\cdot11.26} = 180.41\ \text{N/mm}^2$$

8.3.9.6 Combined hot spot stresses

The combined stress range is corrected for an assumed zero mean stress level, $f_m = 1.0$, and assumed world wide trading routes, $f_e = 0.8$. The combined hot spot stress at the 10^{-4} level is then calculated to be

$$\Delta\sigma = f_e\ \max\begin{cases}\Delta\sigma_g + b\cdot\Delta\sigma_l \\ a\cdot\Delta\sigma_g + \Delta\sigma_l\end{cases}$$ (the combined global and local stress range)

where

a, b Load combination factors, accounting for the correlation between the wave induced local and global stress range equal 0.6

$$\Delta\sigma = 0.8\max\begin{cases}180.41+0.6\cdot113.57 = 248.51 \\ 0.6\cdot180.41+113.57 = 221.82\end{cases}$$

$$\Delta\sigma = 198.84\ \text{N/mm}^2$$

With a correction for mean stress according to 2.2.4 assuming tension over the whole cycle, the stress range to be used in fatigue calculations become.

$$\Delta\sigma_o = f_m\cdot\Delta\sigma$$

$$\Delta\sigma_o = 1.0\cdot198.84 = 198.84\ \text{N/mm}^2$$

8.3.9.7 Long term distribution

The Weibull shape parameter for the location of the considered detail is calculated according to 3.2.2

$$h = h_0 + h_a$$

$$h_0 = 2.21 - 0.54\log_{10}(L)$$

$h_0 = 2.21 - 0.54\log_{10}(275) = 0.893$

$h = 0.893 + 0.05 = 0.943$

(A possible check is here to consult Table 2.8 using the above Weibull parameter, h, and the stress range, $\Delta\sigma_o$.)

8.3.9.8 Fatigue part damage

The part damage in the ballast condition over 20 years fatigue life is calculated according to 2.1.2, for the one slope in Air curve to be

$$D_{ballast} = \frac{v_0 T_d}{\bar{a}} p_{ballast} \cdot q_{ballast}^m \cdot \Gamma\left(1 + \frac{m}{h}\right)$$

where

$$v_0 T_d = \frac{20 \cdot 365 \cdot 24 \cdot 3600}{4 Log_{10}(L)}$$ (the number of cycles during 20 years)

$$\Gamma\left(1 + \frac{m}{h}\right)$$ (the value of the gamma function from Table 2.7)

$$q_{ballast} = \frac{\Delta\sigma_o}{(\ln n_0)^{1/h}}$$

$n_0 = 10^4$ (the total number of cycles associated with 10^{-4} level and stress range)

$p_n = 0.35$ (part of time ballast)

$\Delta\sigma_o = 198.84$ N/mm^2

h = 0.943

$\bar{a} = 5.75 \cdot 10^{12}$ (SN Curve parameter for the curve Ib)

m = 3.0 (SN Curve parameter for the curve Ib)

$$v_0 T_d = \frac{20 \cdot 365 \cdot 24 \cdot 3600}{4 Log_{10}(275)} = 6.46 \cdot 10^7$$

$$\Gamma\left(1 + \frac{m}{h}\right) = 7.671 - 3(7.671 - 7.342)/10 = 7.572$$

$$q_{ballast} = \frac{198.84}{(\ln 10^4)^{1/0.943}} = 18.87 \text{ N/mm}^2$$

$$D_{ballast} = \frac{v_0 T_d}{\bar{a}} p_{ballast} \cdot q_{ballast}^m \cdot \Gamma\left(1 + \frac{m}{h}\right)$$

$$D_{ballast} = \frac{6.46 \cdot 10^7}{5.75 \cdot 10^{12}} 0.35 \cdot 18.87^3 \cdot 7.572 = 0.200$$

8.3.10 Fatigue life calculated from the one slope SN Curve Ib

The total fatigue damage during 20 years is found by summing the part damage from each of the loading conditions and checking the damage against the criteria in 2.1.2.

$$D = \frac{v_0 T_d}{\bar{a}} \sum_{n=1}^{N_{load}} p_n q_n^m \Gamma\left(1 + \frac{m}{h_n}\right) = \sum_{n=1}^{N_{load}} D_n \leq \eta$$

Where η is the usage factor. If the criterion is fulfilled the fatigue damage is considered acceptable. Using the estimated values from the SN Curve Ib.

D = 0.299 + 0.078 + 0.200 = 0.577

When considering the corrosive environment the χ-factor increases the fatigue damage

D = 0.577 χ = 0.577 x 1.3 = 0.750

If the usage factor η = 1.0, the fatigue life of the considered part is

T_{life} = 20/0.750 = 26.7 years

9. Fatigue Analysis of Containerships and Other Ship Types

9.1 Where to analyse

9.1.1

Fatigue damages are known to occur more frequently for some ship types and categories of hull structure elements. The fatigue life is in particular related to the magnitude of the dynamic stress level, the corrosiveness of the environment and the magnitude of notch- and stress concentration factors of the structural details, which all vary depending on ship type and structure considered. The importance of a possible fatigue damage is related to the number of potential damage points of the considered type for the ship or structure in question and to its consequences.

9.1.2

A major fraction of the total number of fatigue damages on ship structures occurs in panel stiffeners on the ship side, in bottom and upper deck. However, the calculated fatigue life depends on the type of stiffeners used, and the detail design of the connection to supporting girder webs, bulkheads, hatch corner and hatch coaming. In general un-symmetrical profiles will have a reduced fatigue life compared to symmetrical profiles unless the reduced effectiveness of the un-symmetrical profile is compensated by an improved design for the attachment to transverse girder webs and bulkhead structures.

9.1.3

Structural elements in the cargo area being of possible interest for fatigue evaluation are listed in Tables 9.1and 9.2.

Hull member	*Structural detail*	*Load type*
Side-and bottom longitudinals	Butt joints and attachment to transverse webs, transverse bulkheads and intermediate longitudinal girders	Hull girder bending, torsion[1], stiffener lateral pressure load and support deformation
Upper deck	Plate and stiffener butt joints, hatch corner curvatures and support details welded on upper deck for container pedestals etc.	Hull girder bending- and torsional warping stress[2].

1) Torsion induced warping stresses in the bilge region may be of significance from the forward machinery bulkhead to the forward quarter length.

2) The fatigue assessment of upper deck structures must include the combined effect of vertical and horizontal hull girder bending and the torsional warping response. For hatch corners, additional stresses introduced by the bending of transverse (and longitudinal) deck structures induced by the torsional hull girder deformation must be included in the fatigue assessment.

Table 9.1 Container carriers

Structure member	*Structural detail*	*Load type*
Side- and bottom longitudinals	Butt joints and attachment to transverse webs, transverse bulkheads and intermediate longitudinal girders	Hull girder bending, stiffener lateral pressure load and support deformation
Racking constraining girders, bulkheads etc.	Stress concentration points at girder supports and at bulkhead openings	Transverse acceleration load[1]

1) It should be noted that the racking constraining girders and bulkheads are in many cases largely unstressed when the ship is in the upright condition. Thus the racking induced stresses may be entirely dynamic, which implies that fatigue is likely to be the primary design criterion. For designs which incorporate "racking bulkheads", the racking deformations are normally reduced such that the fatigue assessment may be limited to stress concentration areas at openings of the racking bulkheads only. If sufficient racking bulkheads are not fitted, racking deformations will be greatly increased, and the fatigue assessment of racking induced stresses should be carried out for primary racking constraining members and vertical girder structures over the ship length as applicable.

Table 9.2 Roll on / Roll off- and Car carriers

9.2 Fatigue analysis

Depending on the required accuracy of the fatigue evaluation it may be recommended to divide the design life into a number of time intervals due to different loading conditions and limitations of durability of the corrosion protection. For example, the design life may be divided into one interval with good corrosion protection and one interval where the corrosion protection is more questionable for which different S-N data should be used, see Section 2.3. Each of these intervals should be divided into that of loaded and ballast conditions. The following guidance may be applied:

For vessels intended for normal, world wide trading, the fraction of the total design life spent at sea, should not be taken less than 0.85. The fraction of design life in the homogeneous design load and ballast conditions, p_n , may be taken from Table 9.3;

Vessel type	Container vessels
Loaded conditions	0.65
Ballast conditions	0.20

Table 9.3 Fraction of time at sea in loaded, ballast condition, p_n respectively

9.3 Simplified Calculation of the Combined Longitudinal Stress in Ships with Large Hatch Openings

9.3.1

The combined longitudinal stress, σ_g, due to horizontal and vertical hull girder bending and torsion, may in general be determined in accordance with the following procedure. The horizontal wave moment and the horizontal wave bending moment are to be defined as given in [1]. The combined stress is generally to be determined for a load combination where the torsional wave moment and the horizontal wave bending moment are combined with a reduced vertical wave bending moment. All are generally to be defined with a positive sign in relation to the axis system and sign convention defined in Figure 9.1.

9.3.2

The combined longitudinal stress range,$\Delta\sigma_g$, is to be determined for both port and starboard side for every member of the cross-section and location for which the fatigue life is to be evaluated. Based on this, the fatigue damage; D_S & D_P, for the port and starboard member respectively is to be determined separately in accordance with 2.1.3. The fatigue damage, D, for the member is then obtained according to the following formula:

$$D = \frac{D_S + D_P}{2}$$

9.3.3

The combined longitudinal stress range, $\Delta\sigma_g$, is determined according to the following formula:

$$\Delta\sigma_g = 2\left|\sigma_h + \sigma_{wt} + \sigma_{gt} + 0.45\sigma_v\right|$$

σ_h = horizontal wave bending stress

$$= \frac{-M_{WH}\ y}{I_C}$$

M_{WH} = horizontal wave bending moment at 10^{-04} probability level is according to (1) given as:

$$= 0.022\ f_r \sqrt{1 - \frac{C_B^2 L^2 B C_{SWP}}{18000\, T_{act}^2}}\, L^{\frac{11}{4}} \left(T_{act} + 0.3B\right) C_B \left(1 - \cos\left(\frac{2\pi x}{L}\right)\right) \text{ (kNm)}$$

f_r = as defined in 4.2.1 inserting h = 0.95

I_C = moment of inertia of hull cross-section about the vertical axis.

y = distance from centre line to considered member, defined in accordance with Figure 9.1

σ_v = stress due to hull girder vertical bending as given in 3.5.1.

σ_{wt} = warping stress at position considered.

$$= \frac{-M_{BWT}\ \Omega}{I_{\Omega\Omega}}$$

σ_{gt} = bending stress of (upper) deck structure due to torsional deformation of hatch openings.

= 0 for members other than (upper) deck.

$$= \frac{-M_D\ y_D}{I_D}$$

M_D = the bending moment of considered upper deck at side structure induced by the torsional deformation of the deck due to wave torque M_{WT}.

I_D = moment of inertia of considered upper deck at side about vertical axis.

y_D = transverse distance positive in the global y-axis direction from neutral axis of the upper deck structure to considered member.

M_{BWT} = warping bimoment at section considered due to wave torque M_{WT}, in accordance with 9.3.5 (with sign as defined in Figure 9.1).

$I_{\Omega\Omega}$ = sectorial moment of inertia of considered cross-section.

Ω = Sectorial co-ordinate (unit warping) for the considered member of the cross-section.

M_{WT} = wave torsional moment at 10^{-04} probability level is according to [1] given by:

$$= 0.26\, f_r \sin^2\left(\frac{\pi x}{L}\right)\cos\left(\frac{\pi x}{3C_B\ L}\right) L^{\frac{4}{3}} B^2 \frac{C_{SWP}}{C_B}$$

$$+ 0.14\, f_r \sqrt{1 - \frac{C_B^2\, L^2 B\, C_{SWP}}{18000\, T_{act}^2}}\ L^{\frac{7}{4}} \left(T_{act} + 0.3B\right) C_B \sin\left(\frac{2\pi x}{L}\right) z_e \ \text{(kNm)}$$

z_e = distance in m from the shear centre of the midship section to a level $0.7T_{act}$ above the vessel base line.

C_{SWP} = A_{WP} / (L B)

A_{WP} = water plane area in m^2 of vessel at draught = T_{act}.

T_{act} = vessel draught in m in considered condition. (Note a draught equal to the design draught may in general be assumed as representative for a condition to be applied for a fatigue analysis related to the ship's cargo conditions)

x = distance in m from A.P. to section considered.

9.3.4

For evaluation of the combined stress of particular stress concentration areas, such as hatch corners, each of the stress components of the formula for $\Delta\sigma_g$ given in 9.3.3 must be adjusted according to its appropriate stress concentration factor.

9.3.5

The torsional constants, I_T, $I_{\Omega\Omega}$, z_e and Ω of the considered hull cross-sections may be determined according to the DNV program Nauticus Hull Section Scantling. Note that Ω-values calculated by the Section Scantling program refer to the half cross-section of the positive y-axis.

The warping bimoment, M_{BWT}, may in general be determined according to calculations based on prismatic beam theory.

For wave torsional moment distributions as defined in [1], the maximum warping bimoments are generally found at the forward machinery bulkhead and in the midship region, and are seen to be mainly related to the warping characteristics of the hull. For container carriers with a normal cargo hold arrangement, the approximate warping bimoment at midship, M_{BWT}(L/2), and at the forward machinery bulkhead, M_{BWT} (x_m), for the wave torque M_{WT} are therefore (tentatively) expressed as:

M_{BWT} (L/2) = $0.8\, M_{BF} - 0.3\,(M_{BA} + 1.8\, M_{BF})$ (kNm^2)

= $-0{,}4\, M_{BA}$, maximum

M_{BWT} (x_m) = $0.8\, M_{BA} + M_{BWT}$ (L/2) (kNm^2)

M_{BA}

$$= \int_{x_m}^{L/2} M_{WT}\, dx$$

$$= K_B \left(\sin\left(\frac{\pi}{6C_B}\right) - \frac{\sin\left(\frac{(6C_B - 1)\pi}{6C_B}\right)}{2(6C_B - 1)} - \frac{\sin\left(\frac{(6C_B + 1)\pi}{6C_B}\right)}{2(6C_B + 1)} \right)$$

$$- \quad K_B \left(\sin\left(\frac{\pi x_m}{3C_B L}\right) - \frac{\sin\left(\frac{(6C_B-1)\pi x_m}{3C_B L}\right)}{2(6C_B-1)} - \frac{\sin\left(\frac{(6C_B+1)\pi x_m}{3C_B L}\right)}{2(6C_B+1)} \right)$$

$$+ \quad 0.0223\sqrt{1-\frac{C_B^2\, L^2 B\, C_{SWP}}{18000\,T^2}}\,L^{\frac{11}{4}}\,(T+0.3B)\,C_B\, z_e\left(1+\cos\left(\frac{2\pi x_m}{L}\right)\right)$$

$$M_{BF} \quad = \quad \int_{L/2}^{L} M_{WT}\, dx$$

$$= \quad K_B \left(\sin\left(\frac{\pi}{3C_B}\right) - \frac{\sin\left(\frac{(6C_B-1)\pi}{3C_B}\right)}{2(6C_B-1)} - \frac{\sin\left(\frac{(6C_B+1)\pi}{3C_B}\right)}{2(6C_B+1)} \right)$$

$$- \quad K_B \left(\sin\left(\frac{\pi}{6C_B}\right) - \frac{\sin\left(\frac{(6C_B-1)\pi}{6C_B}\right)}{2(6C_B-1)} - \frac{\sin\left(\frac{(6C_B+1)\pi}{6C_B}\right)}{2(6C_B+1)} \right)$$

$$- \quad 0.0446\sqrt{1-\frac{C_B^2\, L^2 B\, C_{SWP}}{18000\,T^2}}\,L^{\frac{11}{4}}\,(T+0.3B)\,C_B\, z_e$$

$$K_B \quad = \quad 0.1241 L^{\frac{7}{3}} B^2 C_{SWP}$$

9.3.6

The bending moment of the upper deck member, M_D, may preferably be calculated based on a direct calculation of the deck structure subjected to prescribed transverse- and longitudinal displacements determined according to the prismatic beam torsional response calculation.

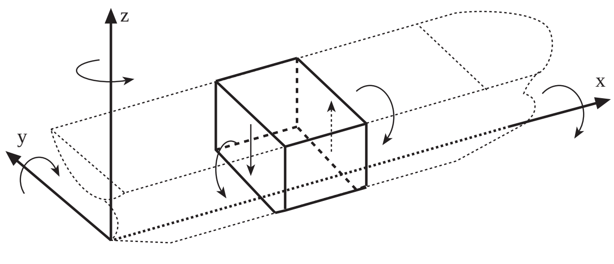

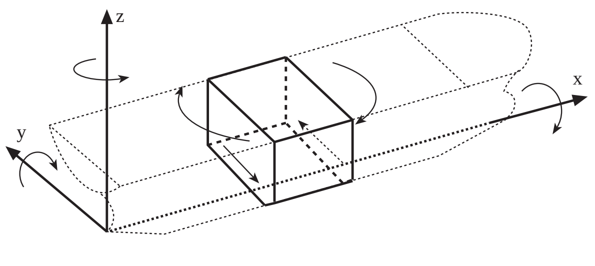

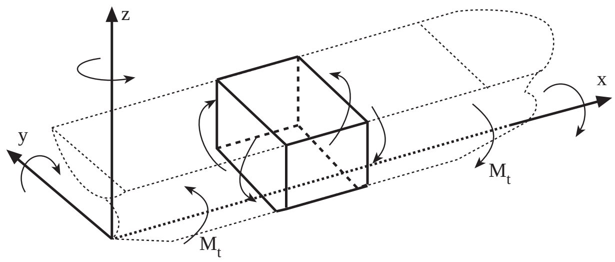

Figure 9.1

Reference:

1) DNVC Report No.: 95-0453 “Rule Calibration and Comparison of Direct Calculations and Rule Values of Torsional and Horizontal Wave induced Moments”.

10. Appendix A Stress Concentration Factors

10.1 General

10.1.1

Stress concentration factors or K-factors may be determined based on fine mesh finite element analyses as described in Section 6.6. Alternatively, K-factors may be obtained from the following selection of factors for typical details in ships.

10.1.2

The fatigue life of a detail is governed by the notch stress range. For components other than smooth specimens the notch stress is obtained by multiplication of the nominal stress by K-factors. The K-factors in this document are thus defined as

$$K = \frac{\sigma_{notch}}{\sigma_{nominal}}$$

The S-N curves in Section 2.3 are given for smooth specimens where the notch stress is equal the nominal stress: K = 1.0.

The relation between the notch stress range to be used together with the S-N-curve and the nominal stress range is

$$\Delta\sigma = K \cdot \Delta\sigma_{nominal}$$

All stress risers have to be considered when evaluating the notch stress. This can be done by multiplication of K-factors arising from different causes. The resulting K-factor to be used for calculation of notch stress is derived as

$$K = K_g \cdot K_w \cdot K_{te} \cdot K_{t\alpha} \cdot K_n$$

where

K_g = stress concentration factor due to the gross geometry of the detail considered

K_w = stress concentration factor due to the weld geometry. K_w=1.5 if not stated otherwise

K_{te} = additional stress concentration factor due to eccentricity tolerance (normally used for plate connections only)

$K_{t\alpha}$ = additionally stress concentration factor due to angular mismatch (normally used for plate connections only)

K_n = additional stress concentration factor for un-symmetrical stiffeners on laterally loaded panels, applicable when the nominal stress is derived from simple beam analyses.

10.2 Examples of K-factors for typical details in ships

10.2.1

The K-factors presented in the following covers typical details in ships. Local stress concentration factors in way of welds depend on level of workmanship. The default values on workmanship tolerances given in the following tables, are based on what appears to be normal shipyard practise. If greater tolerances are used, the K-factors should be calculated based on actual tolerances, see also 10.4

10.2.2

K-factors for flange connections.

K-factors for flange connections are given in Table 10.1.

Geometry	**K-factor**
10.1.a Flange connection with softening toe 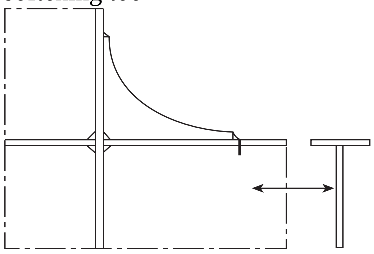	$K_g \cdot K_w = 2.2$
10.1.b Crossing of flanges 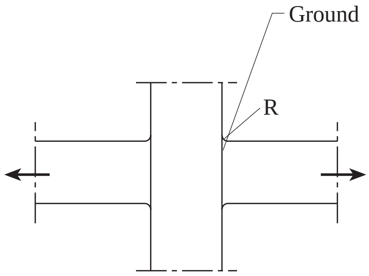 	$K_g \cdot K_w = 2.2$ $R \geq 1.25t$ (ground) welded from both sides t = thickness of flange
10.1.c 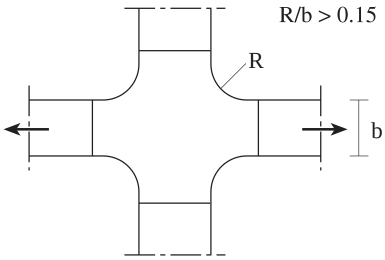 	$K_g = 1.9$ To be used together with S-N curve for base material.
10.1.d Overlap connection 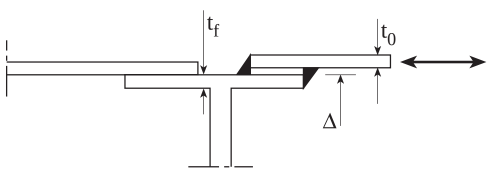 	$K_g = \left(4\frac{t_0}{t_f} + 3\left(\frac{t_0}{t_f}\right)^2 + 6\frac{\Delta t_0}{t_f^{\,2}}\right)$ *Δ=gap = tolerance* *Default: Δ* = 1.0 *mm* $K_w = 1.5$

Table 10.1 K-factors for flange connections

10.2.3

K- factors for stiffener supports.

K-factors for stiffener supports are given in Table 10.2. The factors are applicable to stiffeners subject to axial- and lateral loads. Note that the weld connection area between supporting members and stiffener flange must fulfill the requirements in DNV Rules for Classification of Ships.

<table>
<tr><th>Geometry</th><th colspan="2">K-factor</th></tr>
<tr><td rowspan="3">10.2.a
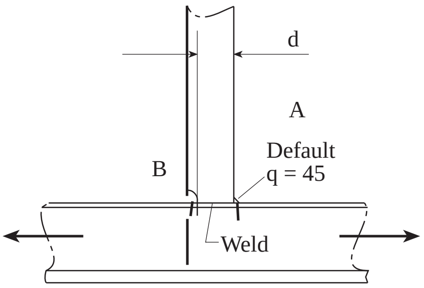
</td><td colspan="2">For supporting members welded to stiffener flange:</td></tr>
<tr><td>Axial stress in the longitudinal direction

At point A:
$K_g \cdot K_w = 2.0 \quad d \leq 150$
$K_g \cdot K_w = 2.1 \quad d > 150$

At point B:
$K_g \cdot K_w = 2.0 \quad d \leq 150$
$K_g \cdot K_w = 2.1 \quad d > 150$</td><td>Bending due to lateral load

At point A:
$K_g \cdot K_w = 2.4$

At point B:
$K_g \cdot K_w = 2.4$</td></tr>
<tr><td colspan="2">Point A denotes the side of the supporting member and point B denotes the opposite side.

For supporting members welded to stiffener web by overlap weld as given in Table 10.5a, the above factors are to be multiplied by a factor 1.15</td></tr>
<tr><td rowspan="3">10.2.b
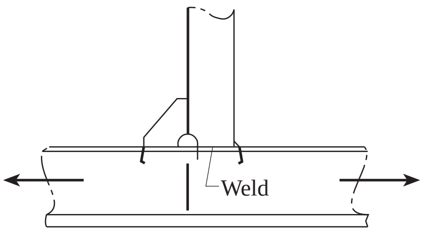
</td><td colspan="2">For supporting members welded to stiffener flange:</td></tr>
<tr><td>Axial stress in the longitudinal direction

$K_g \cdot K_w = 2.2$</td><td>Bending due to lateral load

$K_g \cdot K_w = 2.7$</td></tr>
<tr><td colspan="2">For supporting members welded to stiffener web by overlap weld as given in Table 10.5a, the above factors are to be multiplied by a factor 1.15</td></tr>
<tr><td rowspan="2">10.2.c
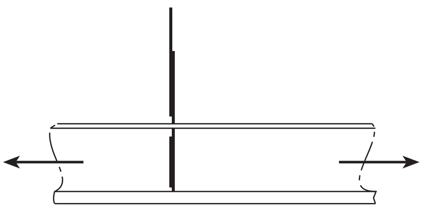</td><td colspan="2">For supporting members welded to stiffener flange:</td></tr>
<tr><td>Axial stress in the longitudinal direction

$K_g \cdot K_w = 1.8$</td><td>Bending due to lateral load

$K_g \cdot K_w = 1.8$</td></tr>
</table>

<table>
<tr>
<td>10.2.d
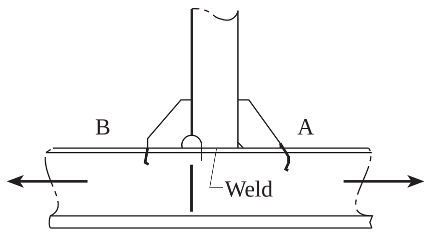
</td>
<td>For supporting members welded to stiffener flange:

<table>
<tr><td>Axial stress in the longitudinal direction

At point A:
$K_g \cdot K_w = 2.1$

At point B:
$K_g \cdot K_w = 2.1$</td>
<td>Bending due to lateral load

At point A:
$K_g \cdot K_w = 2.1$

At point B:
$K_g \cdot K_w = 2.1$</td></tr>
</table>
Point A denotes the side of the supporting member and point B denotes the opposite side.

For supporting members welded to stiffener web by overlap weld as given in Table 10.5a, the above factors are to be multiplied by a factor 1.15</td>
</tr>
<tr>
<td>10.2.e
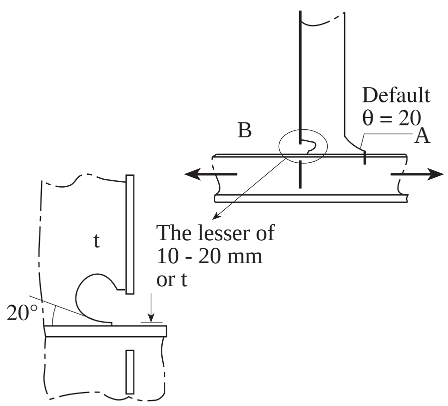
</td>
<td>For soft nose bracket toes with a radius greater than 200 mm and soft heels in scallops with a radius greater than 30 mm:

<table>
<tr><td>Axial stress in the longitudinal direction

At point A:
$K_g \cdot K_w = 2.0 \cdot \left(\frac{60}{R}\right)^{0.05}$

At point B:
$K_g \cdot K_w = 2.1 \cdot \left(\frac{60}{R}\right)^{0.05}$</td>
<td>Bending due to lateral load

At point A:
$K_g \cdot K_w = 1.8$

At point B:
$K_g \cdot K_w = 2.6 \cdot \left(\frac{60}{R}\right)^{0.05}$</td></tr>
</table>
Point A denotes the side of the supporting member and point B denotes the opposite side.

For supporting member welded to stiffener, flange only. It is assumed that the weld is kept clear of flange edge.</td>
</tr>
<tr>
<td>10.2.f
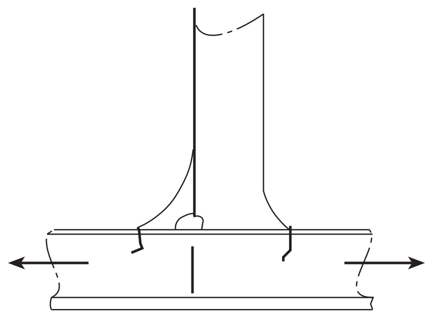</td>
<td>For soft nose bracket toes with a radius greater than 200 mm:

$K_g \cdot K_w = 2.0 \cdot \left(\frac{60}{R}\right)^{0.05}$

R = radius in mm of soft nose or heel

For supporting member welded to stiffener, flange only. It is assumed that the weld is kept clear of flange edge.</td>
</tr>
</table>

Table 10.2 K-factors for stiffener supports

The following should be noted when the value of the K-factor in bending is considered. The K-factors have been determined based on finite element analyses of actual geometries. The hot spot stress has been determined by extrapolation of stresses as defined in Section 6.6. Then the procedure for stress calculation given in 3.5.4 has been followed in a reverse direction to establish the K-factors. Effective plate flange and effective span width between supports are included in the calculation. This will assure that the same hot spot stress is derived using the K-factors based on the specified procedure for the same geometric conditions. Thus the value of the K-factor will depend on the calculation procedure used to obtain the hot spot stress. Therefore, a direct comparison of K-factors from different sources should not be performed without considering how they are defined and derived. A more proper way for comparison is to compare the hot spot stresses due to a specific load.

The K-factors in bending have been evaluated for different boundary conditions for the stiffener at the transverse frames. It was found that the K-factors were not very sensitive to whether free support or fixed condition were used. (It might be added that the effect of boundary conditions would be a function of length of stiffener analysed in relation to geometry of longitudinal and distance between transverse frames. Here, the following geometry has been used: distance from top of longitudinal to end of supporting member equal 560 mm, frames spacing of 3200 mm, plate thickness of 12.5 mm, T-profile 350x12 + 100x17 and spacing 800 mm).

10.2.4

K-factors for termination of stiffeners on plates.

K-factors for termination of stiffeners on plates are given in Table 10.3.

Geometry	**K-factor**
10.3.a Local elements and stiffeners welded to plates 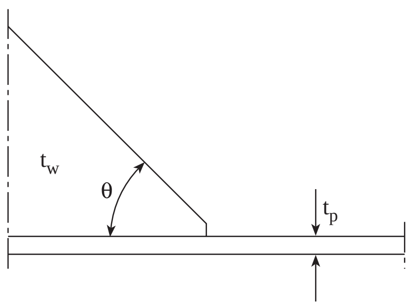 	$K_g \cdot K_w = 2\left(1+\frac{t_w \theta}{t_p 160}\right)$ θ = angle in degrees of sloping termination
10.3.b Sniping of top flanges: 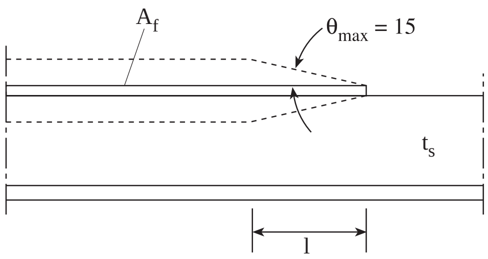 	$K_g \cdot K_w = \frac{3A_f}{l t_s}$ and $K_g \cdot K_w = \min 3.0$

Table 10.3 K-factors for termination of stiffeners on plates

10.2.5

K-factors for butt welds.

K-factors for butt welds are given in Table 10.4. For some geometries, default values have been established for normal design fabrication of the connections and should be used if not otherwise documented. See also 10.4.1.

Geometry	K-factor
10.4.a 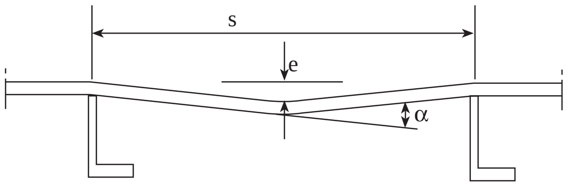 Default: e = 6 mm	Angular mismatch in joints between flat plates results in additional stresses at the butt weld and the stiffener $$K_{t\alpha} = 1 + \frac{\lambda}{4}\alpha\frac{s}{t}$$ where: λ = 6 for pinned ends λ = 3 for fixed ends α = angular mismatch in radians s = plate width t = plate thickness
10.4.b Welding from both sides 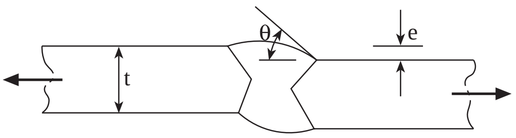 Default: $e = 0.15\ t$	$K_g = 1.0$ $K_w = 1.0 + 0.5(\tan\theta)^{1/4}$ Default value $K_w = 1.5$ for $\theta = 45$deg. $K_{t\alpha}$ from 10.4. a $\mathrm{K}_{te} = 1 + \frac{3e}{t}$
10.4.c Plate not restricted in out-of-plane movement 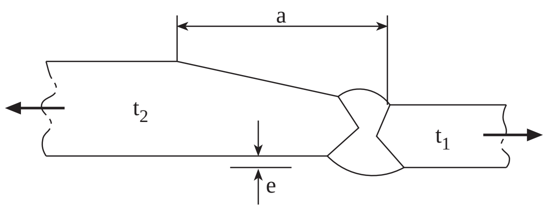 Defaults: $a = \min 3(\Delta t + e)$ $e = 0.15\ t_1$	$\Delta t = t_2 - t_1$ $$K_g = 1 + \frac{3\frac{\Delta t}{t_1}}{1 + \left(1 + \frac{\Delta t}{t_1}\right)^3}$$ $$K_w = 1.4\left(1 + \frac{\Delta t + e}{2a}\right)$$ $$K_{te} = 1 + \frac{6\frac{e}{t_1}}{1 + \left(1 + \frac{\Delta t}{t_1}\right)^3}$$ $K_{t\alpha}$ from 10.4.a

10.4.d Plate restricted in out-of-plane movement (e.g. flanges) 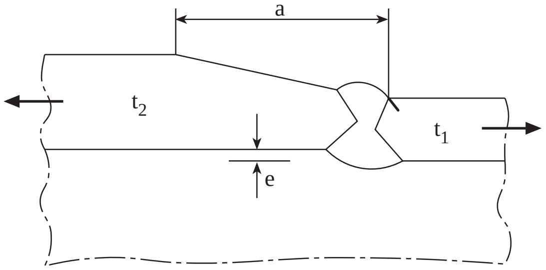 Defaults: $a = \min 3(\Delta t + e)$ $e = 0.15\ t_1$	$\Delta t = t_2 - t_1$ $K_g = 1.0$ $K_w = 1.4\left(1 + \frac{\Delta t + e}{2a}\right)$ $K_{te} = 1.0$ $K_{t\alpha} = 1.0$
10.4.e Welding from one side 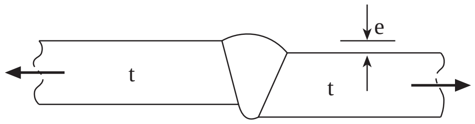 Default: $e = 0.15\ t$.	Welding from one side is not recommended in areas prone to fatigue due to sensitivity of workmanship and fabrication $K_g = 1.0$ Default value: $K_w = 2.2$ $K_{te} = 1 + \frac{3e}{t}$ $K_{t\alpha}$ from 10.4.a

Table 10.4 K-factors for butt-welds

10.2.6

K-factors for doubling plates.

K-factors for doubling plates are given in Table 10.5.

Geometry	K-factor
10.5.a Cover plates on beams 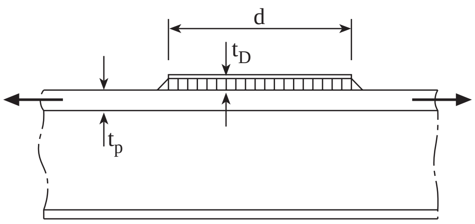	Welded at its end with throat thickness *a* For $a \geq \dfrac{t_p \cdot t_D}{t_p + t_D}$ $K_g \cdot K_w = 1.8 \qquad d \leq 50$ $K_g \cdot K_w = 1.9 \qquad 50 < d \leq 100$ $K_g \cdot K_w = 2.0 \qquad 100 < d \leq 150$ $K_g \cdot K_w = 2.2 \qquad d > 150$
10.5.b Doubling plates welded to plates 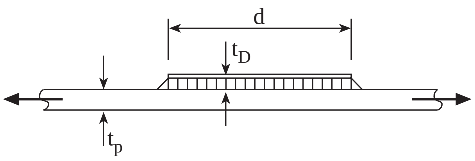	For $a \geq \dfrac{t_p \cdot t_D}{t_p + t_D}$ $K_g \cdot K_w = 1.8 \qquad d \leq 50$ $K_g \cdot K_w = 1.9 \qquad 50 < d \leq 100$ $K_g \cdot K_w = 2.0 \qquad 100 < d \leq 150$ For larger doublers, a more detailed analysis should be performed based on the actual geometry.

Table 10.5 Doubling plates

Note: If the welds of the doubling plates are placed closer to the member (flange, plate) edges than 10 mm, the K-factors in Table 10.5 should be increased by a factor 1.3

10.2.7
K-factors for cruciform joints.

K-factors for cruciform joints are given in Table 10.6.

<table>
<tr><th>Geometry</th><th>K-factor</th></tr>
<tr><td>10.6.a
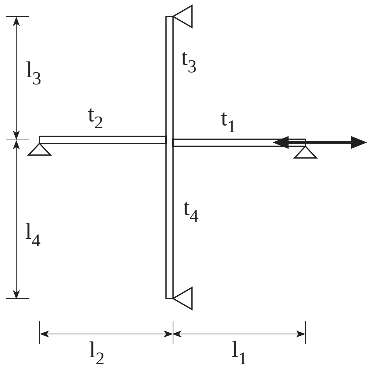
</td><td>$$K_{te} = 1 + \frac{6t^2 \cdot e}{l_1\left(\frac{t_1^{\,3}}{l_1} + \frac{t_2^{\,3}}{l_2} + \frac{t_3^{\,3}}{l_3} + \frac{t_4^{\,3}}{l_4}\right)}$$</td></tr>
<tr><td>10.6.b
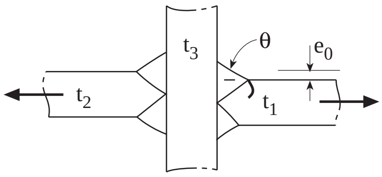

$$e = \frac{t_1}{2} + e_0 - \frac{t_2}{2}$$
$t_1 \leq t_2$
$e_0 \leq 0.3t_1$</td><td>$K_g\ K_w = 0.90 + 0.90\ (\tan\theta)^{1/4}$
Default value: $K_g\ K_w = 1.8$
K_{te} from 10.6.a
$K_{t\alpha} = 1.0$</td></tr>
<tr><td>10.6.c
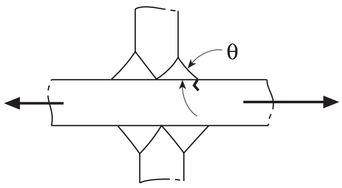

Applicable also for fillet welds</td><td>$K_g\ K_w = 0.90 + 0.90\ (\tan\theta)^{1/4}$
Default value: $K_g\ K_w = 1.8$
$K_{te} = 1$
$K_{t\alpha} = 1.0$</td></tr>
<tr><td>10.6.d
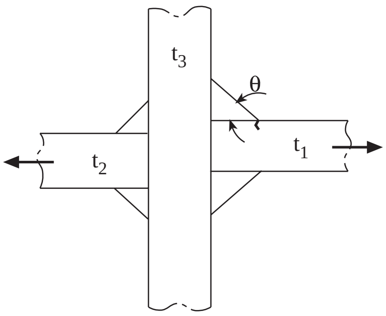
</td><td>$K_g \cdot K_w = 1.2 + 1.3(\tan\theta)^{1/4}$
Default value : $K_g \cdot K_w = 2.5$
K_{te} from 10.6.a with e as given in 10.6.b
$K_{t\alpha} = 1.0$</td></tr>
</table>

<table>
<tr><th>Geometry</th><th>K-factor</th></tr>
<tr><td>10.6.e
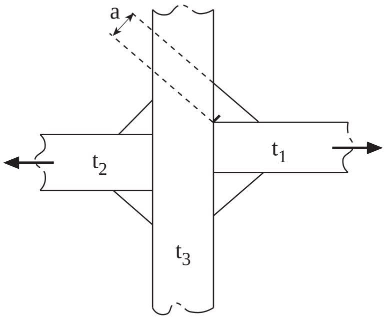

$t_2 \geq t_1$</td><td>Based on nominal stress in member with thickness t_1
$$K_g \cdot K_w = 1.8\frac{t_1}{a}$$
K_g from 10.6.a with e as given in 10.6.b
$K_{t\alpha} = 1.0$</td></tr>
<tr><td>10.6.f
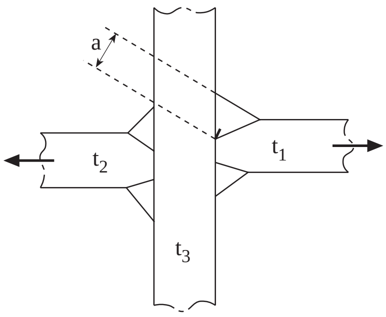
</td><td>$$K_g \cdot K_w = 1.8\frac{t_1}{a}$$
K_g from 10.6.a with e as given in 10.6.b
$K_{t\alpha} = 1.0$</td></tr>
</table>

Table 10.6 K-factors for cruciform joints

10.2.8

K-factors for transverse frames.

For designs with a supporting member welded on top of the longitudinal, it is not likely that the the cut-out in the transverse frame will be initiation point for fatigue as long as normal procedures for design of cut-out geometry are followed and K-factors for stiffener supports should be used.

For designs without a supporting member welded on top of the longitudinal, K-factors are given in Table 10.7. If the geometry is different from the geometries shown in the table, it is recommended to perform a stress concentration analysis.

If a sniped stiffener is welded to a transverse frame, the stiffener may generally be located at a distance of about 50 mm or more away from the edge of web cutout depending on the maximum principal stress level of web frame and the stress concentration factor of the sniped stiffener end

<table>
<tr><th>Geometry</th><th>K-factor</th></tr>
<tr><td>

10.7.a

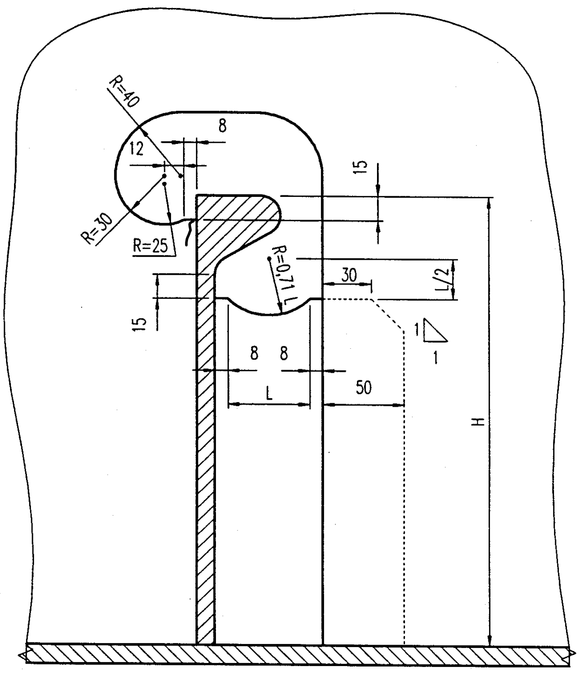

</td><td>

For stiffener heights between 220 mm and 280 mm:

Axial stress in the longitudinal direction

$K_g \cdot K_w = 1.8$

Bending due to lateral load

$K_g \cdot K_w = 1.9$

Note that the K_{n1}–factor for un-symmetrical stiffeners on laterally loaded panels should be included when the bending stress is calculated.

</td></tr>
<tr><td>

10.7.b

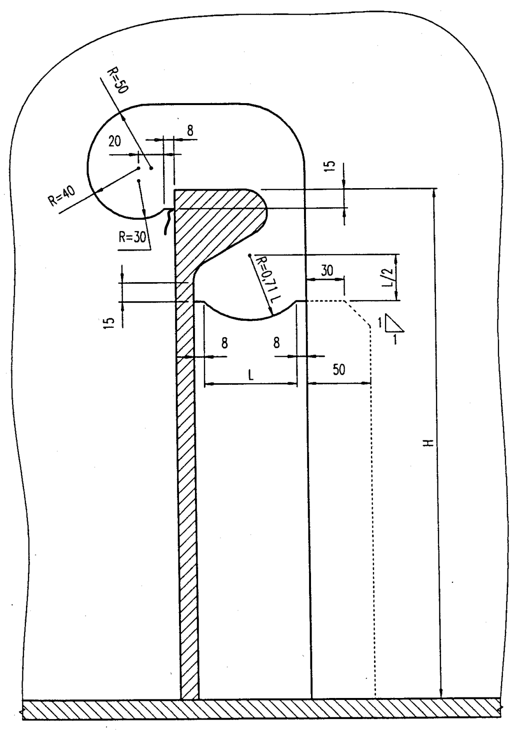

</td><td>

For stiffener heights above 300 mm:

Axial stress in the longitudinal direction

$K_g \cdot K_w = 1.8$

Bending due to lateral load

$K_g \cdot K_w = 1.9$

Note that the K_{n1}–factor for un-symmetrical stiffeners on laterally loaded panels should be included when the bending stress is calculated.

</td></tr>
</table>

Table 10.7 K-factors for transverse frames

10.2.9

K-factors for scallops.

The factors are applicable to stiffeners subject to axial loads. For dynamic pressure loads on the plate these details are susceptible to fatigue cracking ref. /16/ and other design solutions should be considered to achieve a proper fatigue life.

Geometry	K-factor	
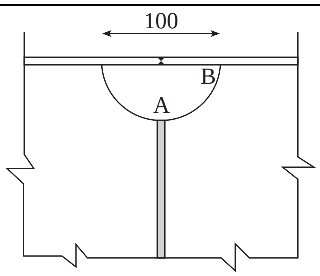	$K_g \cdot K_w = 3.0$ at point A $K_g \cdot K_w = 1.8$ at point B	$K_g \cdot K_w \cdot K_{te} = 4.5$ at point A $K_g \cdot K_w \cdot K_{te} = 1.8$ at point B An eccentricity of 0.15 t included
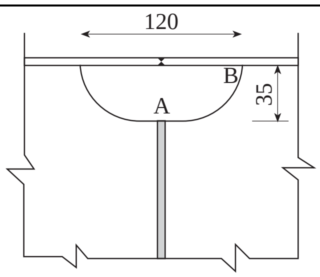	$K_g \cdot K_w = 1.7$ at point A $K_g \cdot K_w = 1.8$ at point B	$K_g \cdot K_w \cdot K_{te} = 2.6$ at point A $K_g \cdot K_w \cdot K_{te} = 1.8$ at point B An eccentricity of 0.15 t included
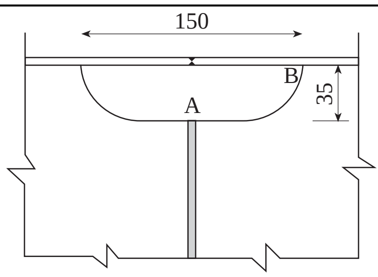	$K_g \cdot K_w = 1.6$ at point A $K_g \cdot K_w = 1.8$ at point B	$K_g \cdot K_w \cdot K_{te} = 2.4$ at point A $K_g \cdot K_w \cdot K_{te} = 1.8$ at point B An eccentricity of 0.15 t included
For scallops without transverse welds, the K-factor at point B will be governing for the design.		

Table 10.8 K–factors for scallops

10.2.10

K-factors for lower hopper knuckles.

Hot-spot stresses in panel knuckles should in general be calculated case by case by a stress concentration model, see e.g. Figure 6.8. However, for a yard standard geometry, a K-factor related to nominal stress in a frame and girder model may be established using the stress concentration model.

The knuckle between inner bottom and hopper plate in oil carriers is called lower hopper knuckle. For this knuckle, the nominal stress should be the transversal membrane stress, ½ a stiffener spacing from the knuckle in the inner bottom plate, and averaged between two floors. For hopper knuckles with angles between inner bottom and hopper plate between 30° and 75° K-factors are given in Table 10.9. It is assumed that brackets are fitted in ballast tanks in line with inner bottom. Geometrical eccentricity in the knuckle should be avoided or kept to a minimum.

Geometry	K-factor
10.9.a 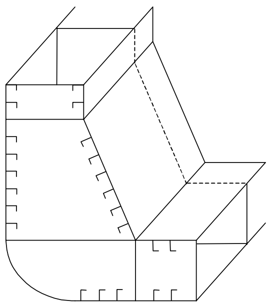	$K_g = 7.0$ $K_w = 1.5$
10.9.b 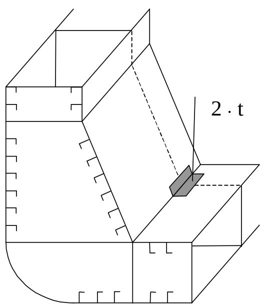	Insert plate of 2,0 times the thickness normally required. Insert plates should be provided in inner bottom, hopper tank top, and web frame. The insert plates should extend approximately 400 mm along inner bottom and hopper plate, approximately 800 mm in longitudinal direction, and 400 mm in the depth of the web. $K_g = 4.5$ $K_w = 1.5$
10.9.c 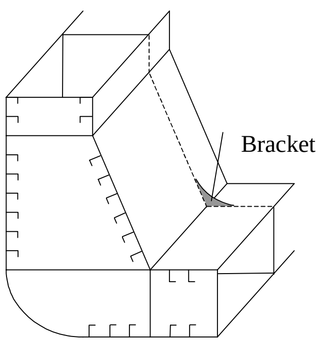	Bracket inside cargo tank. The bracket should extend approximately to the first longitudinals and the bracket toe should have a soft nose design. $K_g = 2.5$ $K_w = 1.5$

Table 10.9 K-factors for lower hopper knuckles

10.2.11

K-factors for cut-outs.

K-factors for rounded rectangular holes are given in Figure 10.1. The factors may be used for hatch opening corners in conventional ships, but not in container carriers.

Cut outs

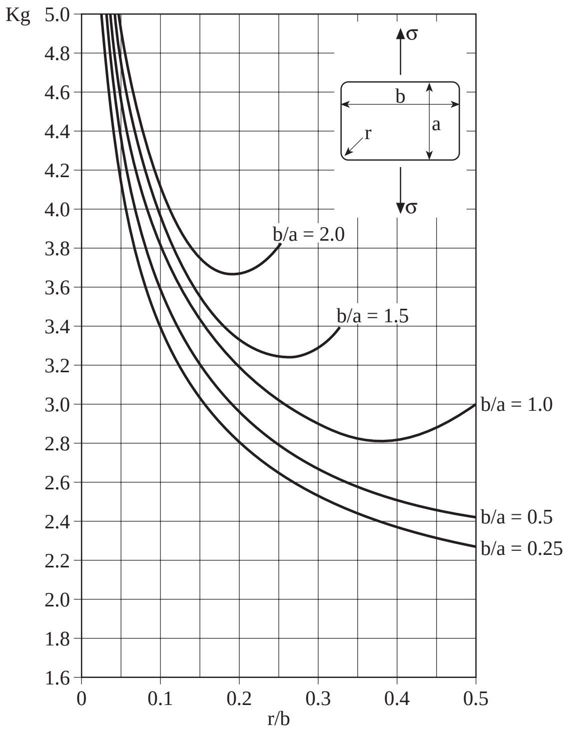

Figure 10.1 Stress concentration factors for rounded rectangular holes

10.2.12

K-factors at the flange of un-symmetrical stiffeners on laterally loaded panels.

The nominal bending stress of laterally loaded panel stiffeners is generally given by:

$$\sigma = \frac{psl^2}{m_b Z}$$

p = lateral pressure load

m_b = moment parameter for stiffener

= 12 for continuous stiffeners at stiffener support

= 24 for continuous stiffeners at stiffener midspan

= 8 at midspan for stiffener with simply supported ends

The stress concentration factors at the flange of un-symmetrical stiffeners on laterally loaded panels as defined in Figure 10.2, are calculated as follows.

At the flange edge

$$K_{n1} = \frac{1+\gamma\beta}{1+\gamma\beta\,\psi}$$

and at the web

$$K_{n2} = \frac{1+\gamma\beta^2}{1+\gamma\beta^2\psi}$$

where

$$\beta = 1 - \frac{2b_g}{b_f} \quad \text{for built up sections} \quad .$$

For definition of b_g, see Figure 10.3

$$\beta = 1 - \frac{t_w}{b_f} \quad \text{for rolled angles}$$

ψ = ratio between section modulus of the stiffener web with plate flange as calculated at the flange and the section modulus of the complete panel stiffener

$$\psi = \frac{(h-t_f)^2 t_w}{4Z} \quad \text{may be used as an approximate value.}$$

Z = section modulus of panel stiffener including plate flange with respect to a neutral axis normal to the stiffener web.

γ is derived from Table 10.10.

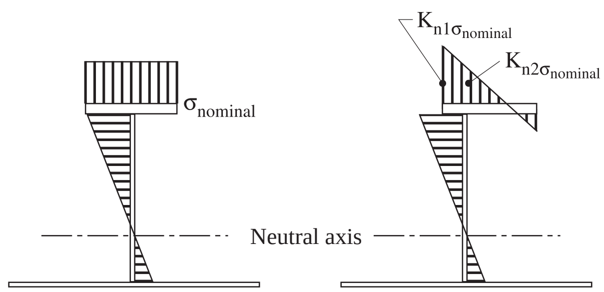

Figure 10.2 Bending stress in symmetrical and un-symmetrical panel stiffener with same web and flange areas.

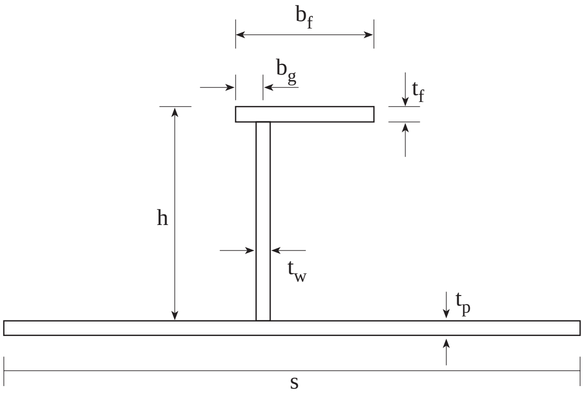

Figure 10.3 Un-symmetrical profile dimensions

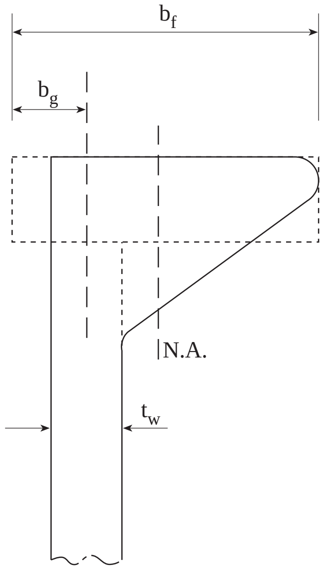

Figure 10.4 Bulb section and equivalent built up flange.

Supporting of flange	*γ-factor*
Fixed ends, at supports (continuous stiffeners)	$\gamma = \dfrac{3\left(1+\dfrac{\mu}{280}\right)}{1+\dfrac{\mu}{40}}$
Fixed ends, at midspan (continuous stiffeners)	$\gamma = \dfrac{3\left(1-\dfrac{\mu}{1120}\right)}{1+\dfrac{\mu}{40}}$ **(= min. 0)**
Simply supported flanges, at midspan	$\gamma = \dfrac{24}{m_b} \cdot \dfrac{1-\dfrac{\mu}{480}}{1+\dfrac{\mu}{8}}$ **(= min. 0)**

where:

$$\mu = \frac{l^4}{b_f^3 t_f h^2 \left(\dfrac{4h}{t_w^3} + \dfrac{s}{t_p^3}\right)}$$

l = stiffener length between supports of flange
b_f = flange width
t_f = flange thickness
h = stiffener height
t_w = stiffener web thickness
s = plate width between stiffeners
t_p = plate thickness
m_b = moment parameter for stiffener.
m_b = 8 for simply supported ends.
m_b = 24 for fixed supported ends.

Table 10.10 γ-factor

The formulations are not directly applicable for bulb profiles. For these the equivalent built up section should be considered, see Figure 10.4, where the assumed built up flange shall have same cross-sectional area, moment of inertia about the vertical axis and neutral axis position as the bulb flange. For the so-called "HP" bulb profiles, the equivalent built up profile dimensions have been determined and are tabulated in Table 10.11

HP- bulb		*Equivalent built up flange*		
Height (mm)	*Web thickness t_w (mm)*	*b_f (mm)*	*t_f (mm)*	*b_g (mm)*
200	9 - 13	t_W + 24.5	22.9	(t_W + 0.9)/2
220	9 - 13	t_W + 27.6	25.4	(t_W + 1.0)/2
240	10 - 14	t_W + 30.3	28.0	(t_W + 1.1)/2
260	10 - 14	t_W + 33.0	30.6	(t_W + 1.3)/2
280	10 - 14	t_W + 35.4	33.3	(t_W + 1.4)/2
300	11 - 16	t_W + 38.4	35.9	(t_W + 1.5)/2
320	11 - 16	t_W + 41.0	38.5	(t_W + 1.6)/2
340	12 - 17	t_W + 43.3	41.3	(t_W + 1.7)/2
370	13 - 19	t_W + 47.5	45.2	(t_W + 1.9)/2
400	14 - 19	t_W + 51.7	49.1	(t_W + 2.1)/2
430	15 - 21	t_W + 55.8	53.1	(t_W + 2.3)/2

Table 10.11 "HP" equivalent built up profile dimensions.

10.2.13

K-factors in web of un-symmetrical stiffener on laterally loaded panels.

The nominal web stress of laterally loaded panel stiffeners is generally given by:

σ = sp/t_w

p = lateral pressure load

s = stiffener spacing

t_w = web thickness

It should be noted that the bending stress in the stiffener web may be significant at the middle of stiffeners with un-symmetrical flange, see Figure 10.2. The stress concentration factor due to this bending is calculated as

$$K_n = 1 + \frac{\alpha_1 \alpha_3}{1 + \frac{\mu}{\alpha_2}}$$

where

α_1 = 0.42 for stiffener with simply supported (or sniped) flange at support

α_1 = 0.094 for continuous stiffener

α_2 = 8 for stiffener with simply supported (or sniped) flange at support

α_2 = 40 for continuous stiffener

$$\alpha_3 = \frac{b_f^2 t_f h \beta \mu}{t_w Z (1 + \gamma \beta^2 \psi)}$$

where γ is taken from Table 10.10 for the midspan position. Parameters in the expression are defined in Section 10.2.12.

For calculation of hot spot stress also the stress concentration due to the weld, K_w, as derived from 10.1.2 with K_{te} = 1.0 has to be included, i.e. $K = K_w \cdot K_n$

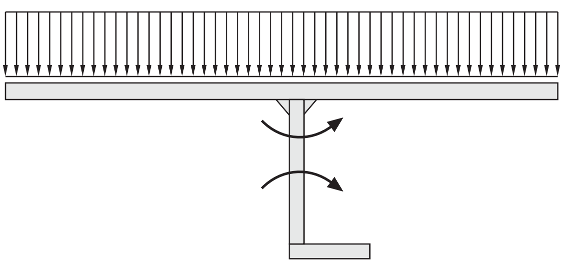

Figure 10.5 Bending stress in webs of un-symmetrical stiffeners subjected to lateral loading.

10.2.14

K-factors due to fabrication tolerances for stiffeners on plates subjected to axial stress variation.

Fabrication tolerances for stiffeners allow for some deviation from straightness. This deviation will introduce some bending in the stiffener when subjected to an axial force.

If not otherwise specified, the following deviations from straightness of flanges should be considered for fatigue analysis.

$$e = 6 + \frac{2l}{1000} \quad \text{(mm)}$$

where,

e_{min} = 8 mm

e_{max} = 13 mm

Reference is made to Figure 10.2 for description of position at stiffener considered and to Figure 10.3 for geometry notations. Notation numbers *i* = 1-3 are used for calculation of the stress concentration factors.

Stress concentration factors due to fabrication tolerances are calculated as,

$$K_{tei} = 1 + \frac{e b_f t_f + \frac{e t_w (h - 3t_f)}{3}}{2 Z_{hi}} \qquad i = 1,2,3$$

where

$$Z_{hi} = \frac{b_f^3 t_f}{12 b_{mi}} \left(1 + \frac{\beta^2}{\frac{1}{3} + \frac{A_f}{A_w}} \right)$$

A_f = $b_f \cdot t_f$

A_w = $(h - t_f) t_w$

$$b_{m1} = \frac{b_f}{2} \left(1 - \frac{\beta}{\frac{3A_f}{A_w} + 1} \right)$$ for position 1, see Figure 10.2

$$b_{m2} = b_{m1} - b_g$$ for position 2, see Figure 10.2

$$b_{m3} = \frac{b_f}{2} \left(1 + \frac{\beta}{\frac{3A_f}{A_w} + 1} \right)$$ for position 3, see Figure 10.2

β = as given in 10.2.12 for unsymmetrical flanged profiles.

β = 0 for symmetrical profiles.

10.3 K-factors for holes with edge reinforcement

10.3.1

K-factors for holes with edge reinforcement.

K-factors for holes with reinforcement are given in 10.3.2. For stresses parallel with the weld the notch stress is obtained with K_g from 10.3.2 and K_w = 1.0. For stresses normal to the weld the resulting notch stress is obtained with K_g from 10.3.2 and K_w = 1.5.

At some locations of the welds there are stress in the plate transverse to the fillet weld,σ_w, and shear stress in the plate parallel with the weld $\tau_{11.}$ Then the fillet weld is designed for a combined stress obtained as

$$\sigma_{comb} = \frac{t}{a}\sqrt{(180\sigma_w)^2 + (0.65\tau_{11})^2}$$

Where

t = plate thickness

a = throat thickness for a double sided fillet weld.

10.3.2 k-factors for holes with edge reinforcement

K-factors at holes in plates with inserted tubular are given in Figures 10.6 to 10.17. K-factors at holes in plates with ring reinforcement are given in Figures 10.18 to 10.22. K-factors at holes in plates with double ring reinforcement given in Figures 10.23 to 10.26.

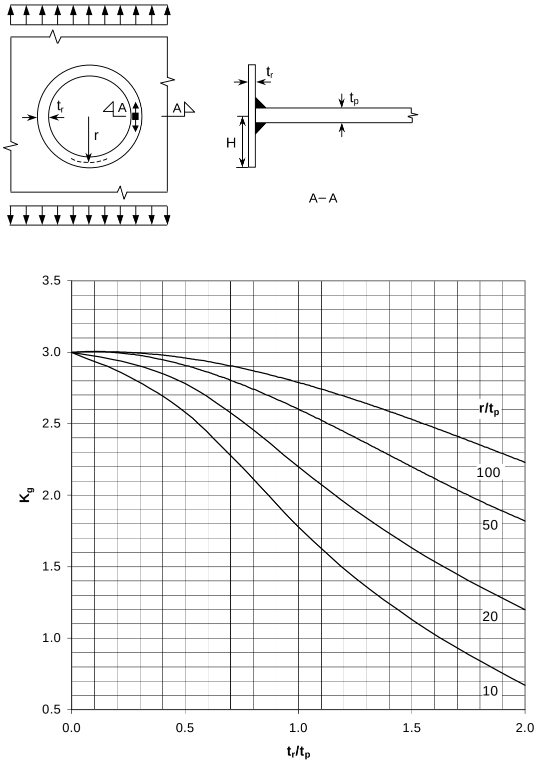

Figure 10.6 K_g at hole with inserted tubular. Stress at outer surface of tubular, parallel with weld. H/t_r = 2

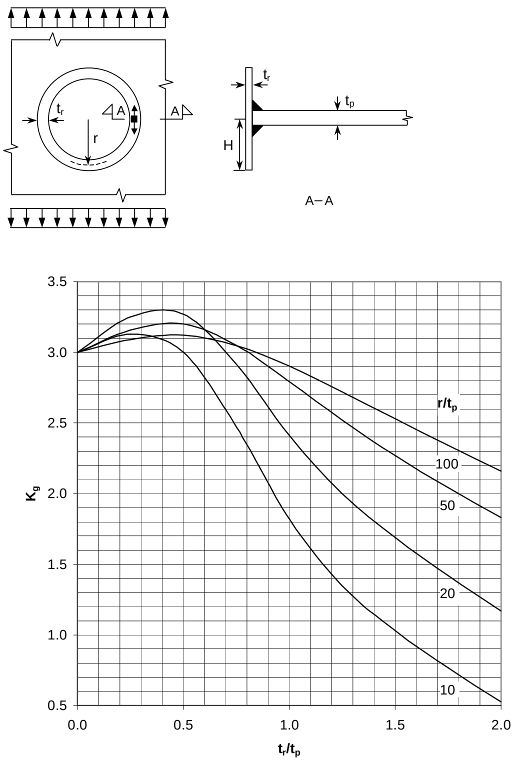

Figure 10.7 K_g at hole with inserted tubular. Stress at outer surface of tubular, parallel with weld. H/t_r = 5

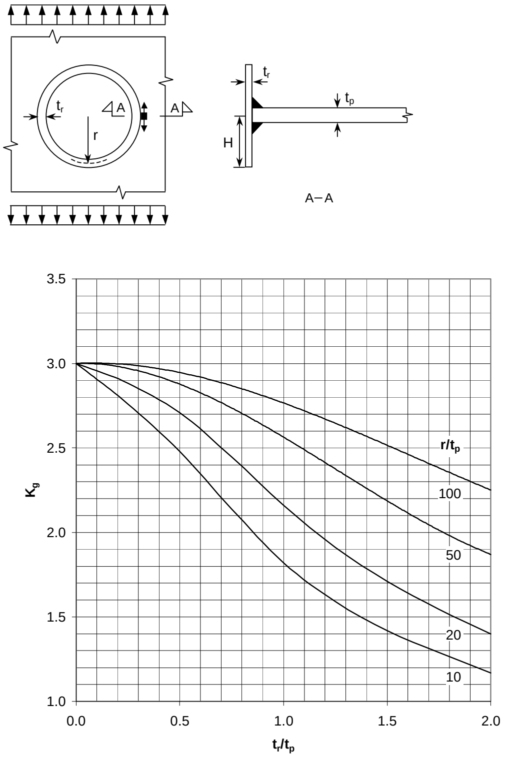

Figure 10.8 K_g at hole with inserted tubular. Stress in plate, parallel with weld. H/t_r = 2

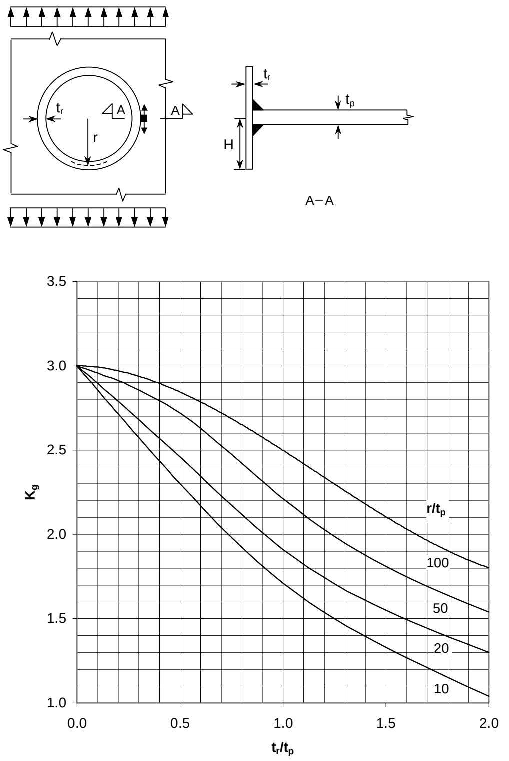

Figure 10.9 K_g at hole with inserted tubular. Stress in plate, parallel with weld. H/t_r = 5

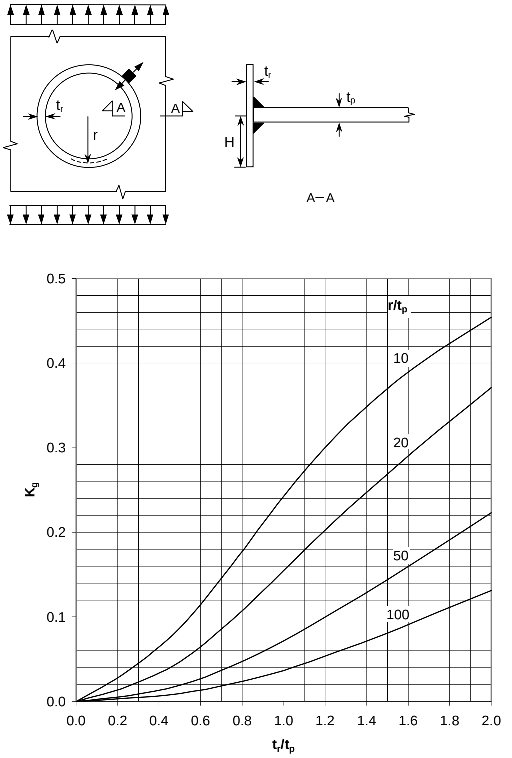

Figure 10.10 K_g at hole with inserted tubular. Stress in plate, normal to weld. $H/t_r = 2$

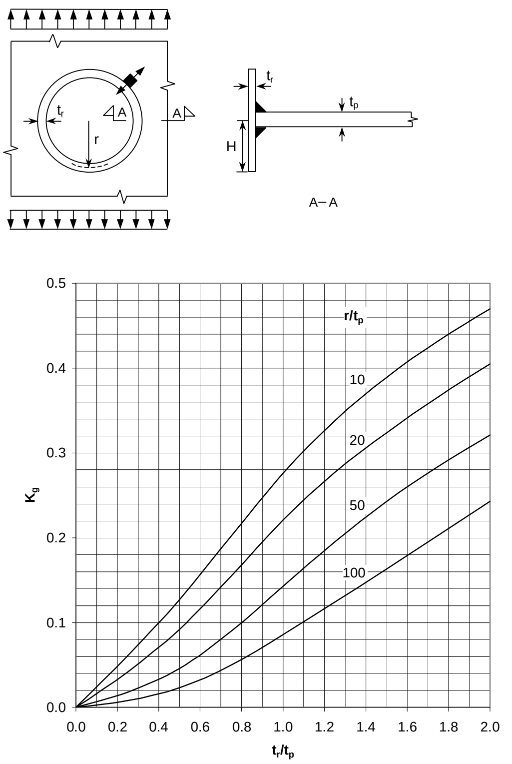

Figure 10.11 K_g at hole with inserted tubular. Stress in plate, normal to weld. $H/t_r = 5$

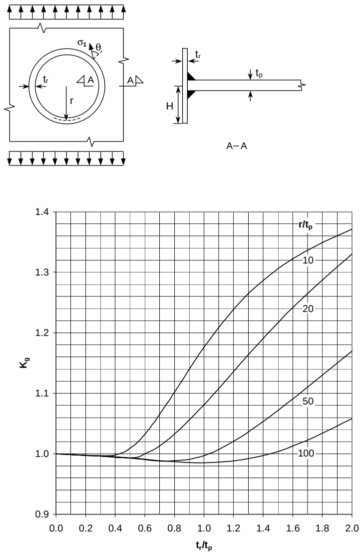

Figure 10.12 K_g at hole with inserted tubular. Principal stress in plate. $H/t_r = 2$

t_r/t_p	r/t_p=10	r/t_p=20	r/t_p=50	r/t_p=100
0.0	90	90	90	90
0.5	72	80	86	88
1.0	56	63	75	82
1.5	50	54	64	73
2.0	46	50	57	66

Table 10.12 Angle to principal stress. H/t_r=2

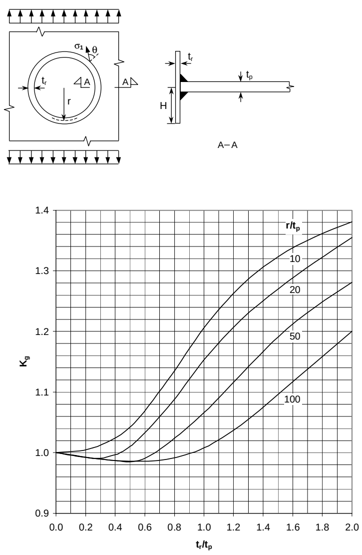

Figure 10.13 K_g at hole with inserted tubular. Principal stress in plate. $H/t_r = 5$

t_r/t_p	r/t_p=10	r/t_p=20	r/t_p=50	r/t_p=100
0.0	90	90	90	90
0.5	66	72	80	85
1.0	54	58	65	72
1.5	49	52	56	62
2.0	46	48	52	56

Table 10.13 Angle to principal stress. H/t_r=5

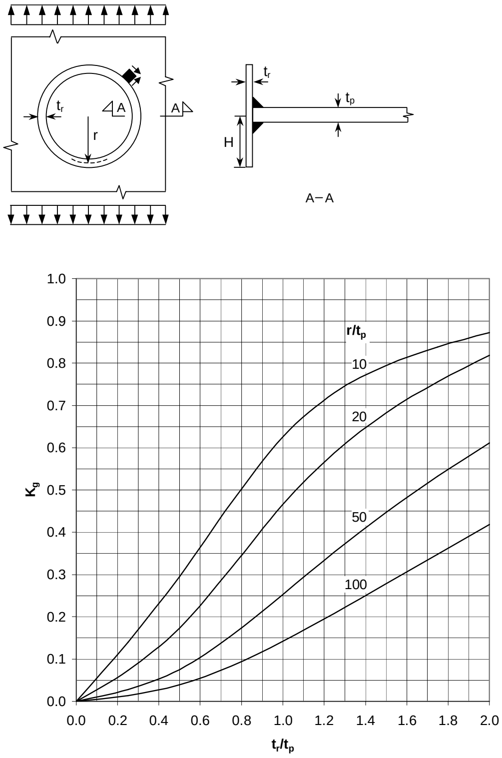

Figure 10.14 K_g at hole with inserted tubular. Shear stress in plate. $H/t_r = 2$

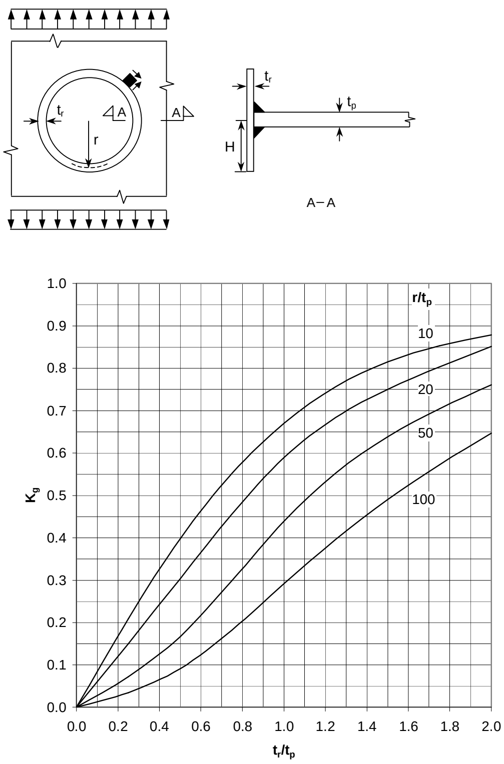

Figure 10.15 K_g at hole with inserted tubular. Shear stress in plate. $H/t_r = 5$

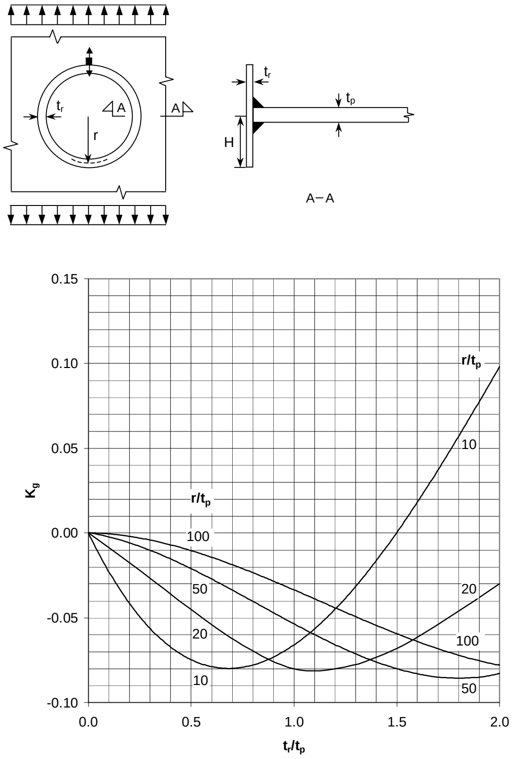

Figure 10.16 K_g at hole with inserted tubular. Stress in plate, normal to weld. $H/t_r = 2$

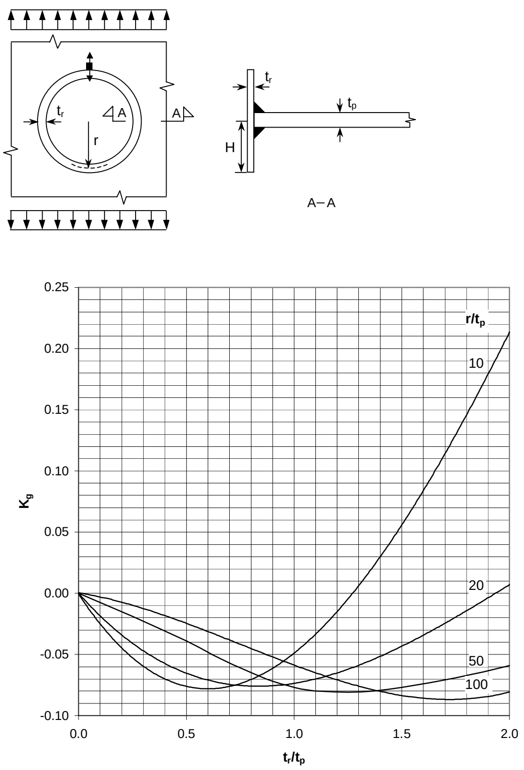

Figure 10.17 K_g at hole with inserted tubular. Stress in plate, normal to weld. $H/t_r = 5$

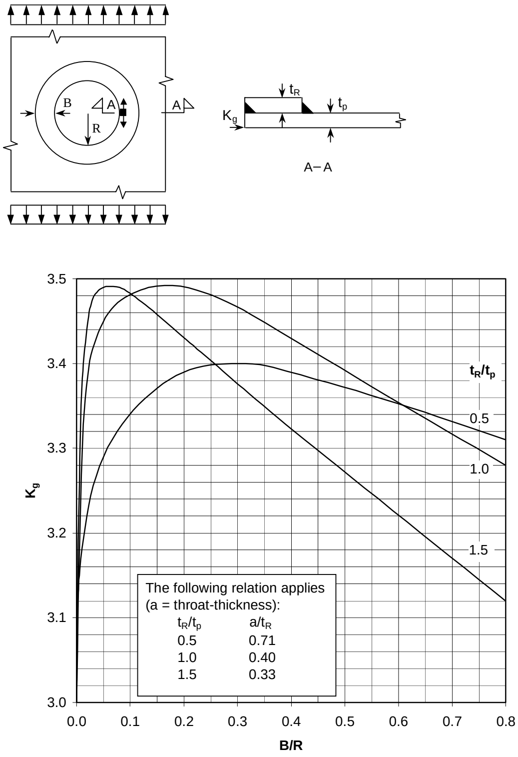

Figure 10.18 K_g at hole with ring reinforcement. Max stress concentration

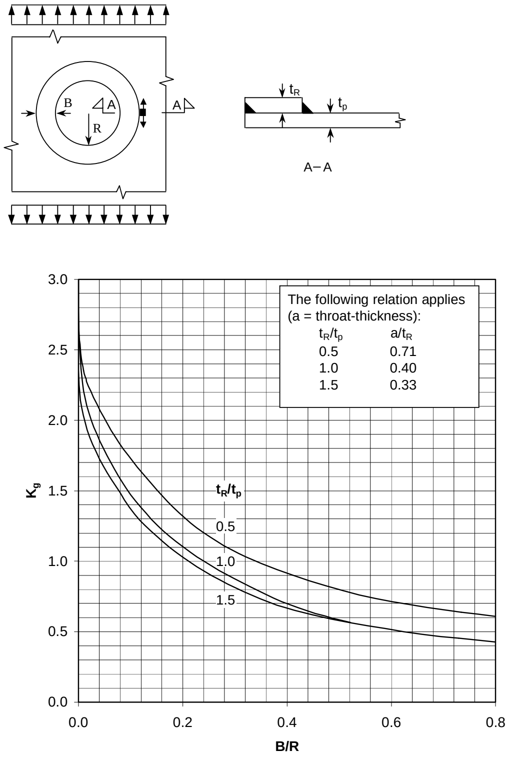

Figure 10.20 K_g at hole with ring reinforcement. Stress in plate, parallel with weld

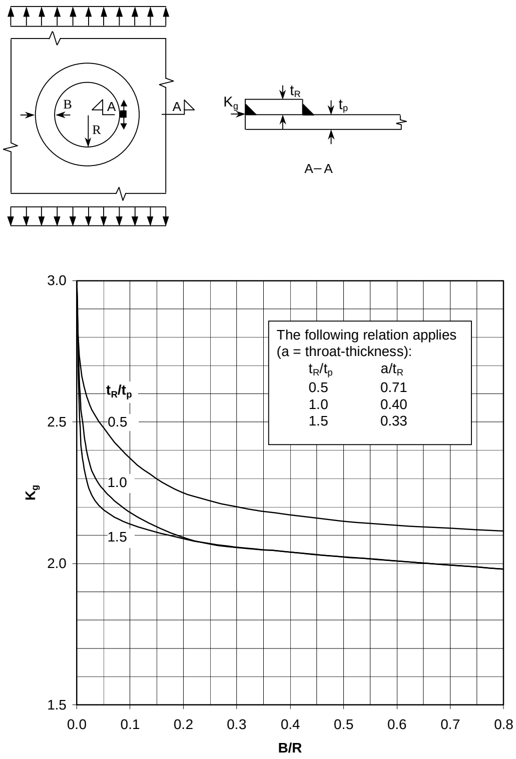

Figure 10.19 K_g at hole with ring reinforcement. Stress at inner edge of ring

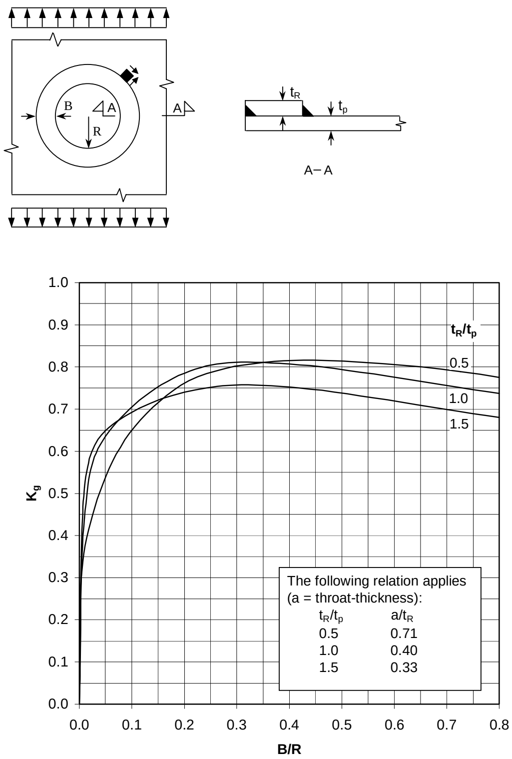

Figure 10.21 K_g at hole with ring reinforcement. Shear stress in weld

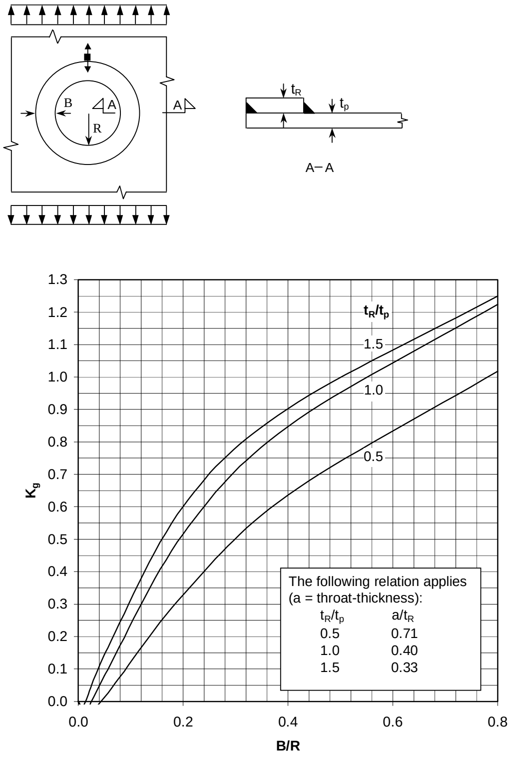

Figure 10.22 K_g at hole with ring reinforcement. Stress in plate, normal to weld

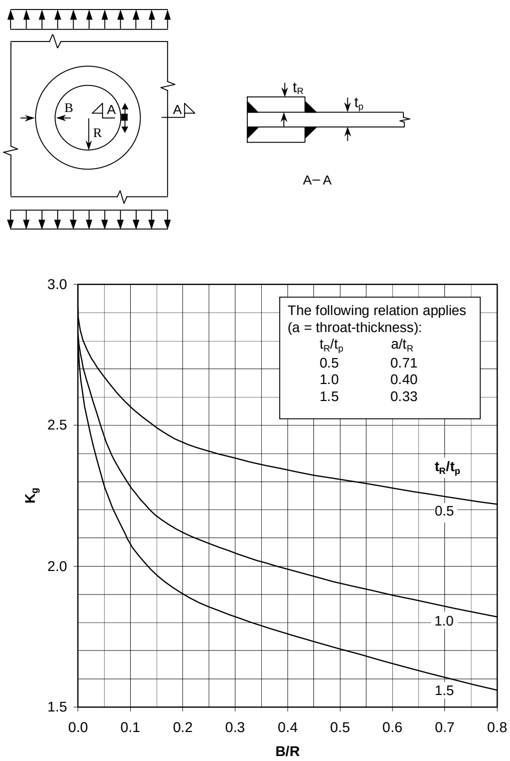

Figure 10.23 K_g at hole with double ring reinforcement. Stress at inner edge of ring

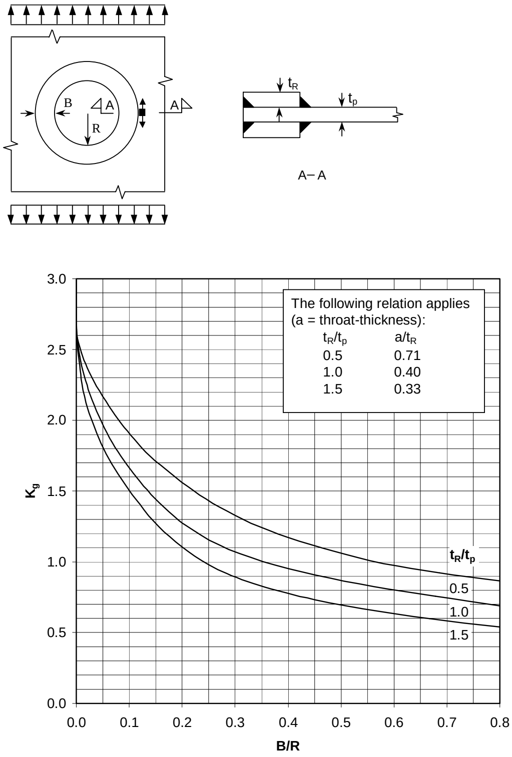

Figure 10.24 K_g at hole with double ring reinforcement. Stress in plate, parallel with weld

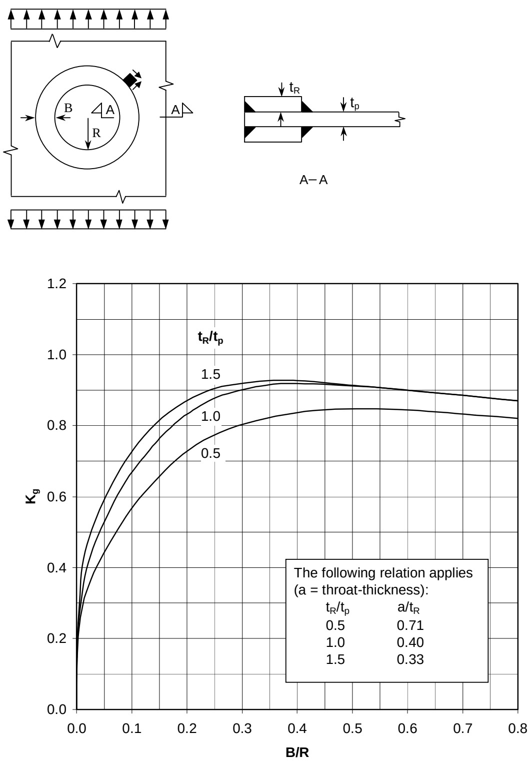

Figure 10.25 K_g at hole with double ring reinforcement. Shear stress in weld

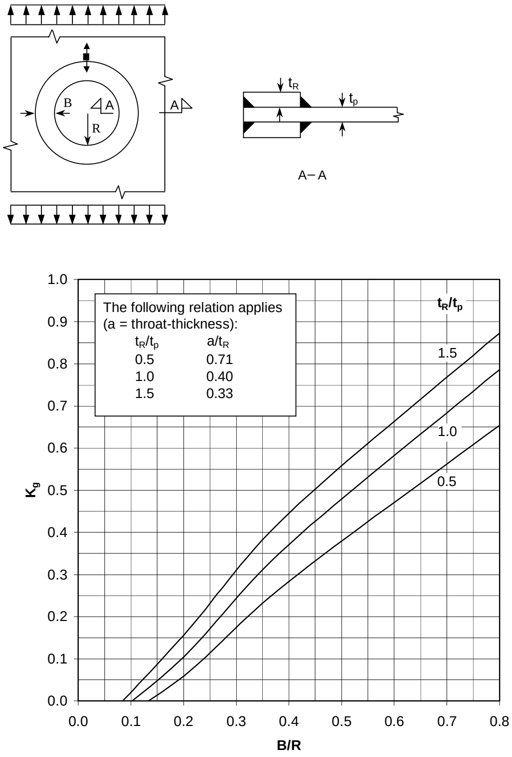

Figure 10.26 K_g at hole with double ring reinforcement. Stress in plate, normal to weld

10.4 Workmanship

10.4.1

The fatigue life of a welded joint is much dependent on the local stress concentrations factors arising from surface imperfections during the fabrication process, consisting of weld discontinuities and geometrical deviations

Surface weld discontinuities are weld toe undercuts, cracks, overlaps, porosity, slag inclusions and incomplete penetration. Geometrical imperfections are defined as misalignment, angular distortion, excessive weld reinforcement and otherwise poor weld shapes.

Embedded weld discontinuities like porosity and slag inclusion are less harmful for the fatigue strength when kept below normal workmanship levels.

Section 10.2 gives equations for calculation of K_g-factors due to fabrication tolerances for alignment of butt joints and cruciform joints, and the local weld geometry. Normally the default values given in the tables in 10.2 should be used if not otherwise defined. These normal default values are estimated assuming geometrical imperfections within limits normally accepted according to good shipbuilding practices, see Table 10.14. The S-N curves given in this note are assumed to include the effect of surface weld discontinuities representative for normal, good workmanship.

In special cases, K-factors may be calculated based on a specified, higher standard of workmanship. However, care should be taken not to underestimate the stress concentration factors by assuming a quality level which is difficult to achieve and follow up during production.

TYPE OF IMPERFECTION	*TYPE OF IMPERFECTION*	*EMBEDDED IMPERFECTIONS*	*SURFACE IMPERFECTIONS*
POROSITY, ISOLATED 2) Max. pore diameter, d: Min. distance to adjacent pore:	Weld Discontinuities	 t/4, max. 4 mm 2.5d	 3 mm 2,5d
POROSITY, CLUSTERED Max. pore diameter, d: 1) Max. length of cluster: 1)	Weld Discontinuities	 3 mm 25 mm	 Not applicable
SLAG INCLUSIONS 1)2)3) Max. width: Max. length:	Weld Discontinuities	 3,0 mm t, max. 25 mm	 Not applicable
UNDERCUT Max. depth: (Smooth transition required)	Weld Discontinuities	 Not applicable	 0.6 mm
UNDERFILL 1)2) Max. depth: Max. length:	Weld Discontinuities	 Not applicable	 1.5 mm t/2
EXCESSIVE WELD REINFORCEMENT 2)4) Max. height:	Geometrical Imperfections	 Not applicable	 b/5, max. 6 mm
OVERLAP 1)2) Max. length	Weld Discontinuities	Not applicable	t
CRACKS	Weld Discontinuities	Not accepted	Not accepted
LACK OF FUSION	Weld Discontinuities	Not accepted	Not accepted
LINEAR MISALIGNMENT 2) Max. eccentricity, butt joints: Max. eccentricity, cruciform joints:	Geometrical Imperfections	 Not applicable	 0.15t, max. 3 mm 0.3t
ANGULAR MISALIGNMENT Max. distortion:	Geometrical Imperfections	 Not applicable	 6 mm
INCOMPLETE PENETRATION 1)2) Max. length: Max. height:	Weld Discontinuities	 t 1.5 mm	 t t/10, max. 1.5 mm

Notes:
1) Defects on a line where the distance between the defects is shorter than the longest defect are to be regarded as one continuous defect.
2) t: Plate thickness of the thinnest plate in the weld connection.
3) If the distance between parallel slag inclusions, measured in the transverse direction of welding is less than 3 times the with of the largest slag inclusion, the slag inclusions are regarded as one defect.
4) b: Width of weld reinforcement

Table 10.14 Assumed normal tolerance limits for fabrication imperfections

10.4.2 Effect of grinding of welds.

For welded joints involving potential fatigue cracking from the weld toe an improvement in strength by a factor of at least 2 on fatigue life can be obtained by controlled local machining or grinding of the weld toe. The final grinding should be carried out by a rotary burr. The treatment should produce a smooth concave profile at the weld toe with the depth of the depression penetrating into the plate surface to at least 0.5 mm below the bottom of any visible undercut (Figure 10.27). The maximum depth of grinding of parrent plate should not exceed 2 mm or 5% of the plate thickness, whichever is smaller. It is recommended that the diameter of rotary burr is 6 mm or greater.

By additional grinding and polishing of the weld profile such that a circular transition between base material and weld surface is achieved, the stress concentration is further reduced (as the grinding radius is increased). This may lead to additional improvement of the joint connection (reduced K-factor).

The benefit of grinding may be claimed only for welded joints which are adequately protected from sea water corrosion.

In the case of partial penetration welds; when failure from the weld root is considered, grinding of the weld toe will not give an increase in fatigue strength.

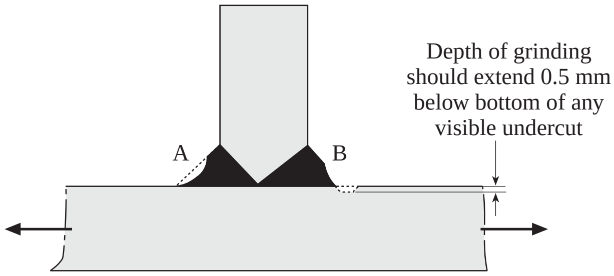

Figure 10.27 Grinding of the weld toe tangential to the plate surface, (as at A) will produce only limited improvement in the fatigue strength. The grinding must extend below the plate surface, (as at B) in order to remove toe defects.

11. Appendix B Assessment of Secondary Bending Stresses

11.1 Objective

When neither 3D-FEM analyses and/or frame analyses results as described in Chapters 6 and 3 respectively, nor experimental data, are available, secondary bending stresses may be assessed by the approximate equations given in 11.2.

The method presented is suitable for a first assessment of secondary bending stresses of large stiffened panels and double skin constructions due to the action of transverse pressure loads. The formulas are intended for

1) double bottom structures between transverse bulkheads and longitudinal bulkheads and/or side structures, Figure 11.1
2) double sides and longitudinal bulkheads between transverse bulkheads and bottom and deck panels.

11.2 Assessment of secondary bending stresses in double hulls

11.2.1

Longitudinal secondary bending stresses in double bottom panels at the intersection with transverse bulkheads may be assessed from the following formulas.

In case the double bottom is longer than wide (a is greater than b) the stresses in the longitudinal direction (*longitudinal direction, short end, Case 1 and 2, Table 11.1)* is found as :

$$\sigma_2 = K_\beta \frac{K_b p_e b^2 r_a}{\sqrt{i_a i_b}} \qquad \rho = \frac{a}{b}\sqrt[4]{\frac{i_b}{i_a}}$$

In case the double bottom is wider than long (b is greater than a) the stresses in the longitudinal direction (*longitudinal direction, long end, Case 3 and 4, Table 11.1)* is found as :

$$\sigma_2 = K_\beta \frac{K_b p_e a^2 r_a}{i_a} \qquad \rho = \frac{b}{a}\sqrt[4]{\frac{i_a}{i_b}}$$

where:

K_β = stress concentration factor as given in Chapter 10 for axial loading

K_b = coefficient dependent on apparent aspect ratio "ρ", $\eta = 1.0$, and actual boundary condition in Table 11.1.

p_e = effective average lateral pressure

r_a = distance from point considered to neutral axis of panel

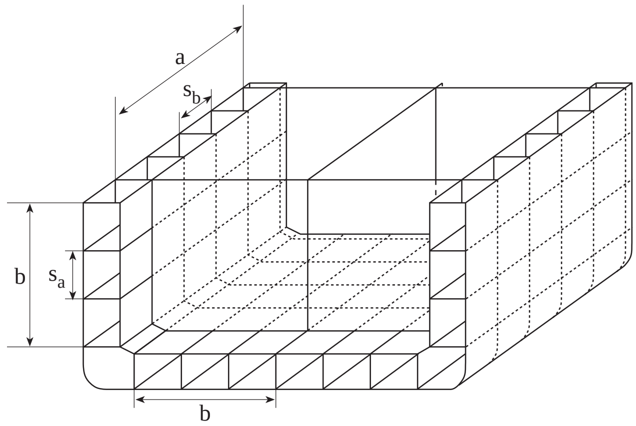

Figure 11.1 Double skin configuration

a = longitudinal length of double bottom panel or double side panel, Figure 11.1

b = Transverse width of double bottom panel or double side panel, Figure 11.1

i_a = smeared out stiffness per longitudinal double panel girder about transverse neutral axis of the girder is normally given by:

$$i_a = \frac{I_a}{s_a}$$

i_b = Smeared out stiffness per transverse double panel girder about longitudinal neutral axis of the girder

$$i_b = \frac{I_b}{s_b}$$

(In case the middle girder is significantly stronger than the other girders or there is only one or less girder in any direction, see Table 11.3 for definition of parameters.)

I_a, I_b = Longitudinal and transverse sectional moment of inertia about the double bottom neutral axis in transverse and longitudinal axes respectively, per girder including effective width of plating. In computation of I_a the area of the longitudinal stiffeners may be added to the plate as a smeared out thickness, conserving the sectional moment of inertia about the double bottom neutral axis.

s_a, s_b = Spacing between girders in longitudinal and transverse directions respectively, Figure 11.1.

11.2.1.1

Transverse secondary bending stresses in double bottom panels at the intersection with longitudinal bulkheads may be assessed from the following formulas.

In case the double bottom is longer than wide (a is greater than b) the stresses in the transverse direction (*transverse direction, long end, Case 3 and 4, Table 11.1)* is found as :

$$\sigma_2 = K_\beta \frac{K_b p_e b^2 r_b}{i_b} \qquad \rho = \frac{a}{b}\sqrt[4]{\frac{i_b}{i_a}}$$

In case the double bottom is wider than long (b is greater than a) the stresses in the transverse direction (*transverse direction, short end, Case 1 and 2, Table 11.1)* is found as :

$$\sigma_2 = K_\beta \frac{K_b p_e a^2 r_b}{\sqrt{i_a i_b}} \qquad \rho = \frac{b}{a}\sqrt[4]{\frac{i_a}{i_b}}$$

11.2.1.2

With double sides, the same formulation as in 11.2.1-11.2.3 can be used. It is, however, important at all times to apply the appropriate boundary conditions.

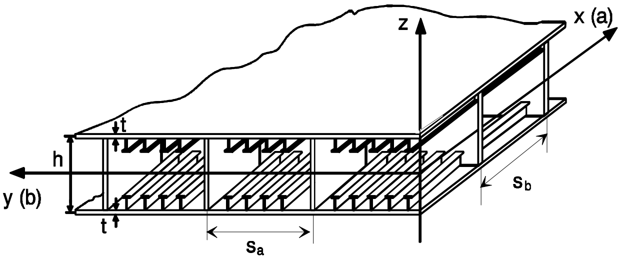

Figure 11.2 Double bottom configuration

Case no. & Stress location	*Boundary conditions*	ρ	η *=0.0*	η*=0.5*	η*=1.0*
Case no. 1:	Long edges:	1.00	0.0952	0.0845	0.0767
Support bending stress in *long*	Simply supported	1.25	0.1243	0.1100	0.0994
direction at middle of short end	Short ends:	1.50	0.1413	0.1261	0.1152
	Clamped	1.75	0.1455	0.1342	0.1251
		2.00	0.1439	0.1374	0.1300
		2.50	0.1388	0.1381	0.1356
		3.00	0.1371	0.1376	0.1369
		3.50	0.1371	0.1373	0.1373
		4.00	0.1373	0.1374	0.1373
		& up	0.1374	0.1374	0.1374
Case no.: 2	All edges:	1.00	-	-	0.0564
Support bending stress in *long* direction at middle of short end	Clamped	1.10	-	-	0.0591
		1.20	-	-	0.0609
		1.30	-	-	0.0619
		1.40	-	-	0.0624
		1.50	-	-	0.0626
		1.60	-	-	0.0627
		& up	-	-	0.0627
Case no.3:	Long edges:	1.00	0.0952	0.0845	0.0762
Support bending stress in *short* direction at middle of long edge	Clamped	1.33	0.1026	0.0949	0.0878
	Short edges:	2.00	0.0972	0.0950	0.0926
	Simply supported	2,66	0.0920	0.0925	0.0922
		4.00	0.0912	0.0915	0.0917
		& up	0.0916	0.0916	0.0916

Case no. & Stress location	*Boundary conditions*	*ρ*	*η =0.0*	*η=0.5*	*η=1.0*
Case no. 4: Support bending stress in *short* direction at middle of long edge	All edges: Clamped	1.00	-	-	0.0564
		1.10	-	-	0.0638
		1.20	-	-	0.0702
		1.30	-	-	0.0755
		1.40	-	-	0.0798
		1.50	-	-	0.0832
		1.60	-	-	0.0857
		1.70	-	-	0.0878
		1.80	-	-	0.0892
		1.90	-	-	0.0903
		2.00	-	-	0.0911
		& up	-	-	0.0911

Table 11.1 Support bending stress coefficients K_b, n = 0.3, (for intermediate values use linear interpolation)

11.3 Assessment of secondary panel stresses in single skin vessels.

11.3.1

The stresses at transverse bulkheads may be assessed from the formulas as for double bottom. However the parameters for aspect ratios ρ and torsion coefficient η shall be taken as given in Table 11.3 and the parameters K_b to be taken as given in Table 11.2.

11.3.2

For *longitudinal bulkheads,* Section 11.2.1 still applies taking the appropriate boundary condition from Tables 11.2 and 11.3 defines the geometric and stiffness properties to be used.

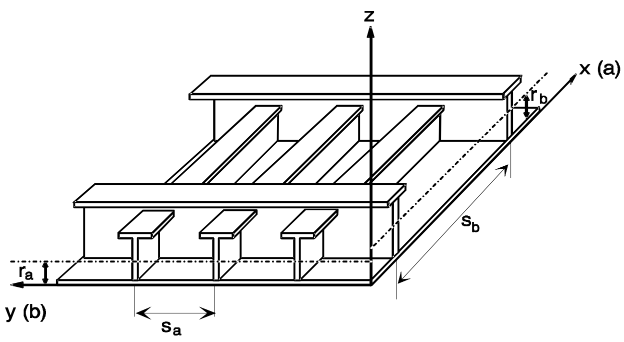

Figure 11.3 Single Bottom Configuration

Case no. & Stress location	*Boundary conditions*	*ρ*	*η=0.0*	*η=0.5*	*η=1.0*
Case no. 5: Support bending stress in *long* direction at middle of short end	Long edges: Simply supported	1.00	0.0866	0.0769	0.0698
		1.25	0.1140	0.1001	0.0904
	Short ends: Clamped	1.50	0.1285	0.1148	0.1049
		1.75	0.1324	0.1221	0.1139
		2.00	0.1310	0.1250	0.1191
		2.50	0.1263	0.1257	0.1234
		3.00	0.1248	0.1253	0.1246
		3.50	0.1248	0.1250	0.1246
		4.00	0.1240	0.1250	0.1250
		& up	0.1250	0.1250	0.1250
Case no.6: Support bending stress in *short* direction at middle of long edge	Long edges: Clamped	1.00	0.0866	0.0769	0.0698
		1.33	0.0934	0.0858	0.0799
	Short edges: Simply supported	2.00	0.0885	0.0865	0.0843
		2.66	0.0837	0.0842	0.0839
		4.00	0.0830	0.0832	0.0835
		& up	0.0834	0.0834	0.0834

Table 11.2 Support bending stress coefficients K_b in free flanges (single skin) n = 0.0, Figure 11.3 (for intermediate values use linear interpolation)

Type	*Sketch*	*Formulas for ρ and η*
A: Cross stiffening Middle girder / stiffener in both directions are stiffer than the others	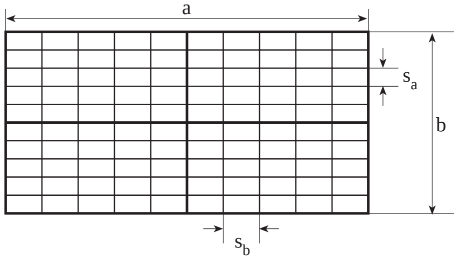	$i_a = \frac{I_{na}}{s_a} + 2\left(\frac{I_a - I_{na}}{b}\right)$ $i_b = \frac{I_{nb}}{s_b} + 2\left(\frac{I_b - I_{nb}}{a}\right)$ $\rho = \frac{a}{b}\sqrt[4]{\frac{i_b}{i_a}}$ $\eta = \sqrt{\frac{I_{pa} I_{pb}}{I_{na} I_{nb}}}$
B: Modified cross stiffening One girder / stiffener in a-direction only	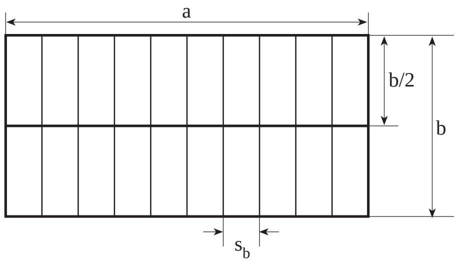	$i_a = 2\frac{I_a}{b}$ $i_b = \frac{I_{nb}}{s_b} + 2\left(\frac{I_b - I_{nb}}{a}\right)$ $\rho = \frac{a}{b}\sqrt[4]{\frac{i_b}{i_a}}$ $\eta = 0.124\sqrt{\frac{I_{pb}^2\, b}{I_a I_{nb}\, s_b}}$
C: Single stiffening Girders / stiffeners in b-direction only	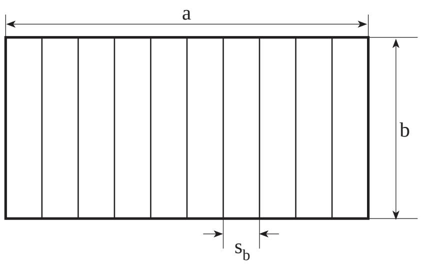	$i_a = 0$ $i_b = \frac{I_{nb}}{s_b}$ ρ = infinite η = indeterminate
D: Unstiffened plate	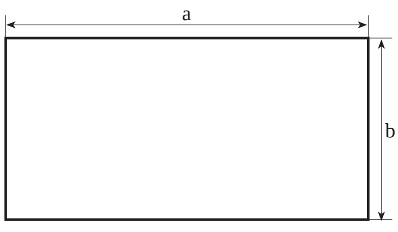	$i_a = i_b = \frac{t^3}{12(1-\nu^2)}$ $\rho = \frac{a}{b}$ $\eta = 1.0$

Table 11.3 Definition of geometry and stiffness parameters

The following notation is applied::

a = Length of panel

b = Width of panel

s_a (s_b) = spacing of long (short) girders in case of double hull and stiffeners in case of single skin.

I_{na} (I_{nb}) = moment of inertia, including effective width of plating, of long (short) repeating less stiff girders or stiffeners (as distinguished from the central girder / stiffener, which may be different).

I_{pa} (I_{pb}) = moment of inertia w.r.t the neutral axis in a (b) direction of effective width of plating only for the central girder.

I_a (I_b) = moment of inertia, including effective width of plating, of *central* long (short) girder / stiffener.

A_a (A_b) = web area of *central* long (short) stiffener

r_a (r_b) = bending lever arm about the combined neutral axis of the stiffened panel combination in a (b) direction respectively, to the stress point of interest

t = plate thickness

i_a (i_b) = unit (smeared out) stiffness

η = torsion coefficient

ρ = (virtual) side ratio

NOTE
The different moment of inertia in the above list are evaluated about the panel neutral axis.

12. Appendix C Simplified Loads for Direct Strength Analysis

12.1
In combination with the loads related to the simplified method described in Chapter 3., direct strength analysis may be applied to determine the stresses in the hull. Each of the load components should then be considered separately and combined according to the formulas in Section 3.4. The stresses from global loads in Section 3.5 are then substituted with those determined from the loads given in 12.2 and 12.3. The local internal and external load induced stress components are to be combined as described in 3.4.

12.2
For direct global finite element calculation purpose, the range of vertical hull girder wave bending moment given in 4.2 may be expressed in terms of counteracting vertical forces, see also Figure12.1:

At A.P. and 0.4L forward of A.P.:

F_1 = +/- $[M_{WO,h} - M_{WO,s}]/(0.4L)$

At 0.65L forward of A.P. and at F.P.:

F_2 = -/+ $[M_{WO,h} - M_{WO,s}]/(0.35L)$

$M_{WO,h}$, $M_{WO,s}$ = as given in 4.2.1.

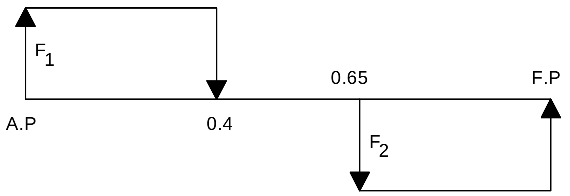

Figure 12.1 Distribution of sectional forces for computation of vertical bending stress range.

12.3
The combined horizontal wave bending- and wave torsion load at 10^{-4} probability level may (in accordance with ref. [1] of 9.3), in a global finite element calculation, be defined as a horizontal line load, q_h, acting at a level 0.7 T above the vessel base line and a line moment load acting in the ship's centreline, m_t, given as:

$$q_h = -0.88\, f_r \sqrt{1 - \frac{C_B^2\, L^2 B\, C_{SWP}}{18000\, T_{act}^2}}\; L^{\frac{3}{4}} \left(T_{act} + 0.3B\right) C_B \cos\left(\frac{2\pi x}{L}\right) \quad \text{(kN/m)}$$

$$m_t = 1.63\, f_r \sin\left(\frac{2\pi x}{L}\right) \cos\left(\frac{\pi x}{3 C_B\, L}\right) L^{\frac{1}{3}} B^2 \frac{C_{SWP}}{C_B}$$

$$-0.27\, f_r \sin^2\left(\frac{\pi x}{L}\right) \cos\left(\frac{\pi x}{3 C_B\, L}\right) L^{\frac{1}{3}} B^2 \frac{C_{SWP}}{C_B^2} \quad \text{(kNm/m)}$$

C_{SWP} = $A_{WP} / (LB)$

A_{WP} = water plane area in m^2 of vessel at draught = T.

T_{act} = vessel draught in m in considered condition. (Note a draught equal to the design draught may in general be assumed as representative for a condition to be applied for a fatigue analysis related to the ship’s cargo conditions)

x = Distance in m from A.P. to considered position on hull girder.

f_r = as defined in 4.2.1 inserting h = 0.95

Note in this connection that the first term of the formula for M_{WT} given in 9.3 is based on an expression for the horizontal wave shear force which is compatible with the formula for the horizontal wave bending moment M_{WH} defined in 9.3.

13. Appendix D Two-Slope S-N Curve Fatigue Damage Expression

13.1 Weibull distributed stress range

When the long-term stress range distribution is defined applying Weibull distributions for the different load conditions, and a one-slope S-N curves is used, the fatigue damage is given by,

$$D = \frac{\nu_0 T_d}{\bar{a}} \sum_{n=1}^{N_{load}} p_n q_n^m \Gamma(1 + \frac{m}{h_n}) \le \eta$$

where

N_{load} = total number load conditions n considered

p_n = fraction of design life in load condition n, $\Sigma p_n \le 1$, but normaly not less than 0.85

T_d = design life of ship in seconds (20 years = 6.3 10^8 sec.)

$\bar{a}, m$ = S-N fatigue parameters

h = Weibull stress range shape distribution parameters, see Section 3.2

q = Weibull stress range scale distribution parameters

ν_0 = average zero-crossing frequency

$\Gamma(1+\frac{m}{h_n})$ = gamma function. Values of the gamma function are listed in Table 2.7

When a bi-linear or two-slope S-N curve is used, the fatigue damage expression is given by,

$$D = \sum_{n=1}^{N_{load}} D_n = \nu_0 T_d \sum_{n=1}^{N_{load}} p_n \left[\frac{q_n^{m_1}}{\bar{a}_1} \Gamma\left(1 + \frac{m_1}{h_n}; \left(\frac{S_0}{q_n}\right)^{h_n}\right) + \frac{q_n^{m_2}}{\bar{a}_2} \gamma\left(1 + \frac{m_2}{h_n}; \left(\frac{S_0}{q_n}\right)^{h_n}\right)\right] \le \eta$$

where,

S_0 = Stress range for which change of slope occure

$\bar{a}_1,\ m_1$ = S-N fatigue parameters for N < 10^7 cycles

$\bar{a}_2,\ m_2$ = S-N fatigue parameters for N > 10^7 cycles

$\gamma(\ )$ = Incomplete Gamma function, to be found in standard tables

$\Gamma(\ ;\ )$ = Complementary Incomplete Gamma function, to be found in standard tables

S-N parameters are given in Section 2.

13.2 Rayleigh distributed stress range

When the long term stress range distribution is defined through a short term Rayleigh distribution within each short term period for the different loading conditions, and a one-slope S-N curve is applied, the fatigue criterion reads,

$$D = \frac{\nu_0 T_d}{\bar{a}} \Gamma(1+\frac{m}{2}) \sum_{n=1}^{N_{load}} p_n \cdot \sum_{i=1, j=1}^{\substack{\text{all seastates}\\ \text{all headings}}} r_{ijn} (2\sqrt{2m_{0ijn}})^m \leq \eta$$

where

r_{ij} = the relative number of stress cycles in short-term condition *i, j*

m_{oij} = zero spectral moment of stress response process

The Gamma function, $\Gamma\left(1+\frac{m}{2}\right)$ is equal to 1.33 for m = 3.0.

When a bi-linear or two-slope S-N curve is applied, the fatigue damage expression is given as,

$$D = \sum_{n=1}^{N_{load}} D_n = \nu_0 T_d \sum_{n=1}^{N_{load}} \rho_n \sum_{i=1, j=1}^{\substack{\text{allseastates}\\ \text{allheadings}}} r_{ijn} \left[\frac{\left(2\sqrt{2m_{0ijn}}\right)^{m_1}}{\bar{a}_1} \Gamma\left(1+\frac{m_1}{2}; \left(\frac{S_0}{2\sqrt{2m_{0ijn}}}\right)^2\right) + \frac{\left(2\sqrt{2m_{0ijn}}\right)^{m_2}}{\bar{a}_2} \gamma\left(1+\frac{m_2}{2}; \left(\frac{S_0}{2\sqrt{2m_{0ijn}}}\right)^2\right)\right] \leq \eta$$

14. Appendix E Background for the S-N curves

14.1 Introduction

Several of the traditional fatigue design codes divide structural details into classes, each with a corresponding design S-N curve. A large number of ship structural details are different from the details the traditional S-N curves have been derived for. It may therefore be difficult to separate the calculated stress into the stress level that is embedded in the S-N curves and the stress level that must be applied together with the S-N curves.

Due to this, it was considered more convenient to develop a basic S-N curve that could be used for fatigue analysis of all welded structural details. This could be achieved by developing appropriate stress concentration factors to be used to obtain the local notch stress used together with the basic S-N curve.

Inherent in the S-N curves for classified details (such as ref. [F1] are both the notch stress and also the stress field over the crack growth area giving the actual crack growth development. This may be considered to give more accurate fatigue lives than the use of a single S-N curve and stress concentration factors. However, the difference between these two concepts is evaluated to be of minor importance for practical fatigue design of ship structural details, as the main portion of the fatigue life is within the initial stage of the crack size development.

14.2 S-N curves for welded connections

14.2.1

Stresses to be Associated with S-N curves

It is important that there is consistency between the way the S-N curves are derived and defined and the way the stress in the structure is calculated. It is necessary to know what stress is inherent in the considered S-N curve, how this stress is determined and how the corresponding stress from numerical analysis should be evaluated.

Definition of stresses used in the Classification Note is as follows (Ref. also Section 6, Figure 6.1):

- Nominal stresses are those derived from beam models or from coarse mesh FEM models. Stress concentrations resulting from the gross shape of the structure are included in the nominal stress.
- Geometric (hot spot) stresses include nominal stresses and stresses due to structural discontinuities and presence of attachments, but excluding stresses due to presence of welds. Stresses derived from fine mesh FEM models are geometric stresses. Effects caused by fabrication imperfections as e.g. misalignment of structural parts, are, however, normally not included in FEM analyses, and must be separately accounted for. The greatest value of the extrapolation to the weld toe of the geometric stress distribution immediately outside the region affected by the geometry of the weld, is commonly denoted hot spot stress.
- Notch stresses are the total stresses at the weld toe (hot spot location) and include the geometric stresses and the stresses due to the presence of the weld. The notch stress may be calculated by multiplying the hot spot stress by a stress concentration factor, or more precisely the theoretical notch factor, K_w. FEM may be used to determine the notch stress. However, because of the small notch radius and the steep stress gradient at a weld, a very fine mesh is needed.

Traditionally fatigue calculations are based on the nominal stresses and the use of geometry dependent S-N curves. S-N curves may also be developed based on the concept of hot spot stresses saying that the effect of the notch stress due to the local weld detail is imbedded in the curve, or alternatively, based on the notch stress where the influence of the weld is included. All concepts have their advantages and disadvantages:

<u>Nominal Stress Approach</u>

Advantages: Inherent in the S-N curves for classified details accounts for both the notch stress and the stress field over the crack growth area.

Disadvantages: It is difficult in practical design of ship structural details to define the nominal stress level to be applied together with the geometry specific S-N curves. Further, the use of a limited number of established S-N curves in the fatigue design, complicates the utilisation of improved local design and workmanship in the fatigue life assessment.

<u>Geometric Stress (Hot Spot Stress) Approach</u>

Advantages: Using the hot spot stress method the local notch effect is embedded in the S-N data, and one may say that the large variation in local notch geometry is accounted for in the scatter of the S-N data.

Disadvantages: The hot spot stress has to be determined by extrapolation of stresses outside the notch region. The finite element mesh has to be fine enough to represent the geometric stress in this region. Extrapolation should be performed from points at least 0.3t outside the notch. Practise for extrapolation has varied as its basis is founded on experience from test measurements and numerical analysis of stress distributions at the hot spot region.

<u>Notch Stress Approach</u>

Advantages: The notch stress need not be separated from the geometric stress, and the notch stress is derived as the finite element size approaches a small value provided the notch root radius is modelled.

Disadvantages: The geometry of the local notch at a weld varies along the weld profile, and it may be difficult to find a geometry to base the analysis on. However, considering that the scatter in local notch geometry is accounted for in the scatter of the S-N data the geometry for local analysis may be based on mean geometry data.

During evaluation of these two concepts, a basic S-N curve was selected for welded connections that was also applicable for smooth machined specimens having a stress concentration factor $K_w = 1.0$ by definition. This corresponds then to the notch stress concept. However, a default value $K_w = 1.5$ is introduced such that the hot spot stress method may be used. The calculated hot spot stress must then be multiplied by the K_w value before the S-N curve is entered.

A procedure that allows the effects of fabrication methods and workmanship to be explicitly accounted for in the fatigue analyses is believed to contribute to improved local geometry and workmanship in shipbuilding. In this way one may say that the advantages of both the concepts described above have been utilised.

14.2.2 Basic S-N Curves

The S-N curves in ref.[F1] was used as basis for derivation of S-N curves for this Classification note.

The S-N curves in ref. [F1] is the same as in ref.[F5] in air (frequently referred to as Department of Energy curves), and with some adjustment for $N \geq 10^7$ for sea water cathodic protection.

The S-N curves are established as mean minus two standard deviation for relevant experimental data.

14.2.3 Basic Transformation to One S-N Curve

The negative inverse slope of S-N curves for typical ship details is m = 3.0. Thus, also the basic curve should have this slope. The slope of the C curve which was considered as a first choice for a basic S-N curve is m = 3.5 (Stress concentration factor 1.0).

The S-N curve with slope m = 3.5 (the C-curve from ref.[F1]) was transferred into a S-N curve with slope m = 3.0 in the following way: A long term stress range distribution for a typical ship was considered that gave fatigue damage equal 1.0 during 20 years service life. A Weibull distribution of the stress ranges with h = 0.95 was used. Then a new curve was established with inverse negative slope m = 3.0 that resulted in the same fatigue damage for the same stress range distribution.

According to Dr. T.R. Gurney of TWI, the S-N data for the C curve are not comprehensive. Therefore the basis for the curve has also been checked for other details such as F and F2 details (Ref.[F1] terminology) and for butt welds, see 14.2.5, and fracture mechanics, see 14.2.6. Also other standards with S-N curves have been looked at.

The F and the F2 curves may be considered as the most reliable S-N curves in the design standards (based on in-house experience). It has been checked that the proposed S-N curve together with proposed procedure for estimation of hot spot stress (determination of K-factors based on FEM ref. Section 6.6) gives fatigue lives corresponding to that obtained by using these curves together with appropriate K-factors.

14.2.4 Thickness Effect

The thickness effect is mainly included as in ref. [F1], but for welds with a small stress concentration (SCF less than 1.3) the thickness effect is negligible. This is substantiated by simple fracture mechanics calculations, and is also in line with experimental data.

14.2.5 Butt Welds

A basic stress concentration factor equal $K_w = 1.5$ is suggested as a default value for welds. This corresponds to $\rho/t \cong 0.15$ and $\theta \cong 45°$ for a butt weld. With thickness $t = 22$ mm this correspond to a radius at the toe of the weld $\rho = 2$ mm applying an equation for the stress concentration factor K_w from Ref.[F14]:

$$K_w \quad = \quad 1 + 0.27 * (\tan\theta)^{0.25} \left(\frac{t}{\rho}\right)^{0.25}$$

where θ denotes the angle between the base plate and the weld face.

This K_w factor together with the basic S-N curve gives appropriate fatigue lives for butt welds. This weld geometry corresponds with that measured (Ref.[F4]), but it should be noted that the scatter of weld toe radius ρ is significant and that this scatter should be accounted for in the design S-N curve.

14.2.6 Fracture Mechanics

It has been verified that the proposed basic S-N curve for welded connections does not result in a fatigue life less than that derived by fracture mechanics assuming a rather shallow crack and with use of relevant crack growth parameters, ref.[F1] (fracture mechanics do not include cycles for initiation):

With reference to Section 4 of ref. [F1], setting I = 9.3, ref. Fig. 4.1a, m = 3.1, $C = 1.1*10^{-13}$, (mean data); w = 22 mm is assumed. Transformation of fracture mechanics into a S-N curve then gives

$\log N = 13.19 - 3.1 \log S$

with initial crack depth $a_i = 0.03$ mm (very small surface crack).

Transformation to slope m = 3.0 assuming a long term Weibull distribution with parameters $n_0 = 10^8$ and h = 1.0:

$\log N = 12.99 - 3.0 \log S.$

Assuming standard deviation in log N equal 0.20 then gives $\log \bar{a} = 12.59$ as mean minus two standard deviations.

14.2.7 S-N curve for Corrosive Environment

The S-N curve for corrosive environment is based on ref. [F1] with a reduction on fatigue life equal 2.0, and a removal of cut-off as compared with cathodic protected structures in sea water.

14.2.8 Comparison of S-N curves

A comparison of S-N curves for welded connections is shown in Table 14.1. It is noted that the basic S-N curve lately proposed by HSE, the D curve, (Ref. [F6]) is 4.9% more optimistic with respect to fatigue strength than that of the basic DNV curve.

S-N curve	*Allowable stress range at $2*10^6$ cycles (MPa)*
DNV curve I *	87.03
HSE curve D (Ref. [F1,F5,F6])	91.27
HSE curve E (Ref. [F1,F5,F6])	80.60
Fracture mechanics with crack growth parameters from Ref. [F1] with initial defect size approaching zero.*	83.22
* The K_w (stress concentration factor due to the local weld geometry) is here taken into account for the DNV curve and the fracture mechanics curve (the allowable stress range has been divided by 1.5) in order to get comparable basis.	

Table 14.1 Comparison of S-N curves for welded connections

14.3 S-N curves for the base material

14.3.1 Background

It is realised that the steepness of S-N curves for base materials is less than that of curves for welded connections. At an early stage of the development of this Classification Note a negative inverse slope equal 4.0 was suggested which is the same as used in ref. [F1]. For structures subject to few dynamic load cycles this led to greater fatigue strength for welded connections than for base material since the curve for base material was crossing the curve for welded connections. It was therefore decided to establish a S-N curve for the base material along similar lines as for the welded joints, i.e. establish a curve that would represent a relatively reliable curve for typical long term distribution of load effects in ships.

It should be noted that the fatigue life of the base material is very dependant on surface finish and how this surface is retained during service life.

It is further noted that the fatigue limit (constant amplitude) is higher for high strength steels than for normal steels. It is likely that this effect is more related to crack initiation (surface finish) and not so much to crack growth. Therefore this effect may be included in a S-N curve for base material with a good surface finish, but should be neglected for notched welds and surfaces. However further investigations is necessary before a higher design S-N curves for high strength steels can be developed.

14.3.2 S-N Curves by the Japanese Society for Steel Construction

Japanese Society for Steel Construction (JSSC) specify an A grade curve for machined and ground surface, while a B grade curve is given for as-flame-cut surface or that with mill-scale. These curves are considered applicable to all kinds of steels intended for welded structures (The yield stress level of steels are not a parameter). From the test data a design A curve is derived as $\log N = 13.14 - 3.0 \log S$, and a B curve is derived as $\log N = 12.87 - 3.0 \log S$.

In Table 14.2, the estimated fatigue strength and fatigue life are presented for the DNV III curve (Base Material) and the JSSC curves. Based on the definition of the JSSC B grade curve, this curve is to be compared with the DNV III curve, accounting for traditional workmanship. The JSSC A grade curve is to be compared with the DNV III curve modified as per Section 2.3.6 for machined or ground smooth base material. As is seen from the table, the JSSC and DNV results are comparable.

S-N curve	*Allowable stress range ($2*10^6$ cycles)*	*Fatigue Life (relative to DNV III)*
DNV curve III	157.1 (MPa)	1.0
JSSC B grade	155.0 (MPa)	0.96
DNV curve III[1]	198.0 (MPa)	2.0
JSSC A grade	190.0 (MPa)	1.77
[1] (machined or ground smooth, see Sect. 2.3.6)		

Table 14.2 Comparison of S-N curves for base materials

14.4 References

The references [F1] to [F17] in this appendix are:

1. Classification Note No. 30.2 Fatigue Strength Analysis for Mobile Offshore Units. Det Norske Veritas, August 1984.
2. Gurney: Fatigue of Welded Structures. Cambridge University Press. Second Edition. 1979.
3. Isao Soya: Fatigue life enhancement by higher standards of workmanship, fax dated August 23 1995.
4. Engesvik: Analysis of Uncertainties in the Fatigue Capacity of Welded Joints. Dissertation Marine Technology NTH 1981.

5. Department of Energy's Offshore Installations. Guidance on design and Construction. Issue N. August 1983. New Fatigue design Guidance for Steel Welded Joints in Offshore Structures.

6. HSE 1995. Proposed Revisions to Guidance Notes.

7. NS-ENV 1993-1-1. Eurocode 3: Design of Steel Structures. Part 1-1: General Rules and Rules for Buildings. 1993.

8. Germanischer Lloyds. Section 20 Fatigue Strength.

9. Berge: On the Effect of Plate Thickness in Fatigue of Welds. Engineering Fracture Mechanics. Vol. 21. No 2. pp 423-435. 1985.

10. Fricke and H. Pettershagen: Detail Design of Welded Ship Structures based on Hot Spot Stresses. PRADS 1992. Newcastle.

11. Aaleskjær: Parametrical Equations for Stress Concentrations at Welds. A/S Veritas Research Report No. 85-2027. DNV 1985.

12. Fatigue Assessment of Ship Structures. Report No 93-0432.

13. Recommendations Concerning Stress Determination for Fatigue Analysis of Welded Components. IIW Doc. XIII-1458-92.

14. Ho, F.V. Lawrence: Fatigue Test Results and Predictions for Cruciform and Lap Welds. Theoretical and Applied Fracture Mechanics. Volume 1., No. 1, March 1984.

15. R.E Peterson: Stress Concentration Factors. John Wiley&Sons New York. 1973.

16. Maddox: Fitness-for-purpose Assessment of Misalignment in Transverse Butt Welds Subject to Fatigue Loading. The Welding Institute 1985.

17. Fatigue Design Recommendations for Steel Structures. Japanese Society of Steel Construction. December 1995.

15. References

1) Det Norske Veritas, Rules for Classification of Ships, Part 3, Chapter 1, *Hull Structural Design, Ships with Length 100 Meters and above*, Høvik, January 1993

2) Hovem, L., Loads and Load Combinations for Fatigue Calculations - Background for the Wave Load Section for the DNVC Classification Note: Fatigue Assessment of Ships, DNVC Report No. 93-0314, Høvik, 1993

3) Cramer, E.H., Løseth, R. and Bitner-Gregersen, E.,. *Fatigue in Side Shell Longitudinals due to External Wave Pressure*, Proceedings OMAE conference, Glasgow, June 1993

4) British Maritime Technology, BMT, (Primary Contributors Hogben, H., Da Cunha, L.F. and Olliver, H.N), *Global Wave Statistics*, Unwin Brothers Limited, London, 1986

5) Det Norske Veritas, Classification Note no. 30.2, *Fatigue Strength Analysis for Mobile Offshore Units*, Høvik, August 1984

6) Recommendations for the Fatigue Design of Steel Structures, ECCS - Technical Committee 6 - Fatigue, First Edition, 1985

7) Maddox, S.J, *Fitness for purpose Assessment of Misalignment in Transverse Butt Welds Subject to Fatigue Loading*, Welding Institute Report 279, 1985

8) Almar - Næss, A., Editor, *Fatigue Handbook*, Tapir, Trondheim 1985

9) Holtsmark, G. *The Bending Response of Laterally Loaded Panels with Unsymmetrical Stiffeners*, DNVC Report No. 93-0152,.Høvik, 1993

10) Det Norske Veritas, PROBAN-Theory Manual, DNVR Report No. 89-2023, Høvik 1989

11) Det Norske Veritas, Classification Note no. 30.6, *Structural Reliability Analysis of Marine Structures*, Høvik, July 1991

12) Gran, S, *A Course in Ocean Engineering*, Developments in Marine Technology, Vol. 8, Elsevier Science Publishers B.V., 1992

13) Lotsberg, I., Nygård, M. and Thomsen, T. : Fatigue of Ship Shaped Production and Storage Units. OTC paper no 8775. Houston May 1998.

14) Lotsberg, I., Jensen, P.G., Cramer, E. and Brodtkorp, B. : Fatigue Assessment of Floating Production Vessels. Side Longitudinals. DNV Report No 97-3266. June 1977.

15) Lotsberg, I. and Unnland, T. : Fatigue Assessment of Floating Production Vessels. Effects of Mean Stress. Stress at Cut-outs. DNV Report No 97-3403. November 1997.

16) Witherby & Co. Ltd 1997: Guidance Manual for Tanker Structures.